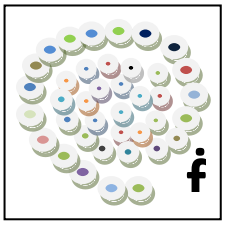

Journal of the Nigerian Society for Mathematical Biology

Volume 4, 2021

ISSN (Print): 2682 - 5694
ISSN (Online): 2682 - 5708

Journal of the Nigerian Society for Mathematical Biology

Volume 4, 2021

ISSN (Print): 2682 – 5694

ISSN (Online): 2682 - 5708

A publication of the Nigerian Society for Mathematical Biology

Editorial Board

Journal of the Nigerian Society for Mathematical Biology
Volume 4 (2021), pp. 1 – 18

SVEIR model of an infectious disease among infected immigrants with nonlinear incidence rate

I. O. Onwubuya[*] and C. E. Madubueze[†]

Abstract

In this paper, the effect of a saturated incidence rate and infectious immigrants on the transmission dynamics of an infectious disease is studied using an SVEIR model. The model exhibits three equilibrium states: the disease-free and endemic equilibrium states when there is no influx of infective immigrants and the endemic equilibrium state when there is an influx of infective immigrants in the population. Besides, the model shows a forward bifurcation when there is no entry of infective immigrants and this aid in establishing the local and global asymptotically stability when the basic reproduction number, $R_0 < 1$ and $R_0 > 1$ respectively. Numerical results are performed to examine the effect of the saturated incidence rate and the infective immigrants on disease transmission. The results indicate that the disease could be controlled or eradicated if there is a strict check to ensure that the infected immigrants are treated before they join the population.

Keywords: SVEIR model; Infectious disease; Non-linear incidence rate; basic reproduction number; global stability; infective immigrants

1 Introduction

Infectious diseases are inconveniences, disorders and a leading cause of death across the globe that man has been fighting to control [1]. They are deadly diseases characterized by rapid progressive deterioration and premature death and this includes severe acute respiratory syndrome (SARS), middle-east respiratory syndrome (MERS), Ebola virus disease, Lassa virus disease, and Yellow fever [2]. They constitute a public health burden to mankind and have profound negative effects on human life and socio-economic activities. These have compelled people of various fields to search for means of halting the spread of infectious diseases in the population. Controlling the spread of infectious diseases could be the administration of herbal and/or traditional remedies, surgery, vaccination, quarantine of infected individuals, and a thorough check on immigrants [3]. The impact of screening

[*] Department of Mathematics, Airforce Institute of Technology, Kaduna, Nigeria; isaacobiajulu@gmail.com
[†]Department of Mathematics/Statistics/Computer Science, University of Agriculture Makurdi, P.M.B. 2373, Makurdi, Nigeria.

and vaccination of immigrants on the spread of infectious diseases in any population is considered in this work.

Vaccination is the administration of antigenic material called vaccine which produces immunity to a disease. Immunity can be temporary or permanent. It has proven to be one of the most effective preventive measures of combating infectious diseases, such as smallpox, measles, hepatitis B, and polio [4]. Vaccines are substances used to build the body's immune system. It produces responses that fight pathogens like viruses, fungi, bacteria, and protects humans from the diseases these pathogens cause. A vaccine can be given by oral, injection, puncture, transdermal, or intranasal. The effect of vaccines is either for life or temporary in the body of the vaccinated person and where it is temporary, the person will become susceptible to the disease again [3, 5].

Immigration is the movement of people from their legal place of origin to another place where they are not native settlers which results in a permanent residence or future citizens. Immigrants are inspired to leave their legal place of origin for some reason, which includes socio-economic, political issues, education (quality of institutions), family reunion, environmental factors like conflict or natural disaster, and the desire of changing one's surroundings. Thus, immigrants from areas where there are infectious diseases can pose a challenge to another area and this makes human migration a major means of spreading infectious diseases to other countries. Infectious immigrants are immigrants with no overt disease who harbors infectious organisms. Infectious immigrants are increasingly important risk factors and sometimes becomes the index case for infections to the host population.

The mathematical modeling of infectious diseases is used to study the mechanisms of the transmission dynamics, the prediction of the future course of an outbreak, and the evaluation of strategies to control the disease. The saturated incidence rate is about the behavioural attitude of susceptible individuals and the crowding effects of infective individuals when there is an outbreak of disease [4, 6]. Significant work on compartmental models such as SEIRS, SEIQV, SIR, SEIR, SEIV with a saturated incidence rate has been done to examine the transmission dynamics of infectious diseases. The global analysis was carried out for these compartmental models except the work of Capasso and Serio [7] who initiated a saturated type incidence rate for generalized Kermack-Mckendrick deterministic model. Authors like Cai and Li [8] studied a SEIV model while Khan et al. [9] considered an SEIRS. Both models [8, 9] incorporate the general incidence rate and a waning preventive vaccine. Liu and Yang [10] used a saturated incidence rate, $\frac{\beta SI}{(1+aI)}$ for a SEIQV with vaccination and quarantine measures. Enatsu et al. [11] discussed a SIR with distributed time delay and found that the global dynamics are not affected by the distributed time delay. Li and Cui [12] incorporate different incidence rates for exposed and infected classes for an SEIR model and assumed permanent immunity for recovered class while Safi and Garba [13] incorporated a Holling type II incidence function with public health education and counseling as control measures for an SEIR. The effect of infected immigrants is considered by Zhang *et al.* [14] with bilinear incidence rate and temporary immunity. They developed an SEIRS model. From the aforementioned authors, none has considered the effect of infected immigrants on the spread of infectious disease with generalized incidence rate. This study investigates the impact of screening and vaccination of infected immigrants on disease dynamics by extending the work of Cai and Li [8]. Our model incorporates the influx of infected immigrants, the recovered class and mortality rate in the work of Cai and Li [8] since the infected immigrants become the index case to the host population as it was seen in the occurrence of the Ebola virus disease and the COVID-19 in Nigeria. It is also important to include the mortality rate because some sufferers can die from the disease itself and most times interventions in place are

non-pharmaceutical interventions. Our work is different from the work of Zhang *et al.* [14] because of the generalized nonlinear incidence rate and the permanent immunity of the recovered class considered in this paper. Thus, an SVEIR compartmental model with a generalized incidence rate and the proportion of infected immigrants is considered in this study. The impact of the different incidence rates is examined.

Based on the above motivation, an SVEIR compartmental model with a saturated incidence rate and the proportion of infected immigrants is considered in this paper. The rest of the paper is organized as follows: Section 2, is the formulation of the SVEIR model. The model analysis is presented in Section 3. In Section 4, numerical simulation is carried out to verify some analytical results while a brief discussion and conclusion are described in Section 5.

2 Model Formulation

We considered a non-linear saturated incidence rate of the form, $\frac{\beta SI}{\varphi(I)}$, which is a more general form of $\frac{\beta I^p S}{(1+\propto I^q)}$ that is used by some researchers (Liu *et al.* [15], Liu *et al.* [16]). The incidence rate is bilinear when $\varphi(I) = 1$. The function, $\varphi(I)$, satisfies $\varphi(0) = 1$ and $\dot{\varphi}(I) \geq 0$. This implies that $\varphi(I) \geq 0$ for $I(t) \geq 0$. The function, $\frac{1}{\varphi(I)}$, is used to measure the psychological or inhibition effect of the behavioral change of susceptible individuals when there is an increase in the number of infectious individuals. We develop a five compartmental model which consists of Susceptible individuals, $S(t)$, Vaccinated individuals, $V(t)$, Exposed individuals, $E(t)$, Infectious individuals $I(t)$, and Recovered individuals $R(t)$ with a general non-linear incidence rate, $\frac{\beta SI}{\varphi(I)}$ and a waning preventive vaccine at the rate, ω. Our model assumed that some proportion, k, of immigrants are infected [14] while some proportions, p, are given vaccination at the point of entrance [9]. Infected immigrants are sometimes the index case to the host population as it happened in Nigeria for the Ebola virus disease and COVID-19 [17, 18]. Also, we assumed that the recovered class has permanent immunity as in the work of [13]. COVID-19 can be a good example of an SVEIR since it has not been confirmed with temporary immunity. This makes up the SVEIR model that is given as follows with the parameter description in Table 1.

$$\frac{dS}{dt} = (1-p-k)\pi - \frac{BSI}{\varphi(I)} - \mu S + \omega V \,, \tag{1}$$

$$\frac{dV}{dt} = p\pi - (\mu+\omega)V \,, \tag{2}$$

$$\frac{dE}{dt} = \frac{BSI}{\varphi(I)} - (\mu+\varkappa)E \,. \tag{3}$$

$$\frac{dI}{dt} = k\pi + \varkappa E - (\mu+\delta+d)I, \tag{4}$$

$$\frac{dR}{dt} = \delta I - \mu R, \tag{5}$$

subject to the initial conditions, $S(0) = S_0, V(0) = V_0,\ E(0) = E_0\,,\ I(0) = I_0,\ \ R(0) = R_0$.

Table 1. Parameter description

Parameters	Description
$\boldsymbol{\pi}$	The recruitment rate of individuals including newborns and immigrants into the population.
$\boldsymbol{p}$	A proportion of recruited individuals that are vaccinated
$\boldsymbol{k}$	A proportion of infected immigrants in the population
$\boldsymbol{\beta}$	The transmission rate
$\boldsymbol{\mu}$	Natural death rate
$\boldsymbol{d}$	The mortality rate due to infection
$\boldsymbol{r}$	The rate at which exposed individuals become infectious
$\boldsymbol{\delta}$	The rate at which infected individuals are treated and recovered
$\boldsymbol{\omega}$	The rate at which the vaccine wanes

3 Model Analysis

3.1 Boundedness of the Solutions

The SVEIR model (1) – (5) is shown to be well-posed and makes biological sense. This is done by proving that the existence of a non-negative solution and its boundedness for an initial solution.

Theorem 1. Let the initial solutions satisfy $S(0) > 0, V(0) \geq 0,\ E(0) \geq 0,\ I(0) \geq 0, R(0) \geq 0$. The SVEIR model of equation (1) - (5) has non-negative solutions which are contained in the feasible region, $\Omega = \left\{\left(S(t), V(t), E(t), I(t), R(t)\right) \in \mathbb{R}_+^5 : N \leq \frac{\pi}{\mu}\right\}$.

Proof. First, we prove the non-negative solution set for the SVEIR model (1) – (5). It follows from (1) that

$$\frac{dS}{dt} = (1-p-k)\pi - \frac{\beta SI}{\varphi(I)} - \mu S + \omega V \geq (1-p-k)\pi - \beta(t)S\,, \qquad (6)$$

where $\beta(t) = \frac{\beta I}{\varphi(I)} + \mu$.

Solving (6), a first-order linear equation in S , using the method of integrating factor on $[0, t]$ with the initial condition, $S(0) > 0$, we have

$$S(t) \geq S(0)exp\left(\int_0^t -\beta(s)ds\right) + exp\left(\int_0^t -\beta(s)ds\right) \times \int_0^t (1 - p - k)\pi exp\left(\int_0^u \beta(\omega)d\omega\right) \geq 0 .$$

Hence, $S(t) \geq 0$ since $S(0) > 0$.

The remaining equations are obtained in a similar way that

$$V(t) \geq V(0)exp\big(-(\mu + \omega)\big)t \geq 0 ,$$

$$E(t) \geq E(0)\exp\big(-(\mu + \curlyvee)\big)\, t \geq 0 ,$$

$$I(t) \geq I(0)\exp\big(-(\mu + \delta + d)\big)\, t \geq 0 ,$$

and

$$R(t) \geq R(0)\exp(-\mu t) \geq 0.$$

Hence, the solution set $\big(S(t), V(t), E(t), I(t), R(t)\big)$ of the SVEIR model of equations (1)-(6) is non-negative for all $t > 0$ since exponential functions and initial solutions are non-negative.

Next, we prove that the non-negative solution set is contained in the feasible region, Ω, which is the boundedness of the solution. This is done by adding the equations of SVEIR model to get the rate of the total population, $N(t)$,

$$\frac{dN}{dt} = \pi - \mu N - dI . \tag{7}$$

If we ignore d, equation (7) yields

$$\frac{dN_h}{dt} \leq \pi - \mu N . \tag{8}$$

Applying the Gronwall's inequality to equation (8) with the initial condition, $N(0) = N_0$, we get

$$N(t) \leq \frac{\pi}{\mu} + \left[N_0 - \frac{\pi}{\mu}\right] e^{-\mu t}. \tag{9}$$

If $N_0 < \frac{\pi}{\mu}$ as $t \to \infty$, the trajectories approach $\frac{\pi}{\mu}$; If $N_0 > \frac{\pi}{\mu}$, the solutions $N(t)$ decreases to $\frac{\pi}{\mu}$ as $t \to \infty$. Therefore, in either case, the total population, $N(t) \to \frac{\pi}{\mu}$ as $t \to \infty$ in (9). This

means that $0 \leq N(t) \leq \frac{\pi}{\mu}$. Hence, the non-negative solution set of the SVEIR model equations (1)-(5) enters the feasible region, Ω, which is a positively invariant set.

3.2 Existence and Stability of Disease-free Equilibrium State and Basic Reproduction Number

3.2.1 Disease-free Equilibrium State

The equilibrium state for the SVEIR model is obtained when $\frac{dS}{dt} = 0$, $\frac{dV}{dt} = 0$, $\frac{dE}{dt} = 0$, $\frac{dI}{dt} = 0$, and $\frac{dR}{dt} = 0$. This yields

$$(1 - p - k)\pi - \frac{BSI}{\varphi(I)} - \mu S + \omega V = 0 , \tag{10}$$

$$p\pi - hV = 0 , \tag{11}$$

$$\frac{BSI}{\varphi(I)} - fE = 0 , \tag{12}$$

$$k\pi + \curlyvee E - gI = 0 , \tag{13}$$

$$\delta I - \mu R = 0, \tag{14}$$

where

$$h = (\mu + \omega), f = (\mu + \curlyvee), \text{and } g = (\mu + \delta + d). \tag{15}$$

Solving equations (10) – (14) when there are no infective immigrants in the population $(i.e. k = 0)$, we have the disease-free equilibrium (DFE) state, E_0, as $E_0 = (S_0, V_0, 0, 0, 0) = \left(\frac{\pi\{(1-p)\mu+\omega\}}{\mu(\mu+\omega)}, \frac{p\pi}{\mu+\omega}, 0, 0, 0\right)$.

This implies that when there is no exposed infective and recovery individuals in the population, the level of susceptible will be approaching $\frac{\pi\{(1-p)\mu+\omega\}}{\mu(\mu+\omega)}$ and the vaccination population will remain at is equilibrium state, $V_0 = \frac{p\pi}{\mu+\omega}$.

3.2.2 Basic Reproduction Number, $\mathbf{R_0}$

The basic reproduction number of an infection denoted by R_0, is a threshold quantity that provides useful information regarding the spreading and control of infectious disease in a population. If $R_0 < 1$, the infection will fizzle out, but, if $R_0, > 1$, the infection will be able to spread and persist in the population. To compute the basic reproduction number for the SVEIR model using the next generation operator, we follow the approach of Van den Driessche and Watmough, [19]. Let $X = (E, I)$, be the vector that represents the infected compartments. Then from the model (1) – (5), we have the rate of new infection in the infected compartments as

$$F = \begin{bmatrix} \frac{\beta SI}{\varphi(I)} \\ 0 \end{bmatrix},$$

and the rate of transfer from in and out the infected compartments as

$$V = \begin{bmatrix} fE \\ -k\pi - \gamma E + gI \end{bmatrix}.$$

Taking the partial derivatives of F and V at the DFE, E_0, yield

$$G = \frac{\partial F(E_0)}{\partial X} = \begin{bmatrix} 0 & \beta S_0 \\ 0 & 0 \end{bmatrix} \text{ and } \qquad U = \frac{\partial V(E_0)}{\partial X} = \begin{bmatrix} f & 0 \\ -\gamma & g \end{bmatrix}.$$

We have the matrix, GU^{-1}, as

$$GU^{-1} = \begin{bmatrix} \frac{\beta S_0 \gamma}{fg} & \frac{\beta S_0}{g} \\ 0 & 0 \end{bmatrix},$$

and the basic reproduction number, R_0, which is the spectral radius of the matrix, GU^{-1}, given as

$$R_0 = \frac{\beta S_0 \gamma}{fg}. \tag{16}$$

Substituting, S_0, and the definition (15) in (21) gives

$$R_0 = \frac{\beta \gamma \pi \{(1-p)\mu + \omega\}}{\mu(\mu+\omega)(\mu+\gamma)(\mu+\delta+d)}. \tag{17}$$

Equation (17) is the basic reproduction number, R_0, for the SVEIR model (1) – (5). The effect of these parameters, $\tau, \beta, \omega, \delta$ on R_0 is illustrate numerically in Figure 1 using the parameter values in [7]. Figure 1 shows that increasing τ, β, ω, and decreasing δ, increases the basic reproduction number, R_0 while other parameters are keep constant.

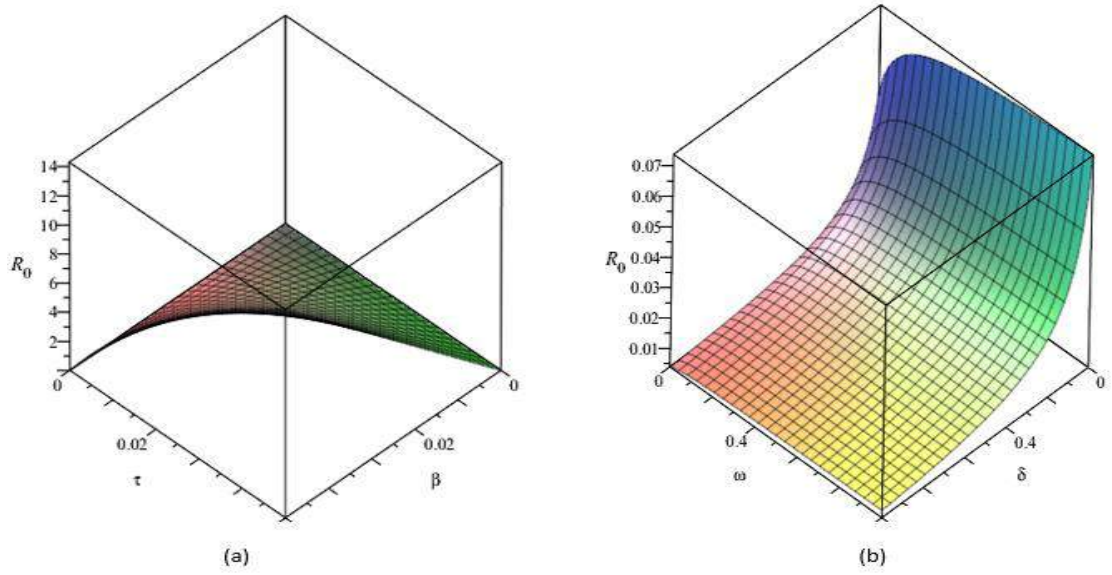

Figure 1. The effect of $\tau, \beta, \omega, \delta$ on the basic reproduction number, R_0. For (a),$p = 0.4,\ \delta = 0.009, \mu = 0.09, d = 0.004, \pi = 10, \omega = 0.05$ and for (b), $p = 0.4,\ \beta = 0.002, \mu = 0.09, d = 0.004, \pi = 10, \tau = 0.003$.

3.2.3 Local Stability of Disease-free Equilibrium (DFE)

Here, we investigate the local stability of the disease-free equilibrium state,$E_0 = (S_0, V_0, 0,\ 0,\ 0)$ without the recovery class, since it does not involve other classes using linearization method by computing its Jacobian matrix at the DFE, $J(E_0)$, as follows

$$J(E_0) = \begin{bmatrix} -\mu & 0 & -\beta S_0 & \omega \\ 0 & -f & \beta S_0 & 0 \\ 0 & r & -g & 0 \\ 0 & 0 & 0 & -h \end{bmatrix}. \tag{18}$$

The characteristics equation of the $J(E_0)$ in (18) is given by

$$(\lambda + \mu)(\lambda + h)[\lambda^2 + (f + g)\lambda + fg - \beta S_0 r] = 0. \tag{19}$$

The SVEIR model (1) – (5) has two negative real roots $-\mu, -h,$ and the roots of the characteristics equation given as

$$\lambda^2 + (f + g)\lambda + fg - \beta S_0 r = 0. \tag{20}$$

Using Routh-Hurwitz criteria, equation (20) has negative root if $A > 0,\ AB > 0$ which implies that $B > 0$.

In equation (20), $A = f + g$; $B = fg - \beta S_0 r$. It is clear that $A > 0$ and $B > 0$ if $fg > \beta S_0 r$ which means that $\frac{\beta S_0 r}{fg} < 1$. Therefore, using the definition in equation (16), we have that DFE, E_0 is locally asymptotically stable if $R_0 < 1$.

3.3 Existence and Stability of Endemic Equilibrium State

3.3.1 Existence of Endemic Equilibrium State

The endemic equilibrium state is established when there is infection in the population ($i.e. I \neq 0$). The endemic equilibrium state for SVEIR model (1) – (5) is obtained by solving equations (10) – (14) simultaneously which gives

$$S^\star = \frac{fA(gI - k\pi)}{r\beta I}, E^\star = \frac{gI - k\pi}{r}, V^\star = \frac{P\pi}{h}. \quad (21)$$

Substituting (21) in (12) and simplifying gives

$$PI^{\star 2} - QI^\star - R = 0, \quad (22)$$

where $A = \varphi(I^\star), P = \beta fgh$, $Q = fgh\mu\left(R_0 + \frac{\beta\pi k}{fg} - A\right)$, $R = A\pi fhk\mu$.

If $k = 0,$ we have $R = 0$ and $A = 1,$ so equation (22) will becomes

$$PI^{\star 2} - Q^* I^\star = 0 \quad (23)$$

with $Q^* = fgh\mu R_0$.

From equation (23), it implies that $I^\star = 0$ or $I^\star = \frac{\mu R_0}{\beta}$. $I = 0$ corresponds to DFE, E_0. So, we have endemic equilibrium state, $E_1,$ when $k = 0$ as

$$E_1 = \left(\frac{fg}{r\beta}, \frac{gR_0}{r\beta fgh}, \frac{R_0}{\beta fgh}, \frac{\mu R_0}{\beta}, \frac{p\pi}{h}\right).$$

When $k > 0,$ we have from equation (22) that

$$I^\star = \frac{Q + \sqrt{Q^2 + 4PR}}{2P}. \quad (24)$$

Substituting equation (24) into equation (21), we have the endemic equilibrium state for $k > 0$ given as

$$E_{1k} = \left(\frac{fAg(Q + \sqrt{Q^2 + 4PR}) - 2pk\pi fA}{r\beta(Q + \sqrt{Q^2 + 4PR})}, \frac{p\pi}{h}, \frac{g(Q + \sqrt{Q^2 + 4PR}) - 2pk\pi}{2pr}, \frac{Q + \sqrt{Q^2 + 4PR}}{2P}, \frac{\delta\left(Q + \sqrt{Q^2 + 4PR}\right)}{2P\mu}\right). \quad (25)$$

Equations (24) and (25) give the endemic equilibrium state,E_{1k}, provided it satisfy the inequality $g\left(Q+\sqrt{Q^2+4PR}\right)>2pk\pi$.

3.3.2 Local Stability of Endemic Equilibrium State

We establish the local stability of endemic equilibrium using the centre manifold theorem by Castillo - Chavez and Song [20] which depends on the existence of bifurcation near $R_0=1$. A forward bifurcation implies that disease-free equilibrium is locally asymptotically stable for $R_0<1$ and also endemic equilibrium is locally asymptotically stable for $R_0>1$ near one. It is possible to have the global asymptotical stability of the two equilibrium states and disease cannot invade the population when $R_0<1$.

Using the concept of Castillo - Chavez and Song [21], we choose $\beta=\beta^*$ as bifurcation parameter so at $R_0=1$ from equation (17) gives

$\beta=\beta^*=\frac{fg\mu(\mu+\varphi)}{\pi\sigma\left((1-p)\mu+\varphi\right)}$.

Also, let represent $S=x_1,\ \ V=x_2,\ E=x_3,\ I=x_4,\ \ \ R=x_5,$ in equations (1) – (5).

If we replacing $\beta=\beta^*$ in the Jacobian matrix $J(E_0)$ of equation (18) at $R_0=1$, we have a simple zero eigenvalue and negative eigenvalues by solving (19) and this yields

$\lambda=-\mu,\lambda=-h,\lambda=-(f+g)$, and $\lambda=0$, since $fg-\beta S_0\gamma=0$ at $R_0=1$.

We derived the right and left eigenvectors associated with zero eigenvalue using the centre manifold theory as $\boldsymbol{w}=(w_1,w_2,w_3,w_4)=\left(-\frac{f}{\mu}w_2,w_2,\frac{\sigma}{g}w_2,0\right)$ and $\boldsymbol{v}=(v_1,v_2,v_3,v_4)=\left(0,v_2,\frac{f}{\sigma}v_2,0\right)$.

Using Theorem 4.1 of [16], the coefficients a and b are given as

$a=-v_2w_2^2\frac{\beta^*f\sigma}{g\mu}$ and $b=v_2w_2\frac{\sigma}{g}S_0$.

It is clear that $a<0$ and $b>0$. This shows the SVEIR model of equations (1) – (5) exhibits a forward bifurcation. This means that the endemic equilibrium state is locally asymptotical stability for $R_0>1$ near one and the disease-free equilibrium state is locally asymptotical stability for $R_0<1$ when $k=0$ and there is the possibility of global stability of the equilibrium states when $k=0$. This is shown graphically in Figure 2.

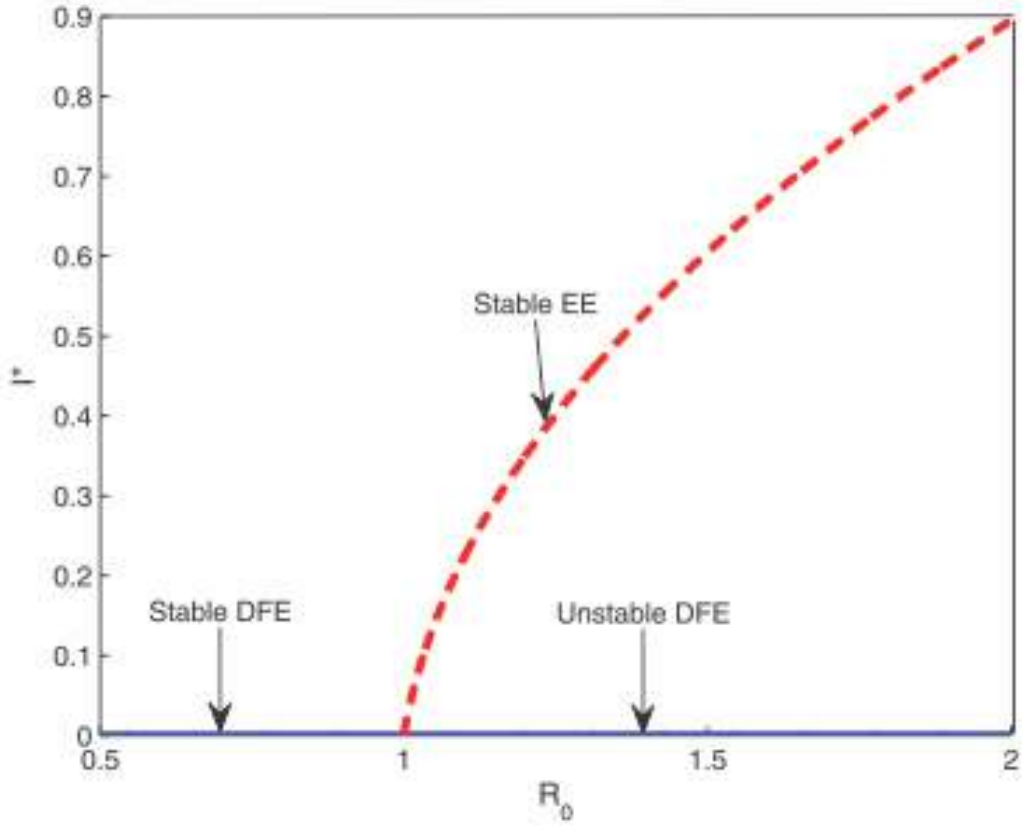

Figure 2. Forward bifurcation plot for the SVEIR model displaying I^* as a function of R_0. Here, $\varphi(I^*) = 1 + I^{*2}$ and the parameter values are $p = 0.4,\ \delta = 0.09, \mu = 0.09, d = 0.004, \pi = 10, \omega = 0.05, \beta = 0.02, \tau = 0.03, k = 0.0, R_0 = 2.243$.

3.4 Global Stability of Equilibrium States

In this subsection, the global stability of the equilibrium states when $k = 0$ is considered. This is done by constructing Lyapunov functions.

3.4.1 Global Stability of Disease-free Equilibrium State

The global stability of the disease-free equilibrium of the SVEIR model equations (1) - (5) is considered by constructing a Lyapunov function and applying LaSalle's invariance principle.

Theorem 2: The DFE, E_0, of the SVEIR model equations (1)-(5) is globally asymptotically stable if $R_0 \leq 1$ in Ω.

Proof: we construct a Lyapunov function using a matrix-theoretic method by Shuai and van Den Driessche [19]. The function is given by

$$L = \frac{r}{fg}E + \frac{1}{g}I \ . \tag{26}$$

Taking the time derivative of equation (26) along the solution of the SVEIR model, we get

$$L' = \frac{r}{fg}E' + \frac{1}{g}I' \ ,$$

$$= \frac{r}{fg}\left(\frac{\beta SI}{\varphi(I)} - fE\right) + \frac{1}{g}(rE - gI) \ . \tag{27}$$

Expanding and simplifying equation (27) yields

$$L' = \left(\frac{\beta rS}{fg\varphi(I)} - 1\right) I \ ,$$

which can be written as

$$L' = \left[\frac{\beta r}{fg}\left(\frac{S}{\varphi(I)} - \frac{S_0}{\varphi(I_0)} + \frac{S_0}{\varphi(I_0)}\right) - 1\right] I \ .$$

But $\varphi(I_0) = 1$ at DFE, E_0. Therefore, we have

$$L' = \left(\frac{\beta rS_0}{fg\varphi(I_0)} - 1\right) I + \frac{\beta r}{fg}\left(\frac{S}{\varphi(I)} - \frac{S_0}{\varphi(I_0)}\right) I \ ,$$

$$= (R_0 - 1)I + \frac{\beta r}{fg}\left(\frac{S}{\varphi(I)} - S_0\right) I \ .$$

Since $\varphi(I) \geq 1,$ then $\frac{S}{\varphi(I)} - S_0 \leq 0.$

Hence,

$$L' \leq (R_0 - 1)I \ .$$

Therefore, it follows that $L' \leq 0$ for $R_0 \leq 1$ with $L' = 0,$ if and only if $E = I = 0.$ This shows that the singleton $\{E_0\}$ is the largest compact invariant set in $\{(S(t), V(t), E(t), I(t), R(t)) \in \Omega : L' = 0\}$. Hence, applying LaSalle's invariance principle, the disease-free equilibrium, $\{E_0\}$ is globally asymptotically stable in Ω If $R_0 \leq 1$.

3.4.2 Global Stability of Endemic Equilibrium State

Theorem 3. The endemic equilibrium, E_1, of the SVEIR model equations (1)-(5) is globally asymptotically stable if $R_0 > 1$ in Ω.

Proof. The global stability of the endemic equilibrium is proved by constructing the Volterra-Lyapunov function.

$$L = \left(S - S^* - S^* ln\frac{S}{S^*}\right) + \left(E - E^* - E^* ln\frac{E}{E^*}\right) + \frac{f}{r}\left(I - I^* - I^* ln\frac{I}{I^*}\right) + \left(V - V^* - V^* ln\frac{V}{V^*}\right).$$

Taking the time derivatives of L along the solutions of the equations (1) – (5), we get

$$L' = \left(1 - \frac{S^*}{S}\right)S' + \left(1 - \frac{E^*}{E}\right)E' + \frac{f}{r}\left(1 - \frac{I^*}{I}\right)I' + \left(1 - \frac{V^*}{V}\right)V',$$

$$L' = \left(1 - \frac{S^*}{S}\right)\left((1-\rho)\pi - \frac{\beta SI}{\varphi(I)} - \mu S + \omega V\right) + \left(1 - \frac{E^*}{E}\right)\left(\frac{\beta SI}{\varphi(I)} - fE\right) + \frac{f}{r}\left(1 - \frac{I^*}{I}\right)(rE - gI) + \left(1 - \frac{V^*}{V}\right)(\rho\pi - hV) \quad . \tag{28}$$

At the endemic equilibrium state, we have

$$(1-\rho)\pi = \frac{\beta S^*I^*}{\varphi(I)} + \mu S^* - \omega V^*, f = \frac{\beta S^*I^*}{\varphi(I^*)E^*}\ ,\ \rho\pi = hV^*,\ g = \frac{rE^*}{I^*}. \tag{29}$$

Substituting equation (29) into equation (28) yields

$$L' = \left(1 - \frac{S^*}{S}\right)\left(\frac{\beta S^*I^*}{\varphi(I^*)} + \mu S - \omega V^* - \frac{\beta SI}{\varphi(I)} - \mu S + \omega V\right) + \left(1 - \frac{E^*}{E}\right)\left(\frac{\beta SI}{\varphi(I)} - \frac{\beta S^*I^*E}{\varphi(I^*)E^*}\right) + \frac{f}{r}(1 - \frac{I^*}{I})\left(rE - \frac{rE^*}{I^*}I\right) + \left(1 - \frac{V^*}{V}\right)(hV^* - hV) \quad . \tag{30}$$

Expanding equation (30) gives

$$L' = \frac{\beta S^*I^*}{\varphi(I^*)} + \mu S^* - \omega V^* - \mu S + \omega V - \frac{\beta S^{*2}I^*}{\varphi(I^*)S} - \frac{\mu S^{*2}}{S} + \omega V^*\frac{S^*}{S} + \frac{\beta S^*I}{\varphi(I)} + \mu S^* - \omega V\frac{S^*}{S} - \frac{\beta S^*I^*E}{\varphi(I^*)E^*} - \frac{\beta SIE^*}{\varphi(I)E} + \frac{\beta S^*I^*}{\varphi(I^*)} + \frac{\beta S^*I^*E}{\varphi(I^*)E^*} - \frac{\beta S^*I}{\varphi(I^*)} - \frac{\beta S^*I^{*2}E}{\varphi(I^*)IE^*} + \frac{\beta S^*I^*}{\varphi(I^*)} + hV^* - hV - \frac{hV^{*2}}{V} + hV^*,$$

which is simplify to get

$$L' = \mu S^*\left(2 - \frac{S^*}{S} - \frac{S}{S^*}\right) + \frac{\beta S^*I}{\varphi(I^*)}\left(3 - \frac{S^*}{S} - \frac{S}{S^*}\frac{I}{I^*}\frac{E^*}{E} - \frac{I^*}{I}\frac{E}{E^*}\right) + \frac{\beta S^*I^*}{\varphi(I^*)}\left(\frac{I}{I^*}\frac{\varphi(I^*)}{\varphi(I)} - \frac{I}{I^*}\right) + hV^*\left(2 - \frac{V}{V^*} - \frac{V^*}{V}\right) + \omega V^*\left(\frac{V}{V^*} + \frac{S^*}{S} - \frac{V}{V^*}\frac{S^*}{S} - 1\right).$$

But $h = \mu + \omega$ in equation (15), then

$$L' = F(S,I,E) + \mu V^*\left(2 - \frac{V}{V^*} - \frac{V^*}{V}\right) + \omega V^*\left(\frac{S^*}{S} - \frac{V}{V^*}\frac{S^*}{S} + 1 - \frac{V^*}{V}\right) + \frac{\beta S^*I^*}{\varphi(I^*)}\left(\frac{I}{I^*}\frac{\varphi(I^*)}{\varphi(I)} - \frac{I}{I^*}\right),$$

where $F(S,I,E) = \mu S^*\left(2 - \frac{S^*}{S} - \frac{S}{S^*}\right) + \frac{\beta S^*I^*}{\varphi(I^*)}\left(3 - \frac{S^*}{S} - \frac{S}{S^*}\frac{I}{I^*}\frac{E^*}{E} - \frac{I^*}{I}\frac{E}{E^*}\right)$.

So,

$$L' = F(S,I,E) + \mu V^*\left(2 - \frac{V}{V^*} - \frac{V^*}{V}\right) + \omega V^*\left(1 - \frac{V^*}{V} + \frac{S^*}{S} - \frac{V}{V^*}\frac{S^*}{S}\right) + \frac{\beta S^* I^*}{\varphi(I^*)}\left(\frac{I}{I^*}\frac{\varphi(I^*)}{\varphi(I)} - \frac{I}{I^*}\right).$$

But, $1 - \frac{V^*}{V} + \frac{S^*}{S} - \frac{V}{V^*}\frac{S^*}{S} \leq 2 - \frac{V^*}{V} - \frac{V}{V^*}$, and $\frac{\varphi(I^*)}{\varphi(I)} - 1 \leq 0$ for $I^* \leq I$ since $S^* < S$ and $\varphi(I)$ is an increasing function.

Therefore,

$$L' \leq \mu S^*\left(2 - \frac{S^*}{S} - \frac{S}{S^*}\right) + \frac{\beta S^* I^*}{\varphi(I^*)}\left(3 - \frac{S^*}{S} - \frac{S}{S^*}\frac{I}{I^*}\frac{E^*}{E} - \frac{I^*}{I}\frac{E}{E^*}\right) + (\mu + \omega)V^*\left(2 - \frac{V}{V^*} - \frac{V^*}{V}\right). \quad (31)$$

Applying the arithmetic-geometric mean inequality theorem to equation (31), we have

$$2 \leq \frac{S^*}{S} + \frac{S}{S^*}, \quad 3 \leq \frac{S^*}{S} + \frac{S}{S^*}\frac{I}{I^*}\frac{E^*}{E} + \frac{I^*}{I}\frac{E}{E^*}, \text{ and } 2 \leq \frac{V}{V^*} + \frac{V^*}{V}.$$

Hence, $L' \leq 0$ for all $\big(S(t), V(t), E(t), I(t), R(t)\big)$ in the region, Ω and $L' = 0$, if and only if $S^* = S,\ E^* = E,\ V^* = V, I^* = I, R^* = R$. This shows that the singleton $\{E_1\}$ is the largest compact invariant set in $\big\{\big(S(t), V(t), E(t), I(t), R(t)\big) \in \Omega : L' = 0\big\}$. Therefore, applying LaSalle's invariance principle, the endemic equilibrium state, $\{E_1\}$ is globally asymptotically stable in Ω If $R_0 > 1$ when $k = 0$.

Global stability implies that with different initial conditions, the model will always converge to the disease-free and endemic equilibrium states when $R_0 < 1$ and $R_0 > 1$ respectively. This is shown in Figure 3 for the infected population. The Infected population is choosing to illustrate the global stability of the equilibrium states.

4 Numerical Simulations

In this section, the numerical simulations for the SVEIR model are implemented to quantify the impact of different incidence rates and proportions of infective immigrants on disease dynamics. The parameter values used in this simulation are mainly from Khan et al. [7] except stated otherwise. The saturated incidence rate, $\varphi(I) = 1 + I^2$ is also used.

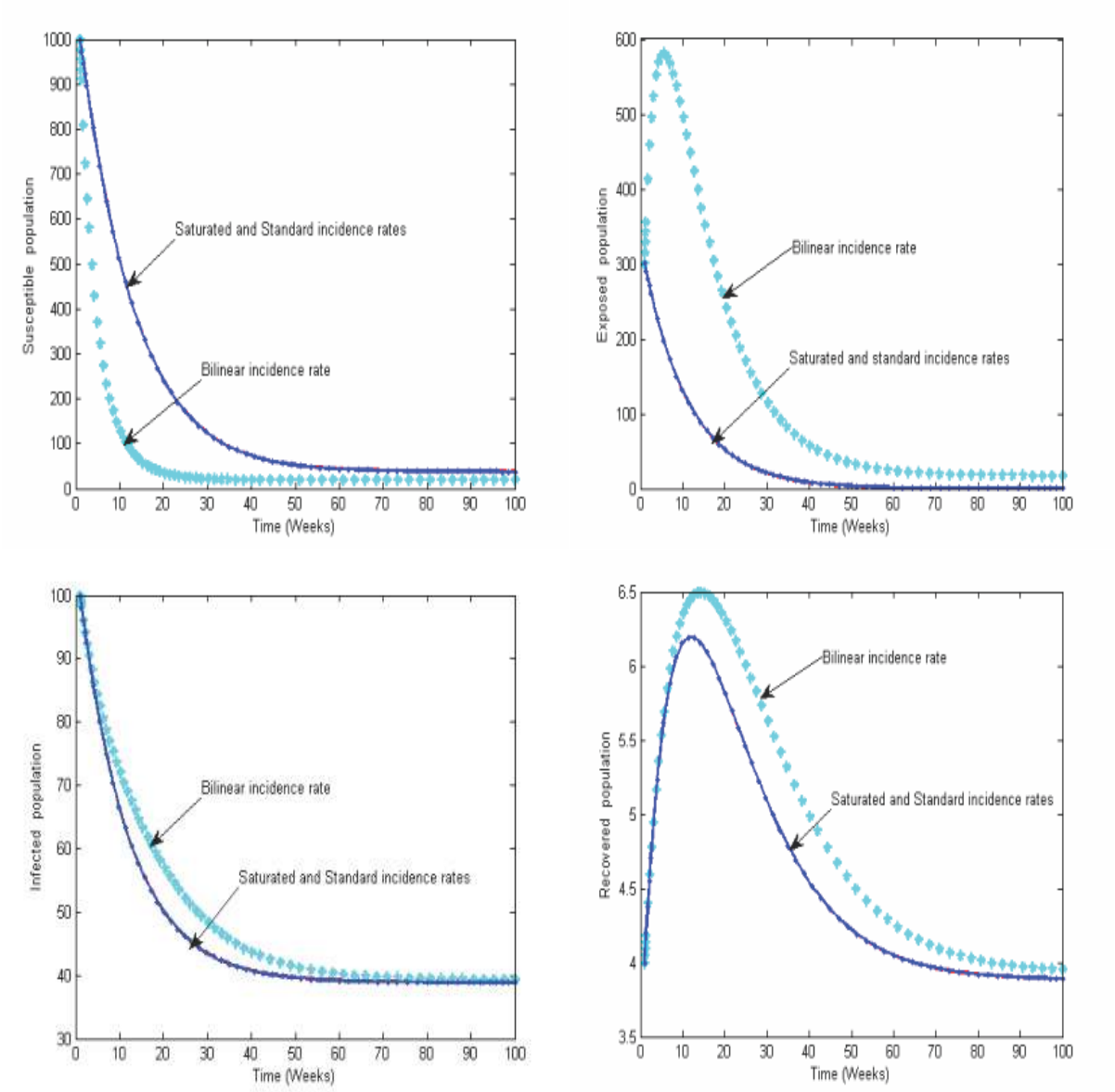

Figure 3. The dynamical behavior of the SVEIR model with different incidence rates. The parameter values are $\beta = 0.002, p = 0.4, k = 0.4, \tau = 0.003, \delta = 0.009, \mu = 0.09, d = 0.004, \pi = 10, \omega = 0.05$.

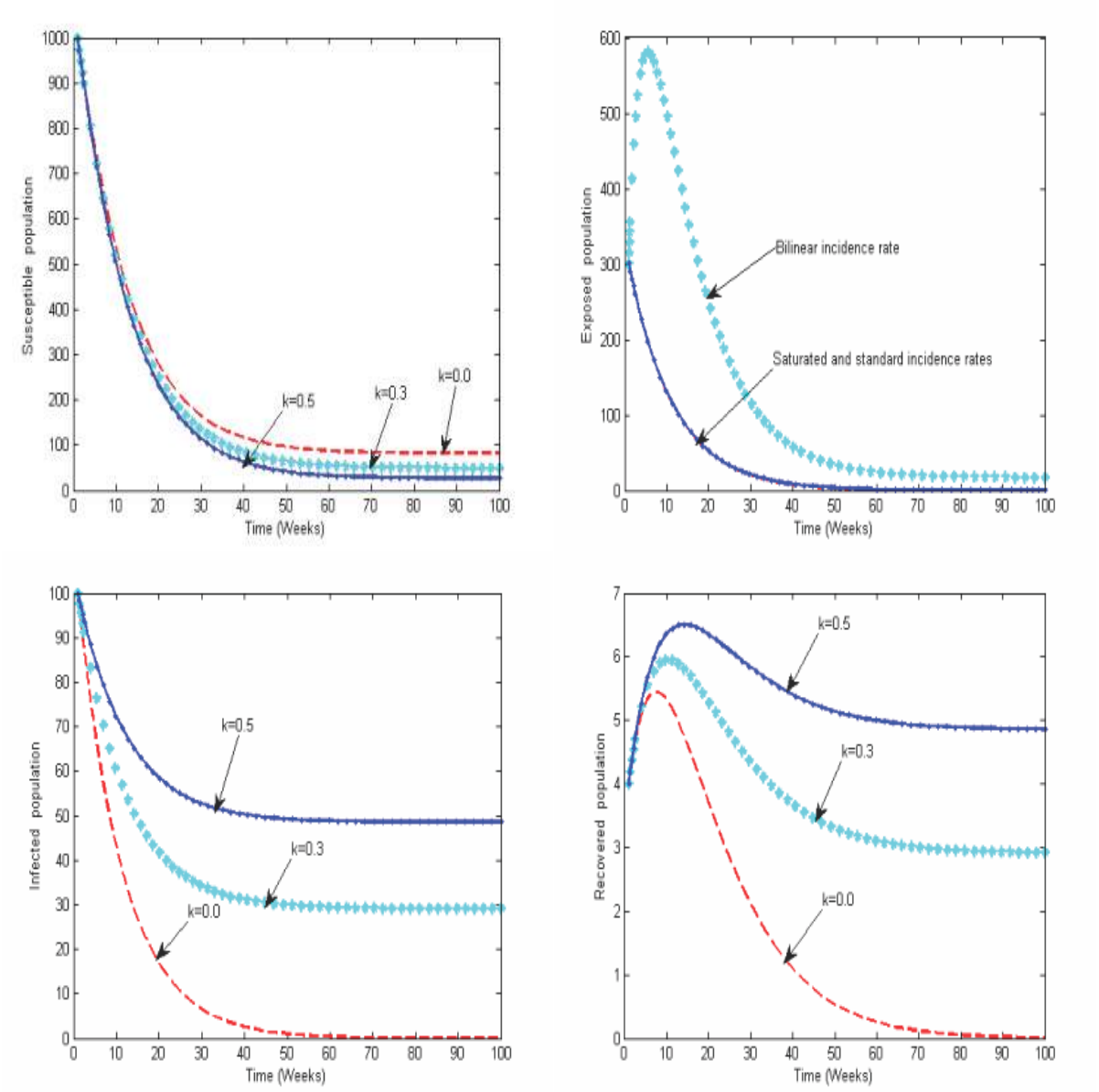

Figure 4. The dynamical behavior of the SVEIR model with different proportions of infective immigrants. The parameter values are $\beta = 0.002, p = 0.4,\ \tau = 0.003, \delta = 0.009, \mu = 0.09, d = 0.004, \pi = 10, \omega = 0.05$.

5 Discussion and Conclusion

This study investigates the transmission dynamics of infectious diseases with a saturated incidence rate and the influx of infected immigrants in the population. The model is a deterministic SVEIR model. The basic reproduction number, R_0, is computed using the next-generation approach. The disease-free and endemic equilibrium states without the influx of infected immigrants are shown to be local

and global asymptomatically stable when $R_0 < 1$ and $R_0 > 1$ respectively. Also, the endemic equilibrium state when there is an influx of infected immigrants in the population is established under certain conditions. A forward bifurcation existed when there is no infective immigrant in the population. Numerical results show that the saturated incidence and the standard incidence rates produce the same results that reduce the number of infected individuals in the population compared to the bilinear incidence rate (Figure 3). The important of infected immigrants is considered and the outcome reveals that infected immigrants do not affect exposed individuals in the population. However, infected individuals increase as the proportion of infected immigrants increase (see Figure 4) and this is comparable with the work of [12] that considered the entrance of infected immigrants in the population for an SEIRS model. This indicates that measures should be taken to reduce the influx of infected immigrants in the population. One of these measures could be screening at the entry point in the population especially for infectious diseases like COVID-19, SARS, MERS, Ebola virus disease and Lassa virus.

References

[1] The Red Cross and the World Health Organization Regional Office for Europe (2001). Infection and Infectious diseases: A manual for nurses and midwives in the WHO Europe Region. https:// www.euro.who.int > assets > pdf_files

[2] Baldassi, F., Carestia, M., Moramarco, S., Malizia, A., and Gaudio, P. (2021). Infectious Diseases Seeker (IDS): An Innovative Tool for Prompt Identification of Infectious Diseases during Outbreaks. Int. J. Environ. Res. Public Health, 18: 3216. https://doi.org/10.3390/ijerph18063216.

[3] Li-Ming Cai and Xue-Zhi Li (2008). Analysis of a SEIV Epidemic Model with a Nonlinear Incidence Rate. J. of Appl. Math Modelling doi: 10.1016/j.apm.2008.01.005.

[4] Liu, W.M., Hethcote, H.W. and Levin, S.A. (1987). Dynamical behavior of epidemiological models with nonlinear incidence rates. J. Math. Biol., 25: 359-380.[5] Zhang, T. and Teng, Z. (2007). Pulse vaccination delayed SEIRS epidemic model with saturated incidence. Appl. Math. Model. doi: 10.1016/J. amp. 2007.06.005.

[6] Liu, W.M., Levin, S.A. and Iwasa, Y. (1986). Influence of nonlinear incidence rates upon the behavior of SIRS epidemiological models. J.Math.Biol., 23:187-204.

[7] Capasso, V. and Serio, G. (1978). A generalization of the Kermack-Mckendrick deterministic epidemic model. Math. Biosci., 42:43-61.

[8] Li-Ming Cai and Xue-Zhi Li (2009). Analysis of a SEIV Epidemic Model with a Nonlinear Incidence Rate. Applied Mathematical Modelling, 33: 2919 – 2926.

[9] Khan, M. A., Badshah, Q., Islam, S, Khan, I., Shafie, S. and Khan, S. A. (2015). Global dynamics of SEIRS epidemic model with non-linear generalized incidences and preventive vaccination. Advances in Difference Equations, 2015:88.

[10] Liu, X. and Yang, L. (2012). Stability Analysis of an SEIQV epidemic model with saturated incidence rate. Nonlinear Analysis. Real World Applications,13(2012):2671-2679.

[11] Enatsu, Y., Nakata, Y. and Muroya, Y. (2012). Global stability of SIRS epidemic models with a class of nonlinear incidence rates and distributed delays. Acta Mathematica Scientia. 32(3): 851-865.

[12] Li, J. and Cui, N. (2013). Dynamics Analysis of an SEIR Model with Distinct Incidence for Exposed and infectives. The Scientific World Journal, 2013: Article ID 871393.
[13] Safi, M. A. and Garba, S. M. (2012). Global Stability Analysis of SEIR Model with Holling Type II incidence Function. Computational and Mathematical Method in Medicine, 2012:Article ID 826052.
[14] Zhang, L., Li, Y., Ren, Q. and Huo, Z. (2013). Global dynamics of an SEIRS epidemic model with constant immigration and immunity. WSEAS Trans. Math. 12(5): 630-640.
[15] Liu, W.M., Hethcote, H.W. and Levin, S.A. (1987). Dynamical behavior of epidemiological models with nonlinear incidence rates. J. math. Boil., 25: 359-380.
[16] Liu, W.M., Levin, S.A. and Iwasa, Y. (1986). Influence of nonlinear incidence rates upon the behavior of SIRS epidemiological models. J.math.Biol., 23:187-204.
[17] CDC (2014). Ebola Disease Outbreak – Nigeria, July – September 2014. Morbidity and Mortality Weekly Report (MMWR), October 3, 2014/ 63(39):867-872.
[18] NCDC (2020). First Case of Corona Virus Disease confirmed in Nigeria. https://ncdc.gov.ng/nes/227/first-case-of-corona-virus-disease-confirmed-in-nigeria. Accessed on 14th July, 2021.
[19] Van den Driessche, P and Watmough, J. (2002). Reproduction number and sub-threshold endemic equilibrium for compartmental models of disease of transmission. Math Biosci. 180: 29-48.
[20] Castillo – Chavez, C. and Song, B. (2004). Dynamical models of tuberculosis and their applications. Mathematical Biosciences and Engineering, 1(2): 361-404.
[21] Shaui, Z. and van den Driessche, P. (2013). Global Stability of Infectious Disease Models Using Lyapunov Functions. SIAM J. Appl. Math., 73(4): 1513 – 1532.

Journal of the Nigerian Society for Mathematical Biology
Volume 4 (2021), pp. 19 – 38

Global stability analysis of endemic equilibrium point of mathematical model for the transmission and control of Zika Virus disease dynamics

K. A. Adeyemo*, N. I. Akinwande†, I. A. Azeez† and E. Philemon‡

Abstract

We constructed Goh Volterra type of Lyapunov function from the transformed model of our formulated mathematical model for the transmission and control of zika virus disease dynamics. Applying the La Salle's invariance principle to the time derivative of the constructed Lyapunov function confirms the existence of global asymptotic stability of unique endemic equilibrium point of the model. The model is solved using differential transformation method based on two different levels of controls. The Graphical simulations of some vital solutions of the model equations showed the impact of the various control measures incorporated into the model. Moreover, the sensitivity analysis of the sensitive parameters is carried out using the effective reproduction number of the model equations. Various characteristics of the vital state variables and the sensitive parameters provide forecasting premises for any possible outbreak of zika virus disease for effective control measure or containment. This study provides a suitable guide for the containment or control measure of any possible outbreak of zika virus disease. Therefore, with strict adherence to the various measures incorporated into the model equations, the outbreak of zika virus disease can be controlled whenever the effective reproduction number is reduced to less than unity.

Keywords: Endemic equilibrium point, global asymptotic stability; sensitive parameters; Zika Virus disease.

1 Introduction

Zika virus (ZIKV) is a microscopic infectious agent which is a member of the family called Flaviviridae and the genus called Flavivirus that causes zika virus fever in human and microcephaly (smaller head than normal) to the infants of infected pregnant women as in [3]. Zika virus has similar characteristic with Dengue and Chikungunya described in [16]. About 80% of the infectious individuals are asymptomatic in any outbreak of zika virus disease; and some symptoms of the

* Department of Computer Science and Mathematics, Nigeria Police Academy, Wudil, Nigeria; k.2a.adeyemo@gmail.com
† Department of Mathematics, Federal University of Technology, Minna, Nigeria
‡Department of Family Medicine, University College Hospital, Ibadan, Nigeria

infection are similar to the mild form of Dengue, Chikungunya and that of Malaria fever. The incubation period of zika infection is between three to twelve days. The illness is generally mild with symptoms not lasting more than a week, and it rarely kill. Differential or co –clinical diagnosis with Dengue, Chikungunya and Malaria could be considered for an infected individual. To detect Zika virus, a blood or tissue sample from the first week of infection is subjected to sophisticated molecular testing. The four major routes of transmission of zika virus are: through female Aedes aegypti mosquitoes' bite as in[11], [8], and [13]; through sexual transmission as in [5] and [9] while [10] worked on the effectiveness of condom in preventing sexual transmission of zika infection; Vertical transmission from infected pregnant women to their fetuses as in [22], during pregnancy and effects on childhood development, [17] showed the potential of zika virus transmission through blood transfusion; [19], worked on the risk of microcephaly induced by zika virus, while [23] showed the possible risk factor of zika virus for autism spectrum disorder. The aim of this study is to show that the unique endemic equilibrium point obtained in [3] is shown to be globally asymptotically stable, in order to provide a valid guide for the control of any possible outbreak of zika virus disease. This is achieved by using the Goh Volteral type of Lyapunov function, constructed from our transformed model and then showed that the time derivative of the function is less or equal to zero. Applying La Salle's invariance principle shows that the unique endemic equilibrium point is globally asymptotically stable. Moreover, the Graphical simulations of some solutions of the model equations are obtained and the sensitivity analysis of the sensitive parameters is carried out using the effective reproduction number of the model equations.

2 Model Formulation

As in [3], the population of the study involves humans and mosquitoes respectively. Human population is divided into female population and male population. SEIR framework is adopted for the state variables (Susceptible – Expose – Infected – Removed), while SI (Susceptible – Infectious) framework is used for the state variables of the mosquito population.

2.1 Model Equations

$$\dot{S_1} = \theta_1\omega_1\Lambda_1 - \frac{S_1}{N_1}\{\alpha_1\phi_3 I_3 + \alpha_{21}\phi_{21}I_{21}(1-\in_c \tau_c) + \alpha_{22}\phi_{22}I_{22}(1-\in_c \tau_c)\} - \mu_1 S_1 \qquad (1)$$

$$\dot{E_1} = (1-\theta_1)\omega_1\Lambda_1 + \frac{S_1}{N_1}\{\alpha_1\phi_3 I_3 + \alpha_{21}\phi_{21}I_{21}(1-\in_c \tau_c) + \alpha_{22}\phi_{22}I_{22}(1-\in_c \tau_c)\} - (\gamma_1 + \sigma_{11} + \sigma_{12} + \mu_1)E_1 \qquad (2)$$

$$\dot{I_{11}} = \sigma_{11}E_1 - (\gamma_{11} + \mu_1)I_{11} \qquad (3)$$

$$\dot{I_{12}} = \sigma_{12}E_1 - (\gamma_{12} + \mu_1)I_{12} \qquad (4)$$

$$\dot{R_1} = (1-\omega_1)\Lambda_1 + \gamma_1 E_1 + \gamma_{11}I_{11} + \gamma_{12}I_{12} - \mu_1 R_1 \qquad (5)$$

$$\dot{S_3} = \Lambda_3 - \frac{S_3}{N_3}(\alpha_3^{11}\phi_{11}I_{11} + \alpha_3^{12}\phi_{12}I_{12} + \alpha_3^{21}\phi_{21}I_{21} + \alpha_3^{22}\phi_{22}I_{22}) - (\mu_3 + \delta)S_3 \qquad (6)$$

$$\dot{\mathrm{I}}_3 = \frac{S_3}{N_3}(\alpha_3^{11}\phi_{11}I_{11} + \alpha_3^{12}\phi_{12}I_{12} + \alpha_3^{21}\phi_{21}I_{21} + \alpha_3^{22}\phi_{22}I_{22}) - (\mu_3 + \delta)\mathrm{I}_3 \qquad (7)$$

$$\dot{S}_2 = \theta_2\omega_2\Lambda_2 - \frac{S_2}{N_2}\{\alpha_2\phi_3 I_3 + \alpha_{11}\phi_{11}I_{11}(1-\in_c \tau_c) + \alpha_{12}\phi_{12}I_{12}(1-\in_c \tau_c)\} - \mu_2 S_2 \qquad (8)$$

$$\dot{E}_2 = (1-\theta_2)\omega_2\Lambda_2 + \frac{S_2}{N_2}\{\alpha_2\phi_3 I_3 + \alpha_{11}\phi_{11}I_{11}(1-\in_c \tau_c) + \alpha_{12}\phi_{12}I_{12}(1-\in_c \tau_c)\} - (\gamma_2 + \sigma_{21} + \sigma_{22} + \mu_2)E_2 \qquad (9)$$

$$\dot{I}_{21} = \sigma_{21}E_2 - (\gamma_{21} + \mu_2)I_{21} \qquad (10)$$

$$\dot{I}_{22} = \sigma_{22}E_2 - (\gamma_{22} + \mu_2)I_{22} \qquad (11)$$

$$\dot{R}_2 = (1-\omega_2)\Lambda_2 + \gamma_2 E_2 + \gamma_{21}I_{21} + \gamma_{22}I_{22} - \mu_2 R_2 \qquad (12)$$

2.2 Model Variables and Parameters

The state variables and parameters of the model equations (1) – (12) are defined in Table 1 and Table 2.

Table 1: Description of variables of the model

Variable	Interpretation
S_1, S_2	Susceptible female, male compartment
E_1, E_2	Exposed female, male compartment
I_{11}, I_{21}	Symptomatic female, male compartment
I_{12}, I_{22}	Asymptomatic female, male compartment
R_1, R_2	Removed female, male compartment
S_3, I_3	Mosquitoes without virus, mosquitoes with virus

Table 2: Description of parameters of system (1) – (12)

Parameter	Interpretation
$\Lambda_1, \Lambda_2, \Lambda_3$	Recruitment rate of females, males and mosquitoes
ω_1, ω_2	Proportion of female and male births without microcephaly
$(1-\omega_1), (1-\omega_2)$	Proportion of female and male births with microcephaly
θ_1, θ_2	Proportion of susceptible female and male births without microcephaly
$(1-\theta_1), (1-\theta_2)$	Proportion of exposed female and male births without microcephaly
μ_1, μ_2, μ_3	Natural death rate of females, males and mosquitoes
δ	Death rate of mosquitoes due to insecticides
α_1, α_2	Transmission rate of ZIKV through mosquito bite to the susceptible females and males
$\alpha_{11}, \alpha_{12}, \alpha_{21}, \alpha_{22}$	Transmission rate of ZIKV through sex from symptomatic and asymptomatic female and males to susceptible females and males
ϕ_3	Is measuring the reduction in effectiveness of mosquito activities in transmitting ZIKV by creating non conducive environment for the mosquitoes including the use of air conditioner
$\phi_{11}, \phi_{12}, \phi_{21}, \phi_{22}$	Is measuring the reduction in effectiveness of sexual transmission through adherence to the preventive instructions
$(1-\in_c \tau_c)$	Reflects the impact of condom usage which is enhanced by public campaign (efficacy and compliance) on sexual transmission where $0 < \in_c, \tau_c < 1$
$\alpha_3^{11}, \alpha_3^{12}, \alpha_3^{21}, \alpha_3^{22}$	Transmission rate of ZIKV from symptomatic and asymptomatic females and males to the susceptible mosquitoes
$\sigma_{11}, \sigma_{12}, \sigma_{21}, \sigma_{22}$	Progression rate of ZIKV from exposed females and males to the symptomatic and asymptomatic compartment
γ_1, γ_2	Recovery rate from exposed females and males to the removed

	compartment
$\gamma_{11}, \gamma_{12}, \gamma_{21}, \gamma_{22}$	Recovery rate from symptomatic and asymptomatic females and males to the removed compartment

2.3 The Transformed Model

In order to obtain condition for the global stability, we transformed equations (1) – (12) from standard incidence function to bilinear incidence function and using the substitutes in (26) and (27) to obtain equations (13) – (24).

$$\dot{S}_1 = \theta_1\omega_1\Lambda_1 - S_1(\overline{\beta_1}I_3 + \overline{\beta_2}I_{21} + \overline{\beta_3}I_{22}) - \mu_1 S_1 \quad (13)$$

$$\dot{E}_1 = (1-\theta_1)\omega_1\Lambda_1 + S_1(\overline{\beta_1}I_3 + \overline{\beta_2}I_{21} + \overline{\beta_3}I_{22}) - k_1 E_1 \quad (14)$$

$$\dot{I}_{11} = \sigma_{11}E_1 - k_2 I_{11} \quad (15)$$

$$\dot{I}_{12} = \sigma_{12}E_1 - k_3 I_{12} \quad (16)$$

$$\dot{R}_1 = (1-\omega_1)\Lambda_1 + \gamma_1 E_1 + \gamma_{11}I_{11} + \gamma_{12}I_{12} - \mu_1 R_1 \quad (17)$$

$$\dot{S}_3 = \Lambda_3 - S_3(\overline{\beta_4}I_{11} + \overline{\beta_5}I_{12} + \overline{\beta_6}I_{21} + \overline{\beta_7}I_{22}) - k_4 S_3 \quad (18)$$

$$\dot{I}_3 = S_3(\overline{\beta_4}I_{11} + \overline{\beta_5}I_{12} + \overline{\beta_6}I_{21} + \overline{\beta_7}I_{22}) - k_4 I_3 \quad (19)$$

$$\dot{S}_2 = \theta_2\omega_2\Lambda_2 - S_2(\overline{\beta_8}I_3 + \overline{\beta_9}I_{11} + \overline{\beta_{10}}I_{12}) - \mu_2 S_2 \quad (20)$$

$$\dot{E}_2 = (1-\theta_2)\omega_2\Lambda_2 + S_2(\overline{\beta_8}I_3 + \overline{\beta_9}I_{11} + \overline{\beta_{10}}I_{12}) - k_5 E_2 \quad (21)$$

$$\dot{I}_{21} = \sigma_{21}E_2 - k_6 I_{21} \quad (22)$$

$$\dot{I}_{22} = \sigma_{22}E_2 - k_7 I_{22} \quad (23)$$

$$\dot{R}_2 = (1-\omega_2)\Lambda_2 + \gamma_2 E_2 + \gamma_{21}I_{21} + \gamma_{22}I_{22} - \mu_2 R_2 \quad (24)$$

$$\left.\begin{array}{c} N_1 = S_1 + E_1 + I_{11} + I_{12} + R_1 \\ N_3 = S_3 + I_3 \\ N_2 = S_2 + E_2 + I_{21} + I_{22} + R_2 \end{array}\right] \quad (25)$$

$$\text{where, } \left.\begin{array}{c} \overline{\beta_1} = \frac{\beta_1\mu_1}{\Lambda_1}, \overline{\beta_2} = \frac{\beta_2\mu_1}{\Lambda_1}, \overline{\beta_3} = \frac{\beta_3\mu_1}{\Lambda_1}, \overline{\beta_4} = \frac{\beta_4\mu_3}{\Lambda_3}, \overline{\beta_5} = \frac{\beta_5\mu_3}{\Lambda_3} \\ \overline{\beta_6} = \frac{\beta_6\mu_3}{\Lambda_3}, \overline{\beta_7} = \frac{\beta_7\mu_3}{\Lambda_3}, \overline{\beta_8} = \frac{\beta_8\mu_2}{\Lambda_2}, \overline{\beta_9} = \frac{\beta_9\mu_2}{\Lambda_2}, \overline{\beta_{10}} = \frac{\beta_{10}\mu_2}{\Lambda_2} \end{array}\right] \quad (26)$$

$$\left.\begin{array}{c} \beta_1 = \alpha_1\phi_3, \beta_2 = \alpha_{21}\phi_{21}(1-\epsilon_c\,\tau_c), \beta_3 = \alpha_{22}\phi_{22}(1-\epsilon_c\,\tau_c), \beta_4 = \alpha_3^{11}\phi_{11}, \beta_5 = \alpha_3^{12}\phi_{12}, k_6 = \gamma_{21} + \mu_2 \\ \beta_6 = \alpha_3^{21}\phi_{21}, \beta_7 = \alpha_3^{22}\phi_{22}, \beta_8 = \alpha_2\phi_3, \beta_9 = \alpha_{11}\phi_{11}(1-\epsilon_c\,\tau_c), \beta_{10} = \alpha_{12}\phi_{12}(1-\epsilon_c\,\tau_c), k_7 = \gamma_{22} + \mu_2 \\ k_1 = \gamma_1 + \sigma_{11} + \sigma_{12} + \mu_1, k_2 = \gamma_{11} + \mu_1, k_3 = \gamma_{12} + \mu_1, k_4 = \mu_3 + \delta, k_5 = \gamma_2 + \sigma_{21} + \sigma_{22} + \mu_2 \end{array}\right] \quad (27)$$

3 Global Stability Analysis

A Goh –Volterra type of Lyapunov function is constructed from equations (14) – (24) as in [12] and [18]. Then the constructed Lyapunov function is given by

$$G = \left[\begin{array}{c} \{S_1 - S_1^{**} - S_1^{**}\ln\frac{S_1}{S_1^{**}} + E_1 - E_1^{**} - E_1^{**}\ln\frac{E_1}{E_1^{**}} + A_1(I_{11} - I_{11}^{**} - I_{11}^{**}\ln\frac{I_{11}}{I_{11}^{**}}) + B_1(I_{12} - I_{12}^{**} - I_{12}^{**}\ln\frac{I_{12}}{I_{12}^{**}}) + \\ S_3 - S_3^{**} - S_3^{**}\ln\frac{S_3}{S_3^{**}} + B_3(I_3 - I_3^{**} - I_3^{**}\ln\frac{I_3}{I_3^{**}}) + S_2 - S_2^{**} - S_2^{**}\ln\frac{S_2}{S_2^{**}} + E_2 - E_2^{**} - E_2^{**}\ln\frac{E_2}{E_2^{**}} + \\ A_2(I_{21} - I_{21}^{**} - I_{21}^{**}\ln\frac{I_{21}}{I_{21}^{**}}) + B_2(I_{22} - I_{22}^{**} - I_{22}^{**}\ln\frac{I_{22}}{I_{22}^{**}})\} \end{array}\right]$$

The time derivative of the Lyapunov function, G now becomes

$$\dot{G} = \left[\begin{array}{c} \{(\dot{S}_1 - \frac{S_1^{**}}{S_1}\dot{S}_1) + (\dot{E}_1 - \frac{E_1^{**}}{E_1}\dot{E}_1) + A_1(\dot{I}_{11} - \frac{I_{11}^{**}}{I_{11}}\dot{I}_{11}) + B_1(\dot{I}_{12} - \frac{I_{12}^{**}}{I_{12}}\dot{I}_{12}) + (\dot{S}_3 - \frac{S_3^{**}}{S_3}\dot{S}_3) + B_3(\dot{I}_3 - \frac{I_3^{**}}{I_3}\dot{I}_3) + \\ (\dot{S}_2 - \frac{S_2^{**}}{S_2}\dot{S}_2) + (\dot{E}_2 - \frac{E_2^{**}}{E_2}\dot{E}_2) + A_2(\dot{I}_{21} - \frac{I_{21}^{**}}{I_{21}}\dot{I}_{21}) + B_2(\dot{I}_{22} - \frac{I_{22}^{**}}{I_{22}}\dot{I}_{22})\} \end{array}\right]$$

Substitute equations (13) –(16), (18), (19), (20) –(23) in the time derivative of the Lyapunov function

and simplifying gives

$$\dot{G}=\left[\begin{array}{c}
\{2\mu_1 S_1^{**}-\mu_1 S_1-\frac{S_1^{**^2}}{S_1}(\overline{\beta_1}I_3^{**}+\overline{\beta_2}I_{21}^{**}+\overline{\beta_3}I_{22}^{**})-\mu_1\frac{S_1^{**^2}}{S_1}+2k_1E_1^{**}-k_1\frac{E_1^{**^2}}{E_1}+\frac{E_1^{**}}{E_1}S_1^{**}(\overline{\beta_1}I_3^{**}+\overline{\beta_2}I_{21}^{**}+\overline{\beta_3}I_{22}^{**})- \\
\frac{E_1^{**}}{E_1}S_1(\overline{\beta_1}I_3+\overline{\beta_2}I_{21}+\overline{\beta_3}I_{22})-\frac{I_{11}^{**}}{I_{11}}A_1\sigma_{11}E_1+A_1k_2I_{11}^{**}-\frac{I_{12}^{**}}{I_{12}}B_1\sigma_{12}E_1+B_1k_3I_{12}^{**}+B_4k_4I_3^{**}+2k_4S_3^{**}+ \\
S_3^{**}(\overline{\beta_4}I_{11}^{**}+\overline{\beta_5}I_{12}^{**}+\overline{\beta_6}I_{21}^{**}+\overline{\beta_7}I_{22}^{**})-\frac{S_3^{**^2}}{S_3}(\overline{\beta_4}I_{11}^{**}+\overline{\beta_5}I_{12}^{**}+\overline{\beta_6}I_{21}^{**}+\overline{\beta_7}I_{22}^{**})-\frac{I_3^{**}}{I_3}B_3S_3(\overline{\beta_4}I_{11}+\overline{\beta_5}I_{12}+\overline{\beta_6}I_{21}+\overline{\beta_7}I_{22})+ \\
2\mu_2 S_2^{**}-\mu_2 S_2-\frac{S_2^{**^2}}{S_2}(\overline{\beta_8}I_3^{**}+\overline{\beta_9}I_{11}^{**}+\overline{\beta_{10}}I_{12}^{**})-\mu_2\frac{S_2^{**^2}}{S_2}+2k_5E_2^{**}-k_5\frac{E_2^{**^2}}{E_2}+\frac{E_2^{**}}{E_2}S_2^{**}(\overline{\beta_8}I_3^{**}+\overline{\beta_9}I_{11}^{**}+\overline{\beta_{10}}I_{12}^{**})- \\
\frac{E_2^{**}}{E_2}S_2(\overline{\beta_8}I_3+\overline{\beta_9}I_{11}+\overline{\beta_{10}}I_{12})-\frac{I_{21}^{**}}{I_{21}}A_2\sigma_{21}E_2+A_2k_6I_{21}^{**}-\frac{I_{22}^{**}}{I_{22}}B_2\sigma_{22}E_1+B_2k_7I_{22}^{**}-k_4S_3-k_4\frac{S_3^{**^2}}{S_3}\}
\end{array}\right.$$

Using the following assumptions:
$S_1\le S_1^{**},E_1\le E_1^{**},I_{11}\le I_{11}^{**},I_{12}\le I_{12}^{**},S_2\le S_2^{**},E_2\le E_2^{**},I_{21}\le I_{21}^{**},I_{22}\le I_{22}^{**},S_3\le S_3^{**},k_1,k_5\le 1,$
$\beta_8>\overline{\beta_8}>\overline{\beta_1},\beta_8>\overline{\beta_9},\beta_8>\overline{\beta_{10}},k_1=k_5\ge k_4$ and since the arithmetic mean exceeds the geometric mean, the following inequalities from $\dot{G}$ hold:

$$\mu_1S_1^{**}(2-\frac{S_1}{S_1^{**}}-\frac{S_1^{**}}{S_1})\le 0,\frac{E_1^{**}}{E_1}S_1^{**}(\overline{\beta_1}I_3^{**}+\overline{\beta_2}I_{21}^{**}+\overline{\beta_3}I_{22}^{**})(1-\frac{S_1^{**}}{S_1})\le 0,$$
$$2k_1E_1^{**}[2-\frac{E_1^{**}}{E_1}-\frac{S_1}{E_1k_1}(\overline{\beta_1}I_3^{**}+\overline{\beta_2}I_{21}^{**}+\overline{\beta_3}I_{22}^{**})]<2k_1E_1^{**}[2-\frac{E_1^{**}}{E_1}-\frac{S_1}{E_1k_1}\frac{(I_3^{**}+I_{21}^{**}+I_{22}^{**})}{\theta_2\omega_2}\frac{\theta_2\omega_2\beta_8}{k_4}],$$
$$2k_1E_1^{**}[2-\frac{E_1^{**}}{E_1}-\frac{S_1}{E_1}\frac{(I_3^{**}+I_{21}^{**}+I_{22}^{**})}{\theta_2\omega_2}\frac{\theta_2\omega_2\beta_2}{k_4}]=2k_1E_1^{**}[2-\frac{E_1^{**}}{E_1}-\frac{S_1}{E_1}\frac{(I_3^{**}+I_{21}^{**}+I_{22}^{**})}{\theta_2\omega_2}R_e]<0,$$
$$A_1\sigma_{11}E_1^{**}(1-\frac{I_{11}^{**}E_1}{I_{11}E_1^{**}})\le 0,B_1\sigma_{12}E_1^{**}(1-\frac{I_{12}^{**}E_1}{I_{12}E_1^{**}})\le 0,k_4S_3^{**}(2-\frac{S_3}{S_3^{**}}-\frac{S_3^{**}}{S_3})\le 0,$$
$$A_2\sigma_{21}E_2^{**}(1-\frac{I_{21}^{**}E_2}{I_{21}E_2^{**}})\le 0,B_2\sigma_{22}E_2^{**}(1-\frac{I_{22}^{**}E_2}{I_{22}E_2^{**}})\le 0,\mu_2S_2^{**}(2-\frac{S_2}{S_2^{**}}-\frac{S_2^{**}}{S_2})\le 0,$$
$$(\overline{\beta_1}S_1^{**}+\overline{\beta_8}S_2^{**})I_3^{**}[1-\frac{I_3^{**}(\overline{\beta_4}I_{11}+\overline{\beta_5}I_{12}+\overline{\beta_6}I_{21}+\overline{\beta_7}I_{22})}{I_3(\overline{\beta_4}I_{11}^{**}+\overline{\beta_5}I_{12}^{**}+\overline{\beta_6}I_{21}^{**}+\overline{\beta_7}I_{22}^{**})}]\le 0,S_3^{**}(\overline{\beta_4}I_{11}^{**}+\overline{\beta_5}I_{12}^{**}+\overline{\beta_6}I_{21}^{**}+\overline{\beta_7}I_{22}^{**})(1-\frac{S_3^{**}}{S_3})\le 0,$$
$$\frac{E_2^{**}}{E_2}S_2^{**}(\overline{\beta_8}I_3^{**}+\overline{\beta_9}I_{11}^{**}+\overline{\beta_{10}}I_{12}^{**})(1-\frac{S_2^{**}}{S_2})\le 0,$$
$$2k_5E_2^{**}[2-\frac{E_2^{**}}{E_2}-\frac{S_2}{E_2k_5}(\overline{\beta_8}I_3^{**}+\overline{\beta_9}I_{11}^{**}+\overline{\beta_{10}}I_{12}^{**})]<2k_5E_2^{**}[2-\frac{E_2^{**}}{E_2}-\frac{S_2}{E_2}\frac{(I_3^{**}+I_{11}^{**}+I_{12}^{**})}{\theta_2\omega_2}\frac{\theta_2\omega_2\beta_2}{k_4}],$$
$$2k_5E_2^{**}[2-\frac{E_2^{**}}{E_2}-\frac{S_2}{E_2}\frac{(I_3^{**}+I_{11}^{**}+I_{12}^{**})}{\theta_2\omega_2}\frac{\theta_2\omega_2\beta_2}{k_4}]=2k_5E_2^{**}[2-\frac{E_2^{**}}{E_2}-\frac{S_2}{E_2}\frac{(I_3^{**}+I_{11}^{**}+I_{12}^{**})}{\theta_2\omega_2}R_e]<0.$$

Thus, $\dot{G}\le 0$ for $R_e>1.$ Hence G is a Lyapunov function. It follows by LaSalle's invariance principle that every solution to the equations of the model (13) – (24) at the endemic equilibrium point ε_E is globally asymptotically stable as explained in [14], in the stability of the dynamical system.

4 Model Solution

Differential transformation method is used in solving the differential equations (15), (16), (19), (22) and (23) as used in [21] and [1]. If the model equation $q(t)$ be a function, then it can be expanded in

Taylor series about a point t = 0 as $q(t) = \sum_{k=0}^{\infty} \frac{t^k}{k} \left[\frac{d^k q}{dt^k} \right]_{t=0}$ (28)

$where, q(t) = \{s_1(t), e_1(t), i_{11}(t), i_{12}(t), r_1(t), s_3(t), i_3(t), s_2(t), e_2(t), i_{21}(t), i_{22}(t), r_2(t)\}$

The differential transformation of $q(t)$ is defined as $Q(t) = \frac{1}{k!} \left[\frac{d^k q}{dt^k} \right]_{t=0}$ (29)

$where, Q(t) = \{S_1(t), E_1(t), I_{11}(t), I_{12}(t), R_1(t), S_3(t), I_3(t), S_2(t), E_2(t), I_{21}(t), I_{22}(t), R_2(t)\}$

The inverse differential transform is $q(t) = \sum_{k=0}^{\infty} t^k Q(t)$ (30)

With the non-negative initial condition and parameters, the recurrence relation of the variables in the program (31) is used for the solutions of the model equations

$$\left.\begin{aligned} I_{11_{k+1}} &= \frac{1}{k+1}[\sigma_{11} E_{1_k} - k_2 I_{11_k}] \\ I_{12_{k+1}} &= \frac{1}{k+1}[\sigma_{12} E_{1_k} - k_3 I_{12_k}] \\ I_{3_{k+1}} &= \frac{1}{k+1}\{\sum_{m=0}^{k} S_{3_m}(\overline{\beta_4} I_{11_{k-m}} + \overline{\beta_5} I_{12_{k-m}} + \overline{\beta_6} I_{21_{k-m}} + \overline{\beta_7} I_{22_{k-m}}) - k_4 I_{3_k}\} \\ I_{21_{k+1}} &= \frac{1}{k+1}[\sigma_{21} E_{2_k} - k_6 I_{21_k}] \\ I_{22_{k+1}} &= \frac{1}{k+1}[\sigma_{22} E_{2_k} - k_7 I_{22_k}] \end{aligned}\right\} \quad (31)$$

to obtain the respective values of the vital state variables, when k = 0, k=1, k=2 and k=3. Using the demographic and epidemic data of zika virus disease outbreak of Cape Verde in 2016 as premises

for the initial values for the model solution, subject to two conditions of 99% and 70% level of the effectiveness at which mosquitoes transmit zika virus.

Table 3: Solutions of System when k = 0

Symbol	**Case one value**	**Case two value**
I_{11_1}	1006.4	1006.4
I_{12_1}	1955.0	1955.0
I_{3_1}	-14511.6	-19057.6
I_{21_1}	998.1	998.1
I_{22_1}	1937.1	1937.1

Table 4: Solutions of System when k = 1

Symbol	**Case one value**	**Case two value**
I_{11_2}	-561.5	-564.8
I_{12_2}	-1571.9	-1580.4
I_{3_2}	5709.8	5975.7
I_{21_2}	-558.8	-558.6
I_{22_2}	-1563.3	-1563.0

Table 5: Solutions of System when k = 2

Symbol	Case one value	Case two value
I_{11_3}	165.6	166.8
I_{12_3}	513.8	517.3
I_{3_3}	-2785.1	-2004.5
I_{21_3}	212.0	205.0
I_{22_3}	630.9	613.1

Table 6: Solutions of System when k = 3

Symbol	Case one value	Case two value
I_{11_4}	-48.6	-47.2
I_{12_4}	-147.1	-143.6
I_{3_4}	1074.6	734.9
I_{21_4}	-49.4	-48.6
I_{22_4}	-154.2	-144.2

The following solutions: (32) – (36) for the case one with the condition of 99%, and (37) – (41) for the case two with the condition of 70% when applying the inverse differential transform are obtained

4.1 Model Solution for Case One

$$i_{11}(t) = 761 + 1006.4t - 280.8t^2 + 55.2t^3 - 12.2t^4 \quad (32)$$

$$i_{12}(t) = 3043 + 1955t - 785t^2 + 171.3t^3 - 36.8t^4 \quad (33)$$

$$i_3(t) = 250,000 - 14,511.6t + 2,854.9t^2 - 928.4t^3 + 268.7t^4 \quad (34)$$

$$i_{21}(t) = 755 + 998.1t - 279.4t^2 + 70.7t^3 - 12.4t^4 \quad (35)$$

$$i_{22}(t) = 3021 + 1937.1t - 781.7t^2 + 210.3t^3 - 38.6t^4 \quad (36)$$

4.2 Model Solution for Case Two

$$i_{11}(t) = 761 + 1006.4t - 282.4t^2 + 55.6t^3 - 11.8t^4 \quad (37)$$

$$i_{12}(t) = 3043 + 1,955t - 790.2t^2 + 172.4t^3 - 35.9t^4 \quad (38)$$

$$i_3(t) = 250,000 - 19,057.6t + 2,987.9t^2 - 668.2t^3 + 183.7t^4 \quad (39)$$

$$i_{21}(t) = 755 + 998.1t - 279.3t^2 + 68.3t^3 - 12.2t^4 \quad (40)$$

$$i_{22}(t) = 3021 + 1,937.1t - 781.5t^2 + 204.4t^3 - 36.1t^4 \quad (41)$$

5 Graphical Simulation of the Solutions of the Model Equations

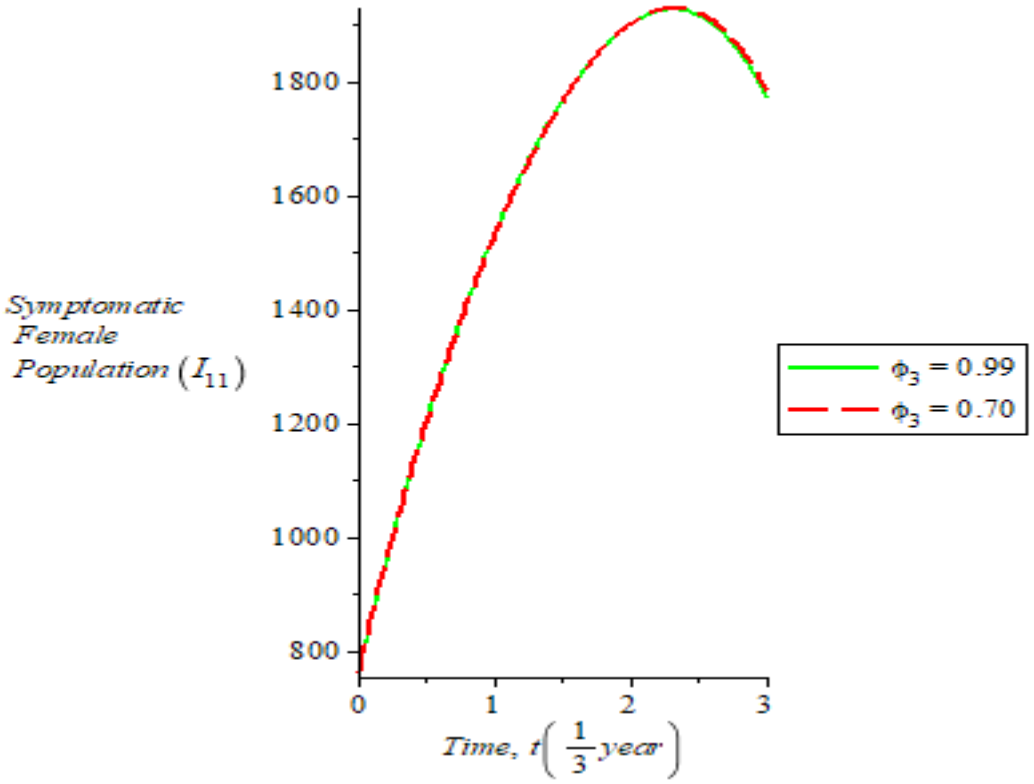

Figure 1: Effect of Reduced Rate in the effectiveness of Mosquito in Transmitting Zika Virus on the Symptomatic Female Population

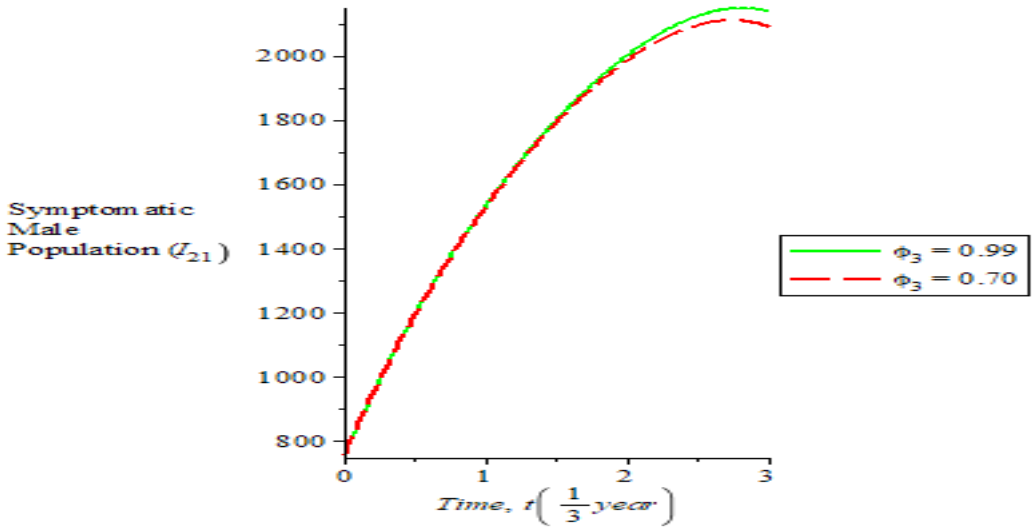

Figure 2: Effect of Reduced Rate in the effectiveness of Mosquito in Transmitting Zika Virus on the Symptomatic Male Population

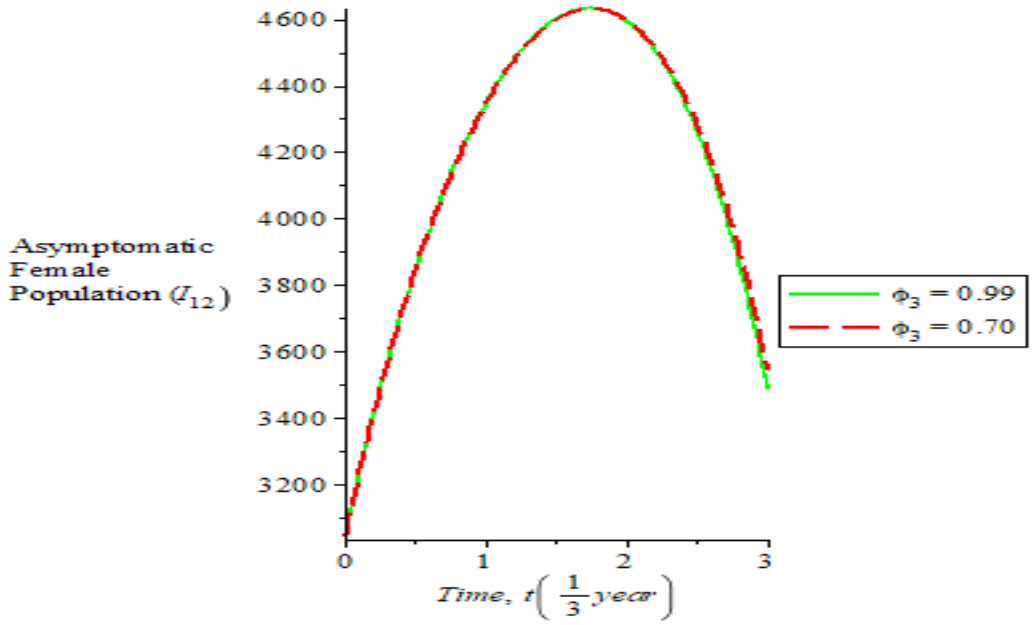

Figure 3: Effect of Reduced Rate in the effectiveness of Mosquito in Transmitting Zika Virus on the Asymptomatic Female Population

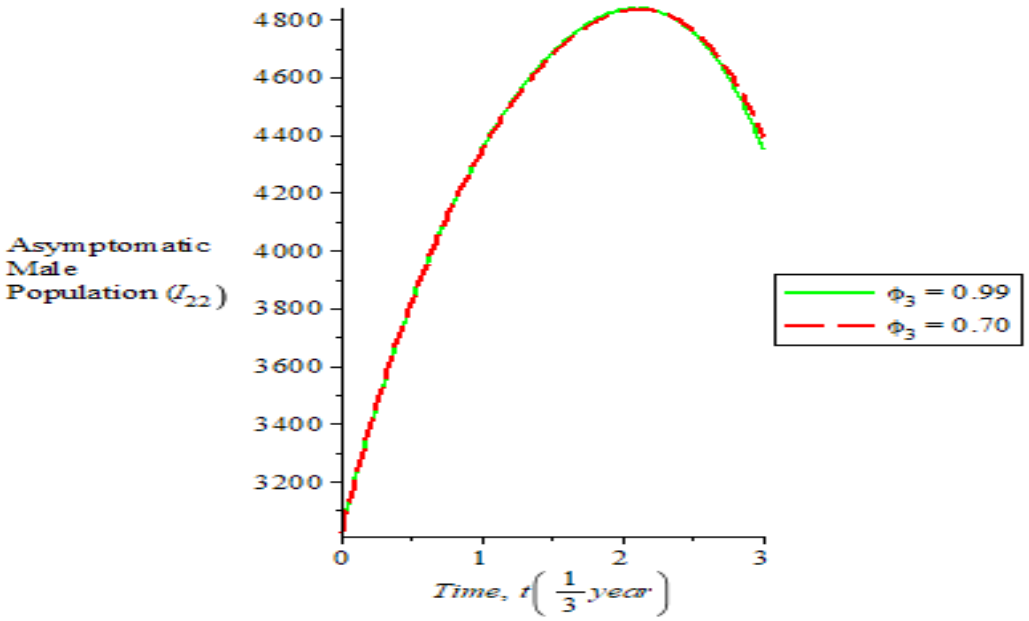

Figure 4: Effect of Reduced Rate in the effectiveness of Mosquito in Transmitting Zika Virus on the Asymptomatic Male Population.

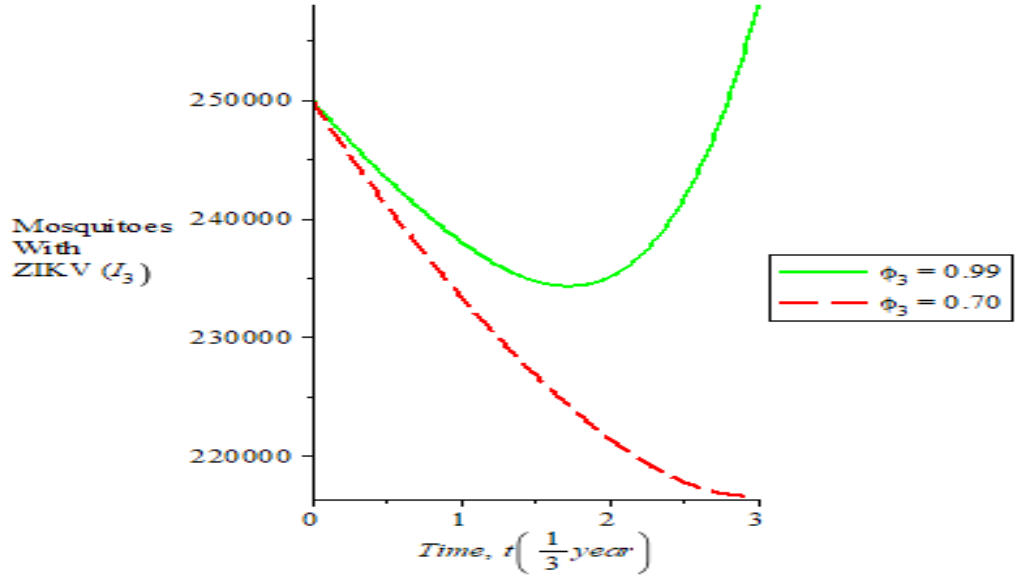

Figure 5: Effect of Reduced Rate in the effectiveness of Mosquitoes in Transmitting Zika Virus on the Population of Mosquitoes with Zika Virus.

6 Sensitivity Analysis of the Effective Reproduction Number

To bring out the importance of the model parameters towards a sound prediction, sensitivity analysis is carried out in a similar approach to the techniques used in [6], [7], [15] and [2]. The sensitivity index of the system is given by $S_{\rho}^{R_0} = \frac{\partial R_0}{\partial \rho} x \frac{\rho}{R_0}$ using the derived effective reproduction number in [3] as given by

$$R_e = \frac{\theta_2 \omega_2 \alpha_2 \phi_3}{\mu_3 + \delta}; \rho = \{\theta_2 = 0.9997, \omega_2 = 0.9982, \alpha_2 = 0.33, \phi_3 = 0.99, \mu_3 = 0.067, \delta = 0.05\} \Rightarrow R_e = 2.78644$$

The sensitive parameters' values are derived from reported cases of zika virus outbreak in Cape (Capo) –Verde in 2016 as in [20] and [24]

Table 7: Sensitivity Indices for the Sensitive Parameters Using the Basic (Effective) Reproduction Number (R_e)

Parameter	Sensitivity index
θ_2	1.000000000
ω_2	1.000000000
ϕ_3	0.9999999999
α_2	0.9999999999
μ_3	-567.1910080
δ	-567.1910080

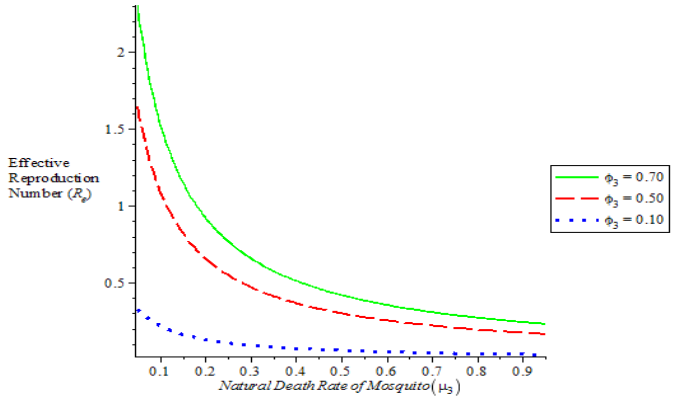

Figure 6: Effect of natural death rate of mosquitoes on the effective reproduction number.

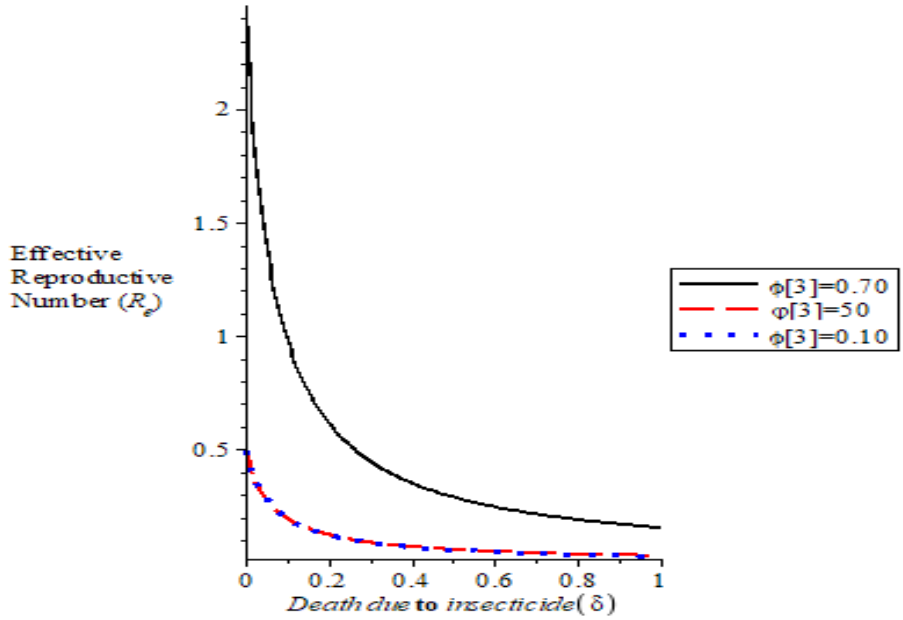

Figure 7: Effect of Death of Mosquitoes due to insecticide on the effective reproduction number

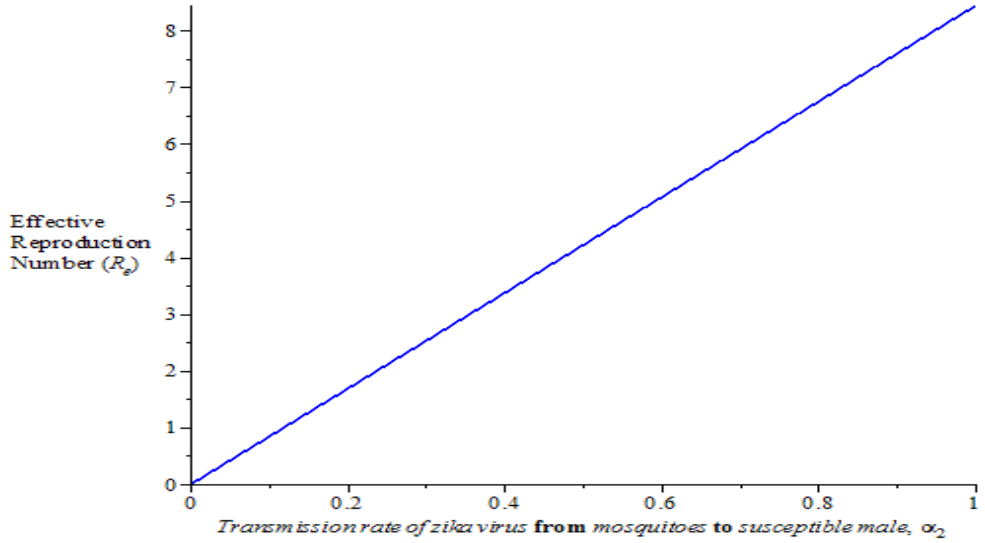

Figure 8: Effect of transmission rate of Zika Virus through mosquito bite on the effective reproduction number

7 Results and Discussion

(i) The time derivative of the constructed Lyapunov function shown to be less than or equal to zero implies that the endemic equilibrium point of the model (13) –(24) is globally asymptotically stable.

(ii) Figures 1 - 4 initially show upward trends as a result of onward progression from the human exposed compartment including females and males, to the infetious compartment (symptomatic and asymptomatic) till peaks of the curves are attained. The direction of the graphs changed from upward to downward because the exposed population is exhausted as a result of reduction in the effectiveness of mosquitoes in transmitting zika virus.

(iii) Figure 5 shows that 70% control of reduction in the effectiveness of mosquitoes in transmitting Zika Virus is more effective in reducing the population of mosquitoes with Zika Virus than 99% control.

(iv) Figures 6 and 7 show that the death of mosquitoes, either natural or through application of insecticides reduces the size of effective reproduction number of the model which implies reduction in the transmission of zika virus. Moreover, if the values of the parameters with negative sensitivity indices increase then the transmission will fall, while increase in the variable with positive sensitivity indices as in Figure 8 will increase the disease but reduction in the variable will make the disease to fall and make the disease to die out if sustained.

8 Conclusion

It is observed that the endemic equilibrium point of the model is globally asymptotically stable when applying LaSalle's invariance principle to the time derivative of Goh Volterral type of Lyapunov function that is shown to be less or equal to zero. The epidemiological implication of the global stability is that the inevitable fate of the outbreak is attained and stabilized irrespective of starting situation. If at the start of the outbreak the number of the infected individual is less than the eventual endemic equilibrium point of the model, then the number of infected individuals will be on the increase until the equilibrium point is attained. On the other hand if the start of the outbreak is higher than the endemic equilibrium point of the model then with strict adherence to the various measures and controls incorporated into the model the size of infections will fall to the equilibrium point of model, which is the inevitable fate of the outbreak. Moreover if the effort is sustained and the effective reproduction number is made to reduce to less than unity, then the outbreak will be brought under control and the disease will die out.

Acknowledgement

The first author wishes to thank the Tetfund through Nigeria Police Academy, Wudil, Kano State, for granting him scholarship and study fellowship during which this research was carried out.

References

[1] Abdel–Halim Hassan, I. H. (2008): Application to differential transformation for solving systems of differential equations. Journal of Applied Mathematical Modeling, 32(12), 2552 – 2559. https://doi.org/10.1016/*j.apm*.2007.09.025

[2] Abdulrahman, S., Akinwande, N. I., Awojoyegbe, O. B and Abubakar, U. Y. (2013) Sensitivity analysis of the parameters of a mathematical model of Hepatitis B virus transmission, Universal Journal of Applied Mathematics, 1(4), 230 – 240.

[3] Adeyemo, K. A., Akinwande, N. I., Abdulrahman, S., and Kuta, F.A. (2018) Formulation of a mathematical model for the transmission and control of zika virus fever dynamics. J. Appl. Sci. Environ. Manage. Vol.22(10) 1363 -1368. DOI:https://dx.doi.org/10.4314/jasem.v22i10.14

[4] Adeyemo, K. A. Akinwande, N.I. and Aye, P. O. (2018) Stability analysis of disease free equilibrium point for transmission and control of zika virus fever dynamics, International Journal of Science Technology, 6(11), 34 -40.

[5] Agusto, F. B., Bewick, S. Fagan, W.F. (2017): Mathematical model for Zika virus dynamics with sexual transmission route. Ecological Complexity, 29:61-81. http://dx.doi.org/10.1016/j.ecocom.2016.12.007

[6] Ariola, I and Hyman, J. (2007): Forward and adjoint sensitivity analysis with applications in Dynamical system, Lecture Notes in Linear Algebra and Optimization.

[7] Chitnis, N., Hyman J. M., and Cushing, J. M. (2008): Determining important parameters in the spread of malaria through the sensitivity analysis of a mathematical model, Bulletin of Mathematical Biology, doi: 10.1007/s11538 – 008 – 9299 – 0.

[8] Funk, S., Kucharski, A. J., Camacho, L. Y. Eggo, A. and Edmunds, W. J. (2016) Comparative analysis of Dengue and Zika outbreaks reveals the differences by setting and virus. PLOS Neglected Tropical Disease, 108(12): e0005173. doi:10.1371/journalpntd.0005173.e0005173.ecollection2016Dec

[9] Gao, D. Lou, Y. He, D. Porce, T. C. Kuang, Y. Chowell, G. Ruan, S. (2016) Prevention and control of Zika a mosquito- borne and sexually transmitted disease: A Mathematical analysis, Scientific Reports, 6:28070. Doi: 10.1038/srep28070.

[10] Holmes, K. K., Levine, R. and Weaver, M. (2004): Effectiveness of condoms in preventing sexually transmitted infections. Bulleting of the World Health Organization, 82, 454 – 461.

[11] Isea, R and Lonngren, K. E. (2016) A preliminary mathematical model for the dynamic transmission of Dengue, Chikungunya and Zika, American Journal of Modern Physics and Application. 3(2): 11-15.

[12] Korobeinikov, A. (2004): Lyapunov functions and global properties for SEIR and SEIS Epidemic models, Mathematics Applied in Medicine and Biology. 1: 1 – 9.

[13] Kucharski, A. J. Funk, S. Eggo, R. M. M. Mallet, H. P. Edmunds, W. J. Nilles E. J. (2016) transmission dynamics of zika virus in island populations: A modeling analysis of the 2013-2014 French Polynesia outbreaks. doi: http//dx.org/10.1101/038588

[14] LaSalle, J. and Lefschetz, S. (1976) The stability of the dynamical system, SIAM, Philadelphia

[15] Mikuchi, M. A. (2012) Sensitivity analysis of the basic reproduction number and other qualities for infectious disease models. An *M.Sc. Thesis*, Colorado state University Fort Collins, Colorado, Spring. 116

[16] Musso, D. Cao - Lormeau, V. M. Gubler. D. J. (2015) Zika virus following the path of Dengue and Chikungunya, The Lancent, 386(9990): 243-244.

[17] Musso, D., Nhan, T., Robin, E. Bierlaire, D. Zisou, K. Shan, Y. A. Cao- Lormeau, V. M. Broult, J. (2014 Potential for Zika virus transmission through blood transfusion demonstrated during an outbreak in French Polynesia November 2013 to February 2014, Eurosurveillance, 19: 20761

[18] Okuonghae, D. and Korobeinikov, A. (2007) Dynamics of tuberculosis: the effect of direct observation therapy strategy (DOTS) in Nigeria. Math. Model of Nat. Phenon., 2(1): 99 – 111.

[19] Pizza, D. M. M. Loaiza, A. M. Montoya, J.F. A. Manrique, O. A. Sossa, V. A. Munoz, C. A. A. Raigosa, S. Contreras, H. M Contreras, I. P. Perea M. E. C and Enriquez, M. A. (2016) A model for the risk of microcephaly induced by the Zika Virus (ZIKV), Open Journal of Modeling and Simulation, 4: 109 - 117. http://dx.doi.org/10.4236/ojmsi.2016.43010.

[20] Rodrigues, F. N. (2018) Epidemiology of Zika Virus Outbreak in the Cabo Verde Islands, West Africa, PLOS Currents, doi: 10.1371/current outbreaks.19433be4d007451c691f138e1e67e8c.

[21] Soltanalizadeh, B (2012). Application of differential transformation method for solving a fourth order parabolic partial differential equations. International Journal of Pure and Applied Mathematics, 78 (3): 299 – 308.

[22] Subissi, L. Dub, T. Besnard, M. Mariteragi –Helle, T. Nhan, T. Lutringer –Magnin, D. and Mallet, H. (2018) Zika virus infection during pregnancy and effects on early childhood development, French Polynesia, 2013 -2016, Emerging Infectious Disease, 24(10), 1850-1858, https://dx.doi.org/10.3201/eid2410.172079

[23] Vianna, P. Gomes, J.D.A. Boquett, J. A Fraga, L.R. Schuch, J.B., Vianna, F.S.L and Schuler –Faccine, L. (2018) Zika virus as a possible risk factor for autism spectrum disorder,

Neuroimmunmodulation, 25(5-6): 320 -327.

[24] World Population Prospects (2018): Cape–Verde population, 2018(Demographics, Maps, Graphs). World populationreview.com/countries/cape –verde –population/ July 11 2019.

Journal of the Nigerian Society for Mathematical Biology
Volume 4 (2021), pp. 39 – 63

Mathematical analysis of Yellow Fever transmission dynamics using Wolbachia and vaccination as control strategies

A.Y. Danjuma[*] and G.C.E. Mbah[†]

Abstract

We present the mathematical analysis of yellow fever transmission dynamics using Wolbachia and vaccination as the control strategies. A deterministic ordinary differential equation model for yellow fever disease transmission dynamics within the human and mosquito populations is formulated. The model equilibrium points were obtained, while the criteria for their macrocosm and stability were investigated. Numerical simulations were carried out using a classical fourth order Runge-kutta method in MATLAB. From the simulations, we investigated and established that the disease can only be eradicated in our society if we encourage the populace to take the vaccines against the disease in the case of the disease insurgence. This is primarily due to the fact that the vaccinated humans do not respond to the infectivity of the Wolbachia-free mosquitoes' biting. Also effective, efficient and timely treatment of infectious persons must be carried out if we must contain the disease when it occurs.

***Keywords*:** booster dose; endemic; Wolbachia; immunity; vaccination; yellow fever; model equation.

1 Introduction

Yellow fever is an acute viral disease that is endemic and enzootic in sub-Saharan Africa and tropical South America, which is marked by three phases of symptoms. These include:" the infectious or acute phase", characterized by fever, chills, loss of appetite, nausea, muscle pains particularly in the back and head ache. These symptoms ameliorate within five days and the "remission phase" set in, this is characterized by the sudden disappearance of the early symptoms. Within 24 hours, the chronic phase set in, which is characterized by the reappearance of the early symptoms along with new and more serious symptoms such as high fever, hemorrhage, abdominal pain and liver impairment begins causing jaundice i.e., yellowing of the skin and eyes which is why this disease is called "yellow fever" [1, 15, 19]. If this occurs, the peril of bleeding and kidney problem is increased [28]. It is caused by a flavivirus (peculiarly yellow fever virus of the genus Flavivirus) transmitted

[*] E-mail: abdulyusufdanjuma@gmail.com
[†] Department of Mathematics, University of Nigeria Nsukka, Nigeria; godwin.mbah@unn.edu.ng

specially by the yellow fever mosquito, and is spread by the bite of an infected female mosquito [11]. It infects only humans, other primates and several types of mosquitoes [21]**.** Particularly in the early stages, this disease may be difficult to differentiate from other illness [31]. For a suspected case to be confirmed, blood sample testing with polymerase chain reaction is needed [11]**.** A safe and effectual vaccine against yellow fever subsist, and some countries demands vaccination for travelers [3, 6, 22]. Other attempts to forestall transmission include reducing the population of the transmitting mosquitoes. In a domain where yellow fever is plebeian, early diagnosis of cases and immunization of large parts of the population are crucial to forestall outbreaks. Up to half of those who got to the severe phase of the disease die within 7-10 days [28].

Yellow fever resulted in about 127,000 serious infection and 450,000 deaths in 2013 [31], with virtually 90 percent of these happening in African nations [11]. In an area of the world where the disease is common, nearly a billion of people lives there. It is plebeian in tropical areas of the continents of south America and Africa but not in Asia [5]. The number of cases of yellow fever has been increasing since the 1980s [13]. This is conceived to be ascribable to fewer people being immuned, more people living in cities, people often moving from one geographical area to another, and changing climate and increasing the mosquitoes home ground. The disease is conceived to have sprung up in Africa and outspread to south America through the slave trade in the 17th century. Several major outbreaks of the disease have occurred in the America, Africa, and Europe since the 17thcentury [14, 20, 24]]. In the 18th and 19th centuries, the yellow fever was seen as one of the lethal, dangerous infections diseases. And the yellow fever virus became the first human virus to be isolated in 1927 [22]. In 1900, Walter Reed established that it was the first sickness shown to be transmissible by filtered human serum and transmitted by mosquitoes [10].

In tropical areas of Africa and the South Americas, Yellow fever virus (YFV) infects human and nonhuman primates, which is transmitted between primate hosts in the saliva of infected mosquitoes. The natural epidemiology of yellow fever on both continents is a cycling of the virus between forest mosquitoes and wild primates. We have **three cycles of secondary transmission to humans,** these are sylvatic (jungle), intermediate (savannah) and urban [16].

Yellow fever is common in tropical and subtropical areas of South America and Africa. Worldwide, about 600million people live in endemic areas. The world Health Organization [WHO] estimates 200,000 cases of disease and 30000 deaths a year occur [26, 27, 29, 30]. An estimated 90% of yellow fever infections occur in African continent [11]. In 2016, a large outbreak originated in Angola and spread to neighboring countries before being contained by a massive vaccination campaign [31, 32].

Yellow fever is distinguished from other viral hemorrhagic fever by the characteristic severity of liver damage and appearance of jaundice (hence flavus; latin for yellow). Moreover, damage to the kidneys frequently leads to extreme albuminuria and acute renal failure. Antibodies can be detected at this stage, while viremia is usually absent. Late central nervous system (CNS) manifestations, such as confusion seizure, and coma, presage death typically follows within seven to ten days of onset [4, 23, 25].

There is no specific treatment for yellow fever infection, only secondary, supportive care exists, i.e., the specialist treatment and support provided by doctors to prevent, control, or relieve complications and side effects and to improve the patients comfort and quality of life) [23]. Secondary care in an intensive care unit is required for complete care. Consequently, supportive care

is critical. Of course, most patients with yellow fever are unable to benefit from state-of-the-heart medical care [17, 18]. Ideally a severe ill patient is admitted to the intensive care unit (ICU) and provided with vaso-active medications, fluid resuscitation, and ventilator support. Symptoms including Dic, hemorrhage, renal and hepatic dysfunction, and possible secondary infection are treated. The use of salicylates is contraindicated in yellow fever cases because of the increased risk of bleeding. Although humans can't spread yellow fever among themselves through casual contact, but the infection could possibly be transmitted directly into the blood through contaminated needles [4]. Viremic patients should be isolated with mosquito netting in areas with potential vectors transmission and until differential diagnoses are eliminated. Although no specific antiviral drugs are available, several compounds with vitro antiviral activity have been described, including ribavirin and interferon-α. However, trials with ribavirin in experimentally infected monkeys have yielded conflicting results [12]. Interferon-γ treatment of monkeys resulted in delayed onset of veremia and illness, but had no effect on survival [2].

2 The Model Equations

Wolbachia is a genus of ***Gram-negative intracellular bacteria*** belonging to the order ***Rickettsiales*** and the family ***Anaplasmataceae,*** which infect invertebrate organisms and are found naturally in more than 50% of all arthropod species and in several nematodes. Nevertheless, wolbachia is naturally absent from Aedes aegypti (stegomyia aegypti), but can be introduced. Wolbachia-infected mosquitoes are not considered to be genetically modified as wolbachia is a naturally occurring symbiont of invertebrates. Moreover, volunteers that are bitten by wolbachia-infected mosquitoes do not show any specific antibody production against wolbachia, which probably means that there is no transmission of the bacteria from mosquitoes to human. As wolbachia is an obligate intracellular bacterium, it cannot survive in the environment (air, soil, water and leaves), but horizontal transmission between arthropods does occur in nature [7]**.**

The principal transmission root of wolbachia is vertically inherited in-virtue-of the cytoplasm of the maternal line, in spite of the fact that, horizontal transmission between insect's species also put up to Wolbachia prevalence [9]**.** Since other mechanisms of transmission are uncommon and may be ignored, then we consider the probability of the vertical transmission as one. The main rationales of using wolbachia for biological control of disease vectors is formulated on cytoplasmic incompatibility (CI), as a result of its infection in the reproductive organs. Mating between an infected male and an uninfected female leads to abnormality in embryonic development with no or limited numbers of viable progenies. In such a transmission cycle, males are the dead-end host of wolbachia and can sterilize the uninfected females.

Mosquitoes with wolbachia have a reduced ability to transmit viruses to people, decreasing the risk of Zika, dengue, Chikungunya and yellow fever outbreaks [4, 8]**.**

Since all the three populations i.e., the human, mosquitoes and wolbachia continuously varies with time, we therefore used a continuous-time model.

2.1 Assumptions of the Model

The following assumptions were made in constructing the model.

i. Death induced by an attempt to suck blood for egg fertilization by both the adult female wolbachia-infected and wolbachia-free mosquitoes is neglected.
ii. The yellow fever virus cannot be transmitted from the wolbachia-infected mosquitoes (I_w) to an adult wolbachia-free mosquitoes (I_m)
iii. Mosquitoes with wolbachia have a reduced ability to transmit viruses to humans.
iv. The non-chronic infectious human, i.e., humans within the 1st and the 2nd phase of infection majorly recovered naturally.
v. Everybody in a given at-risk country cannot be vaccinated
vi. The yellow fever vaccine does not provide an ageless immunity.
vii. The yellow fever disease is not contagious, i.e., cannot be spread from human to human through body contact.
viii. People with weak immune system are considered
ix. Vaccine induced mortality rate is not considered.

Hence, we obtain the Model equations for the transmission dynamics of yellow fever disease using Wolbachia infected mosquitoes as control as follows:

For the wolbachia-free mosquitoes

$$\frac{dS_m}{dt} = \Lambda_m - \alpha S_m - \delta_1 S_m \quad (1)$$

$$\frac{dE_m}{dt} = \alpha S_m - bE_m - \delta_1 E_m \quad (2)$$

$$\frac{dI_m}{dt} = bE_m - \delta_1 I_m \quad (3)$$

For the wolbachia-infected mosquitoes

$$\frac{dS_w}{dt} = \Lambda_W - \beta S_w - \delta_2 S_w \quad (4)$$

$$\frac{dE_w}{dt} = \beta S_w - \xi E_w - \delta_2 E_w \quad (5)$$

$$\frac{dI_w}{dt} = \xi E_w - \delta_2 I_w \quad (6)$$

For human compartment

$$\frac{dS_h}{dt} = \Lambda_h + \theta S_v + \tau R_h - kS_h - \psi S_h - \mu S_h \quad (7)$$

$$\frac{dS_v}{dt} = kS_h - \theta S_v - \lambda_1 S_v - \mu S_v \quad (8)$$

$$\frac{dS_{uv}}{dt} = \psi S_h - \lambda_2 S_{uv} - \mu S_{uv} \quad (9)$$

$$\frac{dE_h}{dt} = \lambda_1 S_v + \lambda_2 S_{uv} - \emptyset E_h - \mu E_h \quad (10)$$

$$\frac{dI_h}{dt} = \emptyset E_h - \rho_1 I_h - \rho_2 I_h - \mu I_h \quad (11)$$

$$\frac{dI_{hN}}{dt} = \rho_1 I_h - \mu I_{hN} - \gamma_1 I_{hN} \quad (12)$$

$$\frac{dI_{hC}}{dt} = \rho_2 I_h - \delta_3 I_{hC} - \mu I_{hC} - \gamma_2 I_{hC} \quad (13)$$

$$\frac{dR_h}{dt} = \gamma_1 I_{hN} + \gamma_2 I_{hC} - \tau R_h - \mu R_h \quad (14)$$

The line of reasoning for the above model is as follows: Wolbachia-infected mothers (S_w) produced the first progeny carrying wolbachia that survived to maturity. Wolbachia-uninfected mothers (S_m) produced the second progenies which are all uninfected. If the female is infected by wolbachia, the possible progenies may be inviable because of cytoplasmic incompatibility (CI).

2.2 Description of the Model Variables and Parameters

Table1: Parameter Description

Parameters	Description
$\boldsymbol{\Lambda_m}$	The basic recruitment level for wolbachia-free mosquitoes.
$\boldsymbol{\Lambda_w}$	The basic recruitment level for wolbachia-infected mosquitoes.
$\boldsymbol{\Lambda_h}$	The basic recruitment level for human
$\boldsymbol{\alpha}$	The rate at which susceptible wolbachia-free mosquitoes are exposed to flavivirus
b	The rate at which an exposed wolbachia-free mosquitoes are infectious
$\boldsymbol{\delta_1}$	Natural death rate of wolbachia-free mosquitoes
$\boldsymbol{\beta}$	The rate at which susceptible wolbachia-infected mosquitoes are exposed to

	flavivirus
ξ	The rate at which an exposed wolbachia-infected mosquitoes are infectious.
δ_2	Natural death rate of wolbachia-infected mosquitoes
K	The rate at which people are vaccinated
ψ	The rate at which people are unvaccinated
λ_1	The force of infection of a susceptible vaccinated human
λ_2	The force of infection of a susceptible unvaccinated human
θ	The rate at which vaccinated humans becomes susceptible.
τ	The rate at which recovered humans become susceptible.
ϕ	The rate at which an exposed humans become infectious.
ρ_1	The rate which an infectious humans progressed to the non-chronic phase of the disease
ρ_2	The rate which an infectious human progressed to the chronic phase of the disease.
γ_1	Natural recovery rate of humans at the non-chronic phase of the disease
γ_2	The recovery rate of humans at the chronic phase of the disease.
μ	The natural death rate of humans
δ_3	Death induced by the disease

Table 2: Variables Description

Variables	Description
S_m	Susceptible class of wolbachia-free mosquitoes
E_m	The class of exposed wolbachia-free mosquitoes
I_m	The class of adult female infectious wolbachia-free mosquitoes
N_m	Total populations of an adult female wolbachia-free mosquitoes, $N_m = S_m + E_m + I_m$
S_w	The susceptible class of an adult wolbachia-infected mosquitoes
E_w	The class of exposed adult wolbachia-infected mosquitoes
I_w	The class of infectious adult wolbachia-infected mosquitoes
N_w	The total populations of an adult wolbachia-infected mosquitoes, $N_w = S_w + E_w + I_w$
S_h	The class of susceptible humans
S_v	The class of vaccinated humans
S_{uv}	The class of unvaccinated humans
E_h	The class of exposed humans to flavivirus
I_h	The class of infectious humans
I_{hN}	The class of infectious humans in the non-chronic phase of the disease
I_{hC}	The class of an infectious humans in the chronic phase of the disease
R_h	The class of humans that recovered from the disease
N_h	The total populations of humans, $N_h = S_h + S_v + S_{uv} + E_h + I_h + I_{hC} + I_{hN} + R_h$

We have that

$$\frac{dN_h}{dt} = \frac{dS_h}{dt} + \frac{dS_v}{dt} + \frac{dS_{uv}}{dt} + \frac{dE_h}{dt} + \frac{dI_h}{dt} + \frac{dI_{hN}}{dt} + \frac{dI_{hC}}{dt} + \frac{dR_h}{dt} \quad (15)$$

$$\frac{dN_m}{dt} = \Lambda_m - \delta_1 N_m \quad (16)$$

$$\frac{dN_w}{dt} = \Lambda_w - \delta_2 N_w \quad (17)$$

3 Analysis of the Model

We investigate the invariant region to determine whether the model is biologically meaningful and that all solutions of our model equations are positive and are attracted in that region.

Lemma 1: The region

Let $\Omega_m = \left(\boldsymbol{S_m, E_m, I_m,}\right)$, $\Omega_w = \left(\boldsymbol{S_w, E_w, I_w}\right)$, $\Omega_h = \left(\boldsymbol{S_h, S_v, S_{uv}, E_h, I_h, I_{hN}, I_{hC}, R_h,}\right)$

So that $\boldsymbol{\Omega} = \Omega_m \times \Omega_w \times \Omega_h$

Then we have:

$\boldsymbol{\Omega} = \left(\boldsymbol{S_m, E_m, I_m, S_w, E_w, I_w, S_h, S_v, S_{uv}, E_h, I_h, I_{hN}, I_{hC}, R_h,}\right) \in \boldsymbol{R_+^{14}}$ to be a relation of the model system with non-negative initial conditions i.e. at t=0, we have:

$$\boldsymbol{S_h > 0, S_v \geq 0, S_{uv} \geq 0, E_h \geq 0, I_h \geq 0, I_{hN} \geq 0, I_{hC} \geq 0, R_h \geq 0,}$$

$$\boldsymbol{S_m \geq 0,\ E_m \geq 0, I_m \geq 0, S_{w,} > 0, E_w \geq 0, I_w \geq 0.}$$

In the absence of the disease (yellow fever) i.e., at disease free equilibrium, we have:

$$\boldsymbol{S_v = 0, S_{uv} = 0, E_h = 0, I_h = 0, I_{hN} = 0, I_{hC} = 0,}$$

then equation (15) becomes:

$$\frac{dN_h}{dt} = \frac{dS_h}{dt}. \quad (*)$$

But from the equation (7) under the human compartment, we now have:

$$\Longrightarrow \frac{dS_h}{dt} = \Lambda_h - \mu S_h\,. \quad (**)$$

This implies that

$$\frac{dN_h}{dt} = \Lambda_h - \mu S_h \Longrightarrow \frac{dN_h}{dt} = \Lambda_h - \mu N_h\,.$$

From the above, we have:

$$\frac{dN_h}{dt} + N_h\,\mu \leq \Lambda_h \qquad (18)$$

Using integrating factor, we solve this to obtain:

$$N_h \leq \frac{\Lambda_h}{\mu} + Ce^{-\mu t}.$$

Using initial conditions: t = 0, $N_h(0) = N_{h\,0}$, this then becomes:

$$N_h \leq \frac{\Lambda_h}{\mu} + \left[N_{h\,0} - \frac{\Lambda_h}{\mu}\right] e^{-\mu t}. \qquad (19)$$

At t = 0, $N_h \leq \frac{\Lambda_h}{\mu} + N_{h\,0} - \frac{\Lambda_h}{\mu} \Longrightarrow N_h \leq N_{h\,0}$

Similarly, at t = ∞, $e^{-\mu t} = 0$ so that $N_h \leq \frac{\Lambda_h}{\mu}$

$$\Longrightarrow 0 \leq N_h \leq \frac{\Lambda_h}{\mu}\ as\ t \to \infty.$$

Therefore, as $t \to \infty$, the human population (N_h) draw close to:

$$K \leq \frac{\Lambda_h}{\mu} \text{ i.e., } N_h \to K = \frac{\Lambda_h}{\mu} \text{ as } t \to \infty.$$

The parameter K is called the carrying capacity. Hence all the viable solution set of the human compartment population model enters the region.

$$\Omega_h = \{(\boldsymbol{S_h, S_v, S_{uv}, E_h, I_h, I_{hN}, I_{hC}, R_h}) \in \mathbf{R_+^8}: \boldsymbol{S_h} > 0, \boldsymbol{S_v} \geq \mathbf{0}, \boldsymbol{S_{uv}} \geq \mathbf{0}, \boldsymbol{E_h} \geq \mathbf{0}, \boldsymbol{I_h} \geq \mathbf{0}, \boldsymbol{I_{hN}} \geq \mathbf{0}, \boldsymbol{I_{hC}} \geq \mathbf{0}, \boldsymbol{R_h} \geq \mathbf{0}\}\, N_h \leq \frac{\Lambda_h}{\mu}$$

Similarly, we can show that the viable solutions for the wolbachia-free and the wolbachia-infected mosquito populations enters the region:

$$\Omega_m = \{(\boldsymbol{S_m, E_m, I_m}) \in \mathbf{R_+^3}: \boldsymbol{S_m} \geq \mathbf{0},\ \boldsymbol{E_m} \geq \mathbf{0}, \boldsymbol{I_m} \geq \mathbf{0}\} N_m \leq \frac{\Lambda_m}{\delta_1}$$

$$\Omega_w = \{(\boldsymbol{S_w, E_w, I_w}) \in \mathbf{R_+^3}: \boldsymbol{S_w} > 0, \boldsymbol{E_w} \geq \mathbf{0}, \boldsymbol{I_w} \geq \mathbf{0}\} N_w \leq \frac{\Lambda_w}{\delta_2}.$$

The solution remains positive for all time t, that is, the domain Ω is positively invariant and the model equation is biologically meaningful and mathematically well posed in the domain. Therefore, meaningful explanation of the disease transmission mechanism can now be carried out.

3.1 Positivity of Solutions

Lemma 3. Let the initial data be:

$$\left\{\boldsymbol{S_m(0), S_w(0), S_h(0),} \begin{pmatrix} \boldsymbol{E_m(0), I_m(0), E_w(0), I_w(0), S_v(0), S_{uv}(0), E_h(0), I_h(0),} \\ \boldsymbol{I_{hN}(0), I_{hC}(0)} \end{pmatrix} \geq \boldsymbol{0}\right\} \in \Omega.$$

Then the solution:

$\{\boldsymbol{S_m, E_m, I_m, S_w, E_w, I_w, S_h, S_v, S_{uv}, E_h, I_h, I_{hN}, I_{hC}, R_h, (t)}\}$ of the system is positive for all t > 0.

Proof:

From the wolbachia-free mosquito compartment, we have:

$$\frac{dS_m}{dt} = \Lambda_m - \alpha S_m - \delta_1 S_m \geq -\alpha S_m - \delta_1 S_m \geq -(\alpha + \delta_1) S_m$$

$$\Longrightarrow \frac{dS_m}{dt} \geq -(\alpha + \delta_1) S_m$$

Using variable separable method, we have:

$\frac{1}{S_m} . \frac{dS_m}{dt} \geq -(\alpha + \delta_1)$ which on integration yields

$S_m \geq A e^{-(\alpha+\delta_1)t}$ where (A=e^{c_1})

At t = 0 $\boldsymbol{S_m(0) = S_{m0}} \geq A \Longrightarrow S_m \geq \boldsymbol{S_{m0}} e^{-(\alpha+\delta_1)t} \geq 0$.

Similarly, we can solve for all the other variables to get:

$S_w \geq \boldsymbol{S_{w0}} e^{-(\beta+\delta_2)t} \geq 0$.

$S_h \geq \boldsymbol{S_{h0}} e^{-(K+\psi+\mu)t} \geq 0$.

Similarly, it can be shown that the human, wolbachia-free and wolbachia-infected mosquito population compartments of the system are all positive for all t > 0

We have thus shown that the model is invariant and has positivity of solutions. As such we can then investigate the existence of the disease equilibrium states and possibly the stability of the disease in the population.

3.2 Equilibrium State

Equilibrium analysis of a given disease model enables us to know whether there could be possible disease free or persistent disease presence (Endemic state) in a given population. There are two types of equilibrium usually studied. These are the **disease-free equilibrium (DFE) and the endemic disease equilibrium (EE).**

3.2.1 Disease Free Equilibrium (DFE)

The disease-free equilibrium is defined as the point at which no disease is present in the population. It enables us to know how the model behaves within a short period of time.

Now we consider the disease classes for the wolbachia-free mosquitoes, wolbachia-infected mosquitoes and the human compartment which can be defined as:

$$E_{m,}I_{m,}E_{w},I_{w},E_{h,}I_{h,}I_{hN,}I_{hC.}$$

The DFE state of equations (1 - 14) is given by:

$$E^{o} = \left(S_{m,}^{0}E_{m,}^{0}I_{m,}^{0}S_{w,}^{0}E_{w,}^{0}I_{w,}^{0}S_{h,}^{0}S_{v,}^{0}S_{uv,}^{0}E_{h,}^{0}I_{h,}^{0}I_{hN,}^{0}I_{hC}^{0}\right).$$

In the absence of the disease or at disease free state, we have:

$\boldsymbol{E_h = I_h = E_m = I_m = E_w = I_w = I_{hN} = I_{hC,} = 0}$, which also implies that:

$\boldsymbol{S_v = S_{uv} = R_h = 0}$.

This is to say that, in the absence of the disease, there won't be need for vaccination, infectious rate is trivial and recovery rate is highly immaterial.

Considering the ***wolbachia-free mosquito's compartment*** and setting the equations to zero, we have:

$$\Lambda_m - \alpha\, S_m^0 - \delta_1 S_m^0 = 0 \qquad \text{(i)}$$

$$\alpha S_m^0 - bE_m^0 - \delta_1 E_m^0 = 0 \qquad \text{(ii)}$$

$$bE_m^0 - \delta_1 I_m^0 = 0 \qquad \text{(iii)}$$

Recall that $E_m = \boldsymbol{I_m = 0}$

Then, from equation (i) we have:

$$\left(S_{m,}^{0}\ E_{m,}^{0}\ \ I_{m,}^{0}\right) = \left(\frac{\Lambda_m}{\alpha+\delta_1}, 0,0\right) \qquad \text{[A]}$$

Similarly we can obtain those of the wolbachia-infected mosquitoes and the humans as::

$$\left(S_{w,}^{0}E_{w,}^{0}I_{w}^{0}\right) = \left(\frac{\Lambda_W}{\beta+\delta_2}, 0,0\right) \qquad \text{[B]}$$

$$\left(S_{h,}^{0}S_{v,}^{0}S_{uv,}^{0}E_{h}^{0}, I_{h}^{0}, I_{hN}^{0}, I_{hC}^{0}, R_{h}^{0}\right) = \left(\frac{\Lambda_h}{\mu}, 0,0,0,0,0,0,0\right) \qquad \text{[C]}$$

From equation A,B,C we have:

$$S^0_{m,} = \frac{\Lambda_m}{\alpha+\delta_1} \quad (20)$$

$$S^0_w = \frac{\Lambda_W}{\beta+\delta_2} \quad (21)$$

$$S^0_h = \frac{\Lambda_h}{\mu} \quad (22)$$

The above **equations (20 - 22)** represents the rate at which there is no infection in the society. Therefore, the disease-free equilibrium state of the model **equation (1- 14)** is given by:

$$E^o = \left(S^0_{m,}E^0_{m,}I^0_{m,}S^0_{w,}E^0_{w,}I^0_w, S^0_{h,}S^0_{v,}S^0_{uv,}E^0_h, I^0_h, I^0_{hN}, I^0_{hC}, R^0_h\right)$$

$$= \left(\frac{\Lambda_m}{\alpha+\delta_1}, 0,0, \frac{\Lambda_W}{\beta+\delta_2}, 0,0, \frac{\Lambda_h}{\mu}, 0,0,0,0,0,0,0\right).$$

3.2.2 Endemic Equilibrium State

From the Wolbachia-free mosquitoes' compartment, we solve for the endemic point(s). However, note that in the endemic case, the derivates on the left-hand side of equations (1 – 14) are still zero but since the disease is endemic, at least some(all) of the disease compartments are non-zero. Thus, we solve the equations to obtain the following:

$$\boldsymbol{S^*_m} = \frac{\boldsymbol{\Lambda_m}}{\boldsymbol{\alpha+\delta_1}} \quad (23)$$

$$\boldsymbol{E^*_m} = \frac{\boldsymbol{\alpha\,\Lambda_m}}{\boldsymbol{\alpha b+\delta_1(b+\alpha+\delta_1)}} \quad (24)$$

$$\boldsymbol{I^*_m} = \frac{\boldsymbol{\alpha b\,\Lambda_m}}{\boldsymbol{\delta_1\left[\alpha b+b\delta_1+\alpha\delta_1+{\delta_1}^2\right]}} \quad (26)$$

$$\boldsymbol{S^*_w} = \frac{\boldsymbol{\Lambda_W}}{\boldsymbol{\beta+\delta_2}} \quad (27)$$

$$\boldsymbol{E^*_w} = \frac{\boldsymbol{\beta S^*_w}}{\boldsymbol{\xi+\delta_2}} \quad (28)$$

$$\boldsymbol{E^*_w} = \frac{\boldsymbol{\beta\Lambda_W}}{\boldsymbol{\xi\beta+\delta_2(\xi+\beta+\delta_2)}} \quad (29)$$

$$\boldsymbol{I^*_w} = \frac{\boldsymbol{\xi\beta\Lambda_W}}{\boldsymbol{\delta_2\left[\xi\beta+\xi\delta_2+{\delta_2}^2\right]}} \quad (30)$$

$$\boldsymbol{S^*_v} = \frac{\boldsymbol{k(\Lambda_h+\tau R^*_h)}}{\boldsymbol{\theta(\psi+\mu)+(\lambda_1+\mu)(k+\psi+\mu)}} \quad (31)$$

$$\boldsymbol{S^*_{uv}} = \frac{\boldsymbol{\psi\left[(\Lambda_h+\tau R^*_h)(\theta(\psi+\mu)+(\lambda_1+\mu)(k+\psi+\mu)+k\theta)\right]}}{(\lambda_2+\mu)(k+\psi+\mu)[\theta(\psi+\mu)+(\lambda_1+\mu)(k+\psi+\mu)]} \quad (32)$$

$$\boldsymbol{E^*_h} = \frac{\boldsymbol{(\Lambda_h+\tau R^*_h)\left[[\lambda_1 k(\lambda_2+\mu)(k+\psi+\mu)]+\lambda_2\psi(k\theta+\theta(\psi+\mu))\right]+\lambda_2\psi[(\lambda_1+\mu)(k+\psi+\mu)]}}{(\theta+\mu)(\lambda_2+\mu)(k+\psi+\mu)[\theta(\psi+\mu)+(\lambda_1+\mu)(k+\psi+\mu)]} \quad (33)$$

$$I_h^* = \frac{\theta(\Lambda_h+\tau R_h^*)\left[[\lambda_1 k(\lambda_2+\mu)(k+\psi+\mu)]+\lambda_2\psi(k\theta+\theta(\psi+\mu))\right]+\lambda_2\psi\theta[(\lambda_1+\mu)(k+\psi+\mu)]}{(\rho_1+\rho_2+\mu)(\theta+\mu)(\lambda_2+\mu)(k+\psi+\mu)[\theta(\psi+\mu)+(\lambda_1+\mu)(k+\psi+\mu)]} \quad (34)$$

$$I_{hN}^* = \frac{\rho_1\theta(\Lambda_h+\tau R_h^*)\left[[\lambda_1 k(\lambda_2+\mu)(k+\psi+\mu)]+\lambda_2\psi(k\theta+\theta(\psi+\mu))\right]+\rho_1\lambda_2\psi\theta[(\lambda_1+\mu)(k+\psi+\mu)]}{(\mu+\gamma_1)(\rho_1+\rho_2+\mu)(\theta+\mu)(\lambda_2+\mu)(k+\psi+\mu)[\theta(\psi+\mu)+(\lambda_1+\mu)(k+\psi+\mu)]} \quad (35)$$

$$I_{hC}^* = \frac{\rho_2\theta(\Lambda_h+\tau R_h^*)\left[[\lambda_1 k(\lambda_2+\mu)(k+\psi+\mu)]+\lambda_2\psi(k\theta+\theta(\psi+\mu))\right]+\lambda_2\psi\theta[(\lambda_1+\mu)(k+\psi+\mu)]}{(\delta_3+\mu+\gamma_2)(\rho_1+\rho_2+\mu)(\theta+\mu)(\lambda_2+\mu)(k+\psi+\mu)[\theta(\psi+\mu)+(\lambda_1+\mu)(k+\psi+\mu)]} \quad (36)$$

$$R_h^* = \frac{(\Lambda_h[\lambda_1 k(\lambda_2+\mu)(k+\psi+\mu)+\lambda_2\psi(k\theta+\theta(\psi+\mu))]+\{(\lambda_2\psi)(\lambda_1+\mu)(k+\psi+\mu)\})\{(\delta_3+\mu+\gamma_2)(\rho_1\gamma_1\theta)+(\mu+\gamma_1)(\rho_2\gamma_2\theta)\}}{\left[(\tau+\mu)(\mu+\gamma_1)(\delta_3+\mu+\gamma_2)(\rho_1+\rho_2+\mu)(\theta+\mu)(\lambda_2+\mu)(k+\psi+\mu)[\theta(\psi+\mu)+(\lambda_1+\mu)(k+\psi+\mu)]\right]} \quad (37)$$
$$.\left[\{\tau(\delta_3+\mu+\gamma_2)(\rho_1\gamma_1\theta)+\tau(\mu+\gamma_1)(\rho_2\gamma_2\theta)\}[\lambda_1 k(\lambda_2+\mu)(k+\psi+\mu)+\lambda_2\psi(k\theta+\theta(\psi+\mu))]\right]$$

$$S_h^* = \frac{\Lambda_h([\theta k+\theta(\psi+\mu)+(\lambda_1+\mu)(k+\psi+\mu)])}{(k+\psi+\mu)[\theta(\psi+\mu)+(\lambda_1+\mu)(k+\psi+\mu)]}+\frac{\tau(\theta k+[\theta(\psi+\mu)+(\lambda_1+\mu)(k+\psi+\mu)])}{(k+\psi+\mu)[\theta(\psi+\mu)+(\lambda_1+\mu)(k+\psi+\mu)]}$$
$$\times\frac{(\Lambda_h[\lambda_1 k(\lambda_2+\mu)(k+\psi+\mu)+\lambda_2\psi(k\theta+\theta(\psi+\mu))]+\{(\lambda_2\psi)(\lambda_1+\mu)(k+\psi+\mu)\})\{(\delta_3+\mu+\gamma_2)(\rho_1\gamma_1\theta)+(\mu+\gamma_1)(\rho_2\gamma_2\theta)\}}{\left[(\tau+\mu)(\mu+\gamma_1)(\delta_3+\mu+\gamma_2)(\rho_1+\rho_2+\mu)(\theta+\mu)(\lambda_2+\mu)(k+\psi+\mu)[\theta(\psi+\mu)+(\lambda_1+\mu)(k+\psi+\mu)]\right]}$$
$$.\left[\{\tau(\delta_3+\mu+\gamma_2)(\rho_1\gamma_1\theta)+\tau(\mu+\gamma_1)(\rho_2\gamma_2\theta)\}[\lambda_1 k(\lambda_2+\mu)(k+\psi+\mu)+\lambda_2\psi(k\theta+\theta(\psi+\mu))]\right] \quad (39)$$

From these computations, we can write the endemic equilibrium state as:

$$E^* = \left(S_m^*, I_m^*, E_{m,}^* I_{m,}^* S_{w,}^* E_{w,}^* I_w^*, S_{h,}^* S_{v,}^* S_{uv,}^* E_h^*, I_h^*, I_{hN}^*, I_{hC}^*, R_h^*\right), \quad (40)$$

with the values of the variables as obtained above.

4 Stability Analyses

Stability analysis is a basic analysis of a dynamical system which is used to study and predict the variability or instability characteristics of the system. It can also be defined as an analysis indicating how a model reacts to perturbation or changes in any of the compartments of the disease population such as the infectious compartments or in the interaction or contact rate of the susceptible and the infectious classes. We shall consider stability at the disease-free equilibrium and endemic equilibrium respectively.

4.1 Local Stability of Disease-Free Equilibrium

The local stability of a disease-free equilibrium enables us to study the short-term dynamics of the disease. The disease-free equilibrium (DFE) is locally asymptotically stable (LAS) if $R_0<1$ and unstable if $R_0>1$". The above theorem simply implies that: if $R_0<1$, then on the average, an infected individual produces less than one new infected individual over the course of its infectious period,

and the infection cannot grow. Conversely, if $\boldsymbol{R_0>1,}$ then each infected individual produces on the average, more than one new infection, and the disease can invade the population.

However, to carry out the analysis this local stability of the disease-free equilibrium, we shall use the Jacobian matrix method. Thus, we obtain from the model equations (1 - 14)) as shown below:

$$J = \begin{bmatrix}
\frac{\partial S'_m}{\partial S_m} & \frac{\partial S'_m}{\partial E_m} & \frac{\partial S'_m}{\partial I_m} & \frac{\partial S'_m}{\partial S_w} & \frac{\partial S'_m}{\partial E_w} & \frac{\partial S'_m}{\partial I_w} & \frac{\partial S'_m}{\partial S_h} & \frac{\partial S'_m}{\partial S_v} & \frac{\partial S'_m}{\partial S_{uv}} & \frac{\partial S'_m}{\partial E_h} & \frac{\partial S'_m}{\partial I_h} & \frac{\partial S'_m}{\partial I_{hN}} & \frac{\partial S'_m}{\partial I_{hC}} & \frac{\partial S'_m}{\partial R_h} \\
\frac{\partial E'_m}{\partial S_m} & \frac{\partial E'_m}{\partial E_m} & \frac{\partial E'_m}{\partial I_m} & \frac{\partial E'_m}{\partial S_w} & \frac{\partial E'_m}{\partial E_w} & \frac{\partial E'_m}{\partial I_w} & \frac{\partial E'_m}{\partial S_h} & \frac{\partial E'_m}{\partial S_v} & \frac{\partial E'_m}{\partial S_{uv}} & \frac{\partial E'_m}{\partial E_h} & \frac{\partial E'_m}{\partial I_h} & \frac{\partial E'_m}{\partial I_{hN}} & \frac{\partial E'_m}{\partial I_{hC}} & \frac{\partial E'_m}{\partial R_h} \\
\frac{\partial I'_m}{\partial S_m} & \frac{\partial I'_m}{\partial E_m} & \frac{\partial I'_m}{\partial I_m} & \frac{\partial I'_m}{\partial S_w} & \frac{\partial I'_m}{\partial E_w} & \frac{\partial I'_m}{\partial I_w} & \frac{\partial I'_m}{\partial S_h} & \frac{\partial I'_m}{\partial S_v} & \frac{\partial I'_m}{\partial S_{uv}} & \frac{\partial I'_m}{\partial E_h} & \frac{\partial I'_m}{\partial I_h} & \frac{\partial I'_m}{\partial I_{hN}} & \frac{\partial I'_m}{\partial I_{hC}} & \frac{\partial I'_m}{\partial R_h} \\
\frac{\partial S'_w}{\partial S_m} & \frac{\partial S'_w}{\partial E_m} & \frac{\partial S'_w}{\partial I_m} & \frac{\partial S'_w}{\partial S_w} & \frac{\partial S'_w}{\partial E_w} & \frac{\partial S'_w}{\partial I_w} & \frac{\partial S'_w}{\partial S_h} & \frac{\partial S'_w}{\partial S_v} & \frac{\partial S'_w}{\partial S_{uv}} & \frac{\partial S'_w}{\partial E_h} & \frac{\partial S'_w}{\partial I_h} & \frac{\partial S'_w}{\partial I_{hN}} & \frac{\partial S'_w}{\partial I_{hC}} & \frac{\partial S'_w}{\partial R_h} \\
\frac{\partial E'_w}{\partial S_m} & \frac{\partial E'_w}{\partial E_m} & \frac{\partial E'_w}{\partial I_m} & \frac{\partial E'_w}{\partial S_w} & \frac{\partial E'_w}{\partial E_w} & \frac{\partial E'_w}{\partial I_w} & \frac{\partial E'_w}{\partial S_h} & \frac{\partial E'_w}{\partial S_v} & \frac{\partial E'_w}{\partial S_{uv}} & \frac{\partial E'_w}{\partial E_h} & \frac{\partial E'_w}{\partial I_h} & \frac{\partial E'_w}{\partial I_{hN}} & \frac{\partial E'_w}{\partial I_{hC}} & \frac{\partial E'_w}{\partial R_h} \\
\frac{\partial I'_w}{\partial S_m} & \frac{\partial I'_w}{\partial E_m} & \frac{\partial I'_w}{\partial I_m} & \frac{\partial I'_w}{\partial S_w} & \frac{\partial I'_w}{\partial E_w} & \frac{\partial I'_w}{\partial I_w} & \frac{\partial I'_w}{\partial S_h} & \frac{\partial I'_w}{\partial S_v} & \frac{\partial I'_w}{\partial S_{uv}} & \frac{\partial I'_w}{\partial E_h} & \frac{\partial I'_w}{\partial I_h} & \frac{\partial I'_w}{\partial I_{hN}} & \frac{\partial I'_w}{\partial I_{hC}} & \frac{\partial I'_w}{\partial R_h} \\
\frac{\partial S'_h}{\partial S_m} & \frac{\partial S'_h}{\partial E_m} & \frac{\partial S'_h}{\partial I_m} & \frac{\partial S'_h}{\partial S_w} & \frac{\partial S'_h}{\partial E_w} & \frac{\partial S'_h}{\partial I_w} & \frac{\partial S'_h}{\partial S_h} & \frac{\partial S'_h}{\partial S_v} & \frac{\partial S'_h}{\partial S_{uv}} & \frac{\partial S'_h}{\partial E_h} & \frac{\partial S'_h}{\partial I_h} & \frac{\partial S'_h}{\partial I_{hN}} & \frac{\partial S'_h}{\partial I_{hC}} & \frac{\partial S'_h}{\partial R_h} \\
\frac{\partial S'_v}{\partial S_m} & \frac{\partial S'_v}{\partial E_m} & \frac{\partial S'_v}{\partial I_m} & \frac{\partial S'_v}{\partial S_w} & \frac{\partial S'_v}{\partial E_w} & \frac{\partial S'_v}{\partial I_w} & \frac{\partial S'_v}{\partial S_h} & \frac{\partial S'_v}{\partial S_v} & \frac{\partial S'_v}{\partial S_{uv}} & \frac{\partial S'_v}{\partial E_h} & \frac{\partial S'_v}{\partial I_h} & \frac{\partial S'_v}{\partial I_{hN}} & \frac{\partial S'_v}{\partial I_{hC}} & \frac{\partial S'_v}{\partial R_h} \\
\frac{\partial S'_{uv}}{\partial S_m} & \frac{\partial S'_{uv}}{\partial E_m} & \frac{\partial S'_{uv}}{\partial I_m} & \frac{\partial S'_{uv}}{\partial S_w} & \frac{\partial S'_{uv}}{\partial E_w} & \frac{\partial S'_{uv}}{\partial I_w} & \frac{\partial S'_{uv}}{\partial S_h} & \frac{\partial S'_{uv}}{\partial S_v} & \frac{\partial S'_{uv}}{\partial S_{uv}} & \frac{\partial S'_{uv}}{\partial E_h} & \frac{\partial S'_{uv}}{\partial I_h} & \frac{\partial S'_{uv}}{\partial I_{hN}} & \frac{\partial S'_{uv}}{\partial I_{hC}} & \frac{\partial S'_{uv}}{\partial S_m} \\
\frac{\partial E'_h}{\partial S_m} & \frac{\partial E'_h}{\partial E_m} & \frac{\partial E'_h}{\partial I_m} & \frac{\partial E'_h}{\partial S_w} & \frac{\partial E'_h}{\partial E_w} & \frac{\partial E'_h}{\partial I_w} & \frac{\partial E'_h}{\partial S_h} & \frac{\partial E'_h}{\partial S_v} & \frac{\partial E'_h}{\partial S_{uv}} & \frac{\partial E'_h}{\partial E_h} & \frac{\partial E'_h}{\partial I_h} & \frac{\partial E'_h}{\partial I_{hN}} & \frac{\partial E'_h}{\partial I_{hC}} & \frac{\partial E'_h}{\partial R_h} \\
\frac{\partial I'_h}{\partial S_m} & \frac{\partial I'_h}{\partial E_m} & \frac{\partial I'_h}{\partial I_m} & \frac{\partial I'_h}{\partial S_w} & \frac{\partial I'_h}{\partial E_w} & \frac{\partial I'_h}{\partial I_w} & \frac{\partial I'_h}{\partial S_h} & \frac{\partial I'_h}{\partial S_v} & \frac{\partial I'_h}{\partial S_{uv}} & \frac{\partial I'_h}{\partial E_h} & \frac{\partial I'_h}{\partial I_h} & \frac{\partial I'_h}{\partial I_{hN}} & \frac{\partial I'_h}{\partial I_{hC}} & \frac{\partial I'_h}{\partial R_h} \\
\frac{\partial I'_{hN}}{\partial S_m} & \frac{\partial I'_{hN}}{\partial E_m} & \frac{\partial I'_{hN}}{\partial I_m} & \frac{\partial I'_{hN}}{\partial S_w} & \frac{\partial I'_{hN}}{\partial E_w} & \frac{\partial I'_{hN}}{\partial I_w} & \frac{\partial I'_{hN}}{\partial S_h} & \frac{\partial I'_{hN}}{\partial S_v} & \frac{\partial I'_{hN}}{\partial S_{uv}} & \frac{\partial I'_{hN}}{\partial E_h} & \frac{\partial I'_{hN}}{\partial I_h} & \frac{\partial I'_{hN}}{\partial I_{hN}} & \frac{\partial I'_{hN}}{\partial I_{hC}} & \frac{\partial I'_{hN}}{\partial R_h} \\
\frac{\partial I'_{hC}}{\partial S_m} & \frac{\partial I'_{hC}}{\partial E_m} & \frac{\partial I'_{hC}}{\partial I_m} & \frac{\partial I'_{hC}}{\partial S_w} & \frac{\partial I'_{hC}}{\partial E_w} & \frac{\partial I'_{hC}}{\partial I_w} & \frac{\partial I'_{hC}}{\partial S_h} & \frac{\partial I'_{hC}}{\partial S_v} & \frac{\partial I'_{hC}}{\partial S_{uv}} & \frac{\partial I'_{hC}}{\partial E_h} & \frac{\partial I'_{hC}}{\partial I_h} & \frac{\partial I'_{hC}}{\partial I_{hN}} & \frac{\partial I'_{hC}}{\partial I_{hC}} & \frac{\partial I'_{hC}}{\partial R_h} \\
\frac{\partial R'_h}{\partial S_m} & \frac{\partial R'_h}{\partial E_m} & \frac{\partial R'_h}{\partial I_m} & \frac{\partial R'_h}{\partial S_w} & \frac{\partial R'_h}{\partial E_w} & \frac{\partial R'_h}{\partial I_w} & \frac{\partial R'_h}{\partial S_h} & \frac{\partial R'_h}{\partial S_v} & \frac{\partial R'_h}{\partial S_{uv}} & \frac{\partial R'_h}{\partial E_h} & \frac{\partial R'_h}{\partial I_h} & \frac{\partial R'_h}{\partial I_{hN}} & \frac{\partial R'_h}{\partial I_{hC}} & \frac{\partial R'_h}{\partial R_h}
\end{bmatrix}$$

$$J^0 = \begin{bmatrix} -\delta_1 & 0 & 0 & 0 & 0 & 0 & 0 & 0 & 0 & 0 & 0 & 0 & 0 & 0 \\ 0 & -(b+\delta_1) & 0 & 0 & 0 & 0 & 0 & 0 & 0 & 0 & 0 & 0 & 0 & 0 \\ 0 & b & -\delta_1 & 0 & 0 & 0 & 0 & 0 & 0 & 0 & 0 & 0 & 0 & 0 \\ 0 & 0 & 0 & -\delta_2 & 0 & 0 & 0 & 0 & 0 & 0 & 0 & 0 & 0 & 0 \\ 0 & 0 & 0 & 0 & -(\xi+\delta_2) & 0 & 0 & 0 & 0 & 0 & 0 & 0 & 0 & 0 \\ 0 & 0 & 0 & 0 & \xi & -\delta_2 & 0 & 0 & 0 & 0 & 0 & 0 & 0 & 0 \\ 0 & 0 & 0 & 0 & 0 & 0 & -(k+\psi+\mu) & \theta & 0 & 0 & 0 & 0 & 0 & \tau \\ 0 & 0 & 0 & 0 & 0 & 0 & k & -(\theta+\mu) & 0 & 0 & 0 & 0 & 0 & 0 \\ 0 & 0 & 0 & 0 & 0 & 0 & \psi & 0 & -\mu & 0 & 0 & 0 & 0 & 0 \\ 0 & 0 & 0 & 0 & 0 & 0 & 0 & 0 & 0 & -(\theta+\mu) & 0 & 0 & 0 & 0 \\ 0 & 0 & 0 & 0 & 0 & 0 & 0 & 0 & 0 & \theta & -(\rho_1+\rho_2+\mu\ ) & 0 & 0 & 0 \\ 0 & 0 & 0 & 0 & 0 & 0 & 0 & 0 & 0 & 0 & \rho_1 & -(\gamma_1+\mu) & 0 & 0 \\ 0 & 0 & 0 & 0 & 0 & 0 & 0 & 0 & 0 & 0 & \rho_2 & 0 & -(\delta_3+\mu+\gamma_2\ ) & 0 \\ 0 & 0 & 0 & 0 & 0 & 0 & 0 & 0 & 0 & 0 & 0 & \gamma_1 & \gamma_2 & -(\tau+\mu) \end{bmatrix}$$

From the above, we have $|J^0 - \lambda I|$=0, and using rows and column transformation, the above matrix is reduced to obtain the following eigen values:

$$\lambda_1 = \lambda_2 = -\delta_1, \lambda_3 = -(b+\delta_1), \lambda_4 = \lambda_5 = -\delta_2, \lambda_6 = -(\xi+\delta_2), \lambda_7 = -\mu.$$

After the reduction of the matrix, MAPLE is further used to obtain the remaining eigenvalues as shown below:

$\lambda_8 = -(\theta+\mu)$, $\lambda_9 = -(\rho_1+\rho_2+\mu\ )$, $\lambda_{10} = -(\gamma_1+\mu)$, $\lambda_{11} = -(\delta_3+\mu+\gamma_2\ )$, $\lambda_{11} = -(\tau+\mu)$, $\lambda_{12} = -(\tau+\mu)$,

$$\lambda_{13} = -\left(\frac{\theta}{2} + \mu - \frac{k}{2} + \frac{\psi}{2} - \sqrt{(k^2 + 2k\psi + 2k\theta - 2\psi\theta + \theta^2)}\right),$$

$$\lambda_{14} = -\left(\frac{\theta}{2} + \mu - \frac{k}{2} + \frac{\psi}{2} + \sqrt{(k^2 + 2k\psi + 2k\theta - 2\psi\theta + \theta^2)}\right).$$

Since all the eigen values are negative, we conclude that the disease-free equilibrium (DFE) is locally stable.

4.2 Local Stability of Endemic Equilibrium (EEP)

The local stability of an endemic equilibrium enables us to study the long-term dynamics of the disease.

To analyse the local stability of the endemic equilibrium, we consider the Jacobian matrix of the model equations (1- 14) above, we use the Jacobian matrix method to obtain:

$$J^* = \begin{bmatrix} -(\alpha+\delta_1) & 0 & 0 & 0 & 0 & 0 & 0 & 0 & 0 & 0 & 0 & 0 & 0 & 0 \\ \alpha & -(b+\delta_1) & 0 & 0 & 0 & 0 & 0 & 0 & 0 & 0 & 0 & 0 & 0 & 0 \\ 0 & b & -\delta_1 & 0 & 0 & 0 & 0 & 0 & 0 & 0 & 0 & 0 & 0 & 0 \\ 0 & 0 & 0 & -(\beta+\delta_2) & 0 & 0 & 0 & 0 & 0 & 0 & 0 & 0 & 0 & 0 \\ 0 & 0 & 0 & \beta & -(\xi+\delta_2) & 0 & 0 & 0 & 0 & 0 & 0 & 0 & 0 & 0 \\ 0 & 0 & 0 & 0 & \xi & -\delta_2 & 0 & 0 & 0 & 0 & 0 & 0 & 0 & 0 \\ 0 & 0 & 0 & 0 & 0 & 0 & -(k+\psi+\mu) & \theta & 0 & 0 & 0 & 0 & 0 & \tau \\ 0 & 0 & 0 & 0 & 0 & 0 & k & -(\theta+\lambda_1+\mu) & 0 & 0 & 0 & 0 & 0 & 0 \\ 0 & 0 & 0 & 0 & 0 & 0 & \psi & 0 & -(\lambda_2+\mu) & 0 & 0 & 0 & 0 & 0 \\ 0 & 0 & 0 & 0 & 0 & 0 & 0 & \lambda_1 & \lambda_2 & -(\theta+\mu) & 0 & 0 & 0 & 0 \\ 0 & 0 & 0 & 0 & 0 & 0 & 0 & 0 & 0 & \theta & -(\rho_1+\rho_2+\mu\ ) & 0 & 0 & 0 \\ 0 & 0 & 0 & 0 & 0 & 0 & 0 & 0 & 0 & 0 & \rho_1 & -(\gamma_1+\mu) & 0 & 0 \\ 0 & 0 & 0 & 0 & 0 & 0 & 0 & 0 & 0 & 0 & \rho_2 & 0 & -(\delta_3+\mu+\gamma_2\ ) & 0 \\ 0 & 0 & 0 & 0 & 0 & 0 & 0 & 0 & 0 & 0 & 0 & \gamma_1 & \gamma_2 & -(\tau+\mu) \end{bmatrix}$$

and by row and column transformation, we have the following eigenvalues thereby reducing the matrix to 8 by 8 matrix as shown below:

$$\lambda_1 = -(\alpha+\delta_1), \lambda_2 = -(b+\delta_1), \lambda_3 = -\delta_1, \lambda_4 = -\delta_2, \lambda_5 = -(\xi+\delta_2), \lambda_6 = -(\beta+\delta_2)$$

$$\begin{bmatrix} -(k+\psi+\mu) & \theta & 0 & 0 & 0 & 0 & 0 & \tau \\ k & -(\theta+\lambda_1+\mu) & 0 & 0 & 0 & 0 & 0 & 0 \\ \psi & 0 & -(\lambda_2+\mu) & 0 & 0 & 0 & 0 & 0 \\ 0 & \lambda_1 & \lambda_2 & -(\theta+\mu) & 0 & 0 & 0 & 0 \\ 0 & 0 & 0 & \theta & -(\rho_1+\rho_2+\mu\ ) & 0 & 0 & 0 \\ 0 & 0 & 0 & 0 & \rho_1 & -(\gamma_1+\mu) & 0 & 0 \\ 0 & 0 & 0 & 0 & \rho_2 & 0 & -(\delta_3+\mu+\gamma_2\ ) & 0 \\ 0 & 0 & 0 & 0 & 0 & \gamma_1 & \gamma_2 & -(\tau+\mu) \end{bmatrix}$$

Simplifying the above matrix using MAPLE, the following eigenvalues were obtained:

$\lambda_7 = -(\rho_1+\rho_2+\mu\ ), \lambda_8 = -(\lambda_2+\mu), \lambda_9 = -(\delta_3+\mu+\gamma_2\ ), \lambda_{10} = -(\theta+\mu), \lambda_{11} = -(\gamma_1+\mu),$
$\lambda_{12} = -(\tau+\mu)$,

$$\lambda_{13} = -\frac{k}{2} - \mu - \frac{\psi}{2} - \frac{\theta}{2} - \frac{\lambda_1}{2} + \frac{1}{2}\sqrt{\left(k^2 + 2k\psi + 2k\theta - 2k\lambda_1 + \psi^2 - 2\psi\theta - 2\psi\lambda_1 + \theta^2 + 2\theta\lambda_1 + {\lambda_1}^2\right)}$$

$$= -\left[\frac{k}{2} + \mu + \frac{\psi}{2} + \frac{\theta}{2} + \frac{\lambda_1}{2} - \frac{1}{2}\sqrt{\left(k^2 + 2k\psi + 2k\theta - 2k\lambda_1 + \psi^2 - 2\psi\theta - 2\psi\lambda_1 + \theta^2 + 2\theta\lambda_1 + {\lambda_1}^2\right)}\right],$$

$$\lambda_{14} = -\frac{k}{2} - \mu - \frac{\psi}{2} - \frac{\theta}{2} - \frac{\lambda_1}{2} - \frac{1}{2}\sqrt{\left(k^2 + 2k\psi + 2k\theta - 2k\lambda_1 + \psi^2 - 2\psi\theta - 2\psi\lambda_1 + \theta^2 + 2\theta\lambda_1 + {\lambda_1}^2\right)}$$

$$= -\left[\frac{k}{2} + \mu + \frac{\psi}{2} + \frac{\theta}{2} + \frac{\lambda_1}{2} + \frac{1}{2}\sqrt{\left(k^2 + 2k\psi + 2k\theta - 2k\lambda_1 + \psi^2 - 2\psi\theta - 2\psi\lambda_1 + \theta^2 + 2\theta\lambda_1 + {\lambda_1}^2\right)}\right].$$

If all the eigenvalues are negative, we conclude that the endemic equilibrium is locally stable and unstable if otherwise.

5 Simulation of the Model Equations

A numerical simulation of the model equations is conducted using Runge-kutta method of order 4 in MATLAB and MAPPLE software in other to find out the dynamics of the disease in both human, wolbachia-free and wolbachia-infected mosquitoes' populations.

The initial conditions for the three populations are:
$\boldsymbol{S_{h(0)}}$ =4200,$\boldsymbol{S_{v(0)}}$ =3200, $\boldsymbol{S_{uv(0)}}$ =2000, $\boldsymbol{E_{h(0)}}$ =1000, $\boldsymbol{I_{h(0)}}$ =1070, $\boldsymbol{I_{hN(0)}}$ =1200, $\boldsymbol{I_{hC(0)}}$ =450, $\boldsymbol{S_{m(0)}}$ =300, $\boldsymbol{E_{m(0)}}$ =5000, $\boldsymbol{I_{m(0)}}$ =4000, $\boldsymbol{S_{w(0)}}$ =600, $\boldsymbol{E_{w(0)}}$ =4000, $\boldsymbol{I_{w(0)}}$ =3000, $\boldsymbol{R_{h(0)}}$ =300.

Table3: Parameter values for model

Parameter	Description	Base Value	Source
$\boldsymbol{\Lambda_m}$	The basic recruitment level for wolbachia-free mosquitoes.	3000	Assumed
$\boldsymbol{\Lambda_w}$	The basic recruitment level for wolbachia-infected mosquitoes.	1500	Assumed

Λ_h	The basic recruitment level for human	2000	Assumed
α	The rate at which susceptible wolbachi-free mosquitoes are exposed to flavivirus	0.02	[8]
b	The rate at which an exposed wolbachia-free mosquitoes are infectious	0.1000	[8]
δ_1	Natural death rate of wolbachia-free mosquitoes	0.061	[15]
β	The rate at which susceptible wolbachia-infected mosquitoes are exposed to flavivirus	0.004	Assumed
ξ	The rate at which an exposed wolbachia-infected mosquitoes are infectious.	0.51	
δ_2	Natural death rate of wolbachia-infected mosquitoes	0.068	[24]
k	The rate at which people are vaccinated	0.01	[32]
ψ	The rate at which people are unvaccinated	0.99	[32]
λ_1	The force of infection of a susceptible vaccinated humans	0.05	[27]
λ_2	The force of infection of a susceptible unvaccinated human	0.2	Assumed
θ	The rate at which vaccinated humans becomes susceptible.	0.005	Assumed
τ	The rate at which recovered humans become susceptible.	0.89	Assumed
ϕ	The rate at which an exposed humans become infectious.	0.31	[27]
ρ_1	The rate at which infectious humans progress to the non-chronic phase of the disease	0.85	[27]
ρ_2	The rate at which infectious humans progress to	0.25	[27]

	the chronic phase of the disease.		
γ_1	Natural recovery rate of humans at the non-chronic phase of the disease	0.9	Assumed
γ_2	The recovery rate of humans at the chronic phase of the disease.	0.143	[21]
μ	The natural death rate of humans	0.000035	[21]
δ_3	Death induced by the disease	0.068	[21]
u_1	The rate of contact between an infectious wolbachia-free mosquitos and vaccinated human	0.05	Assumed
u_2	The rate of contact between an infectious wolbachia-free mosquitos and unvaccinated human	0.04	Assumed
v_1	The rate of contact of an infectious wolbachia-infected mosquitoes and vaccinated human	0.003	Assumed
v_2	The rate of contact of an infectious wolbachia-infected mosquitoes and unvaccinated human	0.002	Assumed
m_1	The rate of contact of a non chronic infectious human and a susceptible wolbachia-free mosquitoes	0.00025	Assumed
m_2	The rate of contact of a chronic infectious human and a susceptible wolbachia-free mosquitoes	0.00031	Assumed
n_1	The rate of contact of a non chronic infectious human and a susceptible wolbachia-infected mosquitoes	0.000011	Assumed
n_2	The rate of contact of a chronic infectious human and a susceptible wolbachia-infected mosquitoes	0.00021	Assumed

Here, the effect of interaction between human, Wolbachia-free and Wolbachia-infected mosquitoes were investigated. Since interaction occurs on a faster timescale, the dynamics of an outbreak can be affected. Thus, we present the following graphical results:

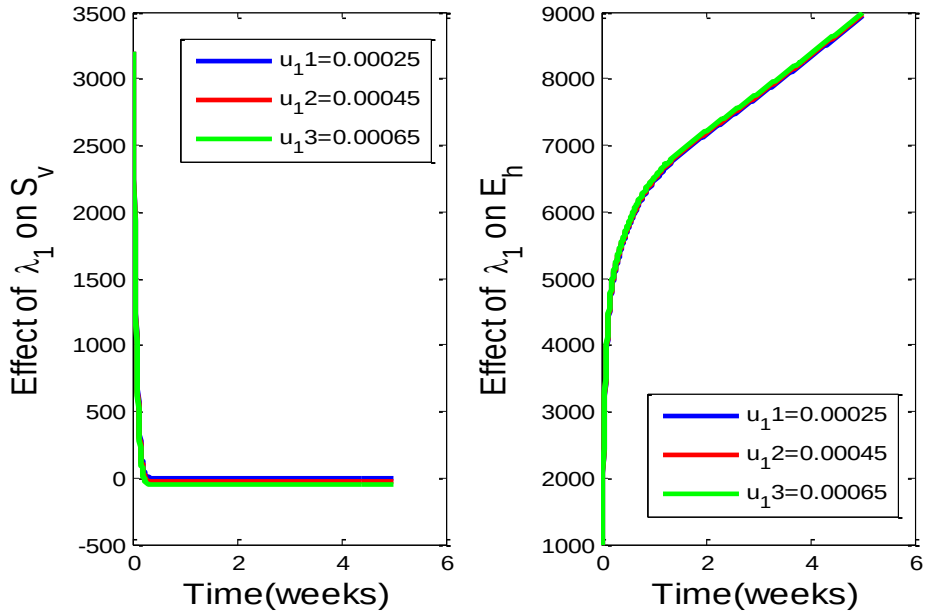

Figure 1.

Figure 1 above shows that, the increasing biting rate of the wolbachia-free infectious mosquitoes on vaccinated human, does not in any way change the trend of the infection in the population since the susceptible is pretected against the disase. We can equally see that the population of the exposed persons does not change irrespective of the level of contact of the Wolbachia-free mosquito with susceptible human population. This now confirm the fact in our assumption of this model that **"the population of the vaccinated humans only decreases as the average daily biting rate of the mosquito increases if the vaccination effect wanes with time in the susceptible.**

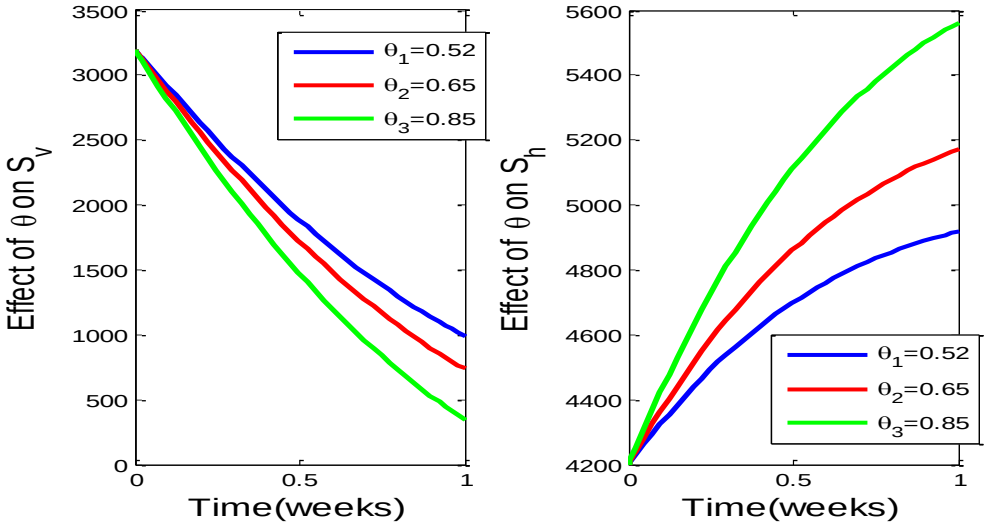

Figure 2.

From Figure 2, we can see that as more vaccinated persons loose their immunity, the population of vaccinated compartment reduces while the population of the exposed class increases. What this shows is that as we loose immunity due to the wanning of the vaccine, people become more exposed to the disease because they are no longer protwcted. This is the reason for asking persons even though vaccinated, to be careful about exposing oneself to yellow fever by carefully avoided any interactions with yellow-fever infectious individuals.

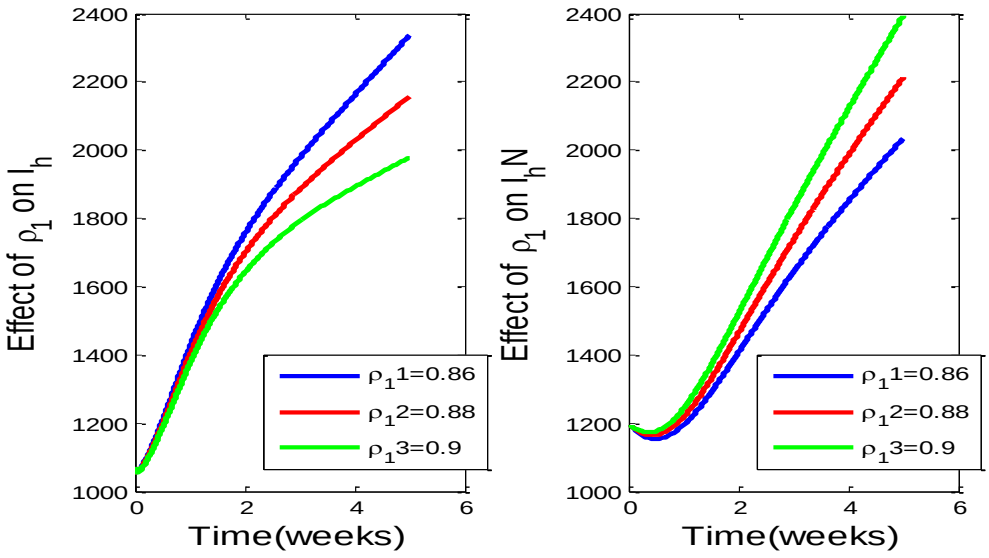

Figure 3.

Figure 3 above clearly shows that if there is increment in the rate at which infectious persons move to the remission stage, that is the non-chronic stage, then the population of the infectious compartment reduces while that of the non-chronic compartment increases. A look at the second graph shows that the population decreased first before increasing. Practically, this explains that it takes more time for infectious individual to remain in the non-chronic stage than for the non-chronic persons to remain in the non-chronic stage. This implies that the domicility time in this stage is transient, that is very small, and so people must have moved more to the chronic stage before the mass movement from the infectious class dominates the movement from the non-chronic stage or compartment and so the cause of the increment in the population of the non-chronic compartment.

6 Conclusion

This work is basically centered on a mathematical model consisting of three compartmental populations i.e. the human population, wolbachia-free mosquitoes and wolbachia-infected mosquito populations. The dynamical system was studied using a classical fourth order Runge-Kutta method in MATLAB for the ordinary differential equation model,. We investigated the stability analysis of both disease free and endemic equilibrium states and found that its locally and asymptotically stable. Numerical simulations were presented for various values of parameters which aid us in sensitivity analysis. From these analyses we found that in other to completely eradicate yellow fever disease, there is need for vaccination against the disease. Futhermore, we needed to ensure that the rate at which people move from infectious class to the non-chronic stage must be effectively controlled if the yellow fever disease has to be eradicated. This means that appropriate and early detection and treatment of yellow fever disease must be handled appropriately, timely and efficiently .

References

[1] Amer, A. and Mehlhorn, H. (2006). Effects of various essential oils against Aedes, Anopheles, and Culex larvae (Diptera, Culicidae). Parasitol. Res., 99: 66-472.

[2] Arroyo, J.I., Apperson, S.A. and Cropp, C.B. (1988). Effect of human gamma interferon on Yellow fever virus infection. Am J Trop Med Hyg.., 38(3):647-50.

[3] Bryan, C.S., Moses, S.W. and Kahn, R.J. (2004). Yellow fever in the Americas. Infect Dis clin North Am., 18(2):275-292.

[4] Carol, D. (2019). Transmission of yellow fever. Retrieved from https://www.webmd.com/a-to-z-guides/qa/how-does-yellow-fever- spread#.

[5] Chambers, T.J., Weir, R.C. and Grakoui, A. (1990). Evidence that the N-terminal domain of nonstructural protein NS3 from yellow fever virus is a serine protease responsible for site-specific cleavages in the viral polyprotein. Proc Natl Acad Sci USA, 87(22):8898-902.

[6] Chambers, T.J., Mccourt, D.W. and Rice, C.M. (1990). Production of yellow fever virus

proteins in infected cells: identification of discrete polyprotein species and analysis of cleavage kinectics using region-specific polyclonal antiseral. Virology, 177(1):159-74.

[7] Chang, G.J., Cropp, C.B., Kinney, R.M., Trent, D.W. and Gubbler, D.J.(1995). Neuclotide sequence variation of the envelope protein gene identifies two distinct genotypes of yellow fever virus, Virol J., 69(9):5773-80.

[8] Chitins, N., Cushing, J.M. and Hyman, J.M. (2006). Bifurcation analysis of a mathematical model of malaria transmission, SIAM (Appl. Maths.), 67(1): 24-45.

[9] Digouette, JP., Cornet, M., Deubel, V. and Downs, W.G. (1995). Yellow fever in Porterfield JS, Exotic Viral Infections. London: pp 67-102.

[10] Ellis, B.R. and Barrette AD. (2008). The enigma of yellow fever in east Africa, Rev. Med. Virol., 18(5):331-346.

[11] Gould, E.A. and Solomon, T. (2008). Pathogenic flavivirus. Lancet, 371(9611):500-9.

[12] Huggings, J.W., Hsiang, C.M. and Cosgriff, T.M. (1991). Prospective, double-blind, concurrent, placebo-controlled clinical trial of intravenous ribavirin therapy of hemorrhagic fever with renal syndrome. J. Infect. Dis., 164(6):1119-27.

[13] John, M. (1814). Mitchell account of the yellow fever in Virginia in 1741-2, [Archived 2017-02-23] at the wayback machine, the Philadelphia Medical Museum, 1 (1):1-20

[14] Liu, N. (2015). Insecticide resistance in mosquitoes impact, mechanisms, and research Directions, Annu. Rev. Entomol., 60,537-559.

[15] McMeniman, C.J., Lane, R.V., Cass, B.N., Fong, A.W.C., Seidu, M., Wang, Y.F. and O'Neil, S.L. (2009). Stable introduction of a life-shortening wolbachia infection into the mosquito aedes agytpi. Science, 323(5910): 141-144.

[16] Monath, T.P. (1999). Facing up to re-emergence of urban yellow fever, Lancet, 353:1541.

[17] Monath, T.P. (1987). Yellow fever: a medically neglected disease. Report on a seminar. Rev. Infect. Dis., 9(1):165-75.

[18] Monath, T.P. (2008). Treatment of yellow fever. Antiviral Res., 78(1):116-24.

[19] Mutebi, J.P. and Barrette, A.D. (2002). The epidemiology of Yellow fever in Africa, Microbes Infect., 4(14):1459-1468.

[20] Netochukwu, O., Onah, S.I. and Mbah, G.C.E. (2018). A mathematical model on the biological control of malaria transmission using Wolbachia, International Journal of Scientific and Engineering Research, 9(9):

[21] Raimundo, S.M., Amaku, M. and Massad, E.(2015) Equilibrium analysis of Yellow fever dynamical model with vaccination. Comput. Math. Methods. Med., 482019.

[22] Sfakianos, J. and Hecht, A. (2009). Babcock Hillary (ed). West Nile Virus: Deadly disease and epidemics. New York: Chelsea House, p.17

[23] Thomas, M.Y. (2020). Yellow fever. Retrieved from https://www.msdmanuals.com/professional/infectious

[24] Walker, T.J.P., Johnson, P.H., Moreira, L.A., Inaki, I.O., Frentiu, F.D., McMeniman, C.J., Leong, Y.S., Dong, Y., Jasson, A. and Kriesner, P. (2011) The wmel wolbachia strain blocks dengue and invade caged aegypti populations, Nature, 476:450.

[25] Wikipedia. Retrieved from https://en.wikipedia.org/wiki/Yellow fever.

[26] Woodall, JP. And Yuill, T.M. (2016). Why is the yellow fever outbreak in Angola a threat to the entire world.

[27] World Health Organization. WHO Global Advisory committee on vaccine safty(2005).Weekly Epidemial. Record, 80(1):3-7.

[28] World Health Organization. WHO factsheet on Yellow fever; 2013. [Retrieved February,2014], https://www.who.int/en/news-room/factsheets/detail/yellow fever.

[29] World Health Organization. (2017). Yellow fever-China. [Retrieved 9 February,2017]. Available:https://www.who.int/en/news-room/factsheets/detail/yellow fever-china.
[30] World Health Organization. WHO factsheet on Yellow fever; 2018. [Retrieved May, 2018]. Available:https://www.who.int/en/news-room/factsheets/detail/yellowfever.
[31] World Health Organization. WHO factsheet on Yellow fever, 2019. [Retrieved May, 2019]. Available:https://www.who.int/en/news-room/factsheets/detail/yellow fever.
[32] Zhao, S., Stone, L., Gao, D. and Daihai, H. (2018). Modeling the large scale yellow fever outbreak in Luanda, Angola and the impart of vaccination. PLOS. Negl. Trop. Dis., doi.org/10.1371/journal.pntd.0006158.

Journal of the Nigerian Society for Mathematical Biology
Volume 4 (2021), pp. 64 – 75

Sensitivity analysis of the parameters of a co-infection model of Malaria and Dengue Fever disease

T.J. Oluwafemi[*†‡], N.I. Akinwande[*], R.O. Olayiwola[*] and D. Bako[*]

Abstract

In the paper, we present a mathematical model of malaria and dengue fever co-infection. We state the Disease Free and Endemic Equilibrium of the model equations. We compute the reproduction number using the next generation matrix method. Sensitivity analysis of the reproduction number was carried out. Our results shows that the disease vectors death rate is the most sensitivity parameters which further imply that eliminating or reducing the disease vector is the most effective control measure in controlling the transmission of malaria-dengue co-infection.

***Keywords*:** Malaria; Dengue Fever; co-infection; sensitivity analysis

1 Introduction

Malaria and Dengue Fever (DF) are common vector-borne diseases that pose major public health challenges [1, 2].

Malaria is vector-borne disease caused by protozoan parasites belonging to Plasmodium species. The parasites are transmitted through the bites of an infected female Anopheles mosquitoes [3, 4, 5]. According to the 2018 World Malaria Report, 219 million cases of malaria occurred globally in 2017 resulting into 435, 000 death. African region having the highest cases of 92%, South-East Asia 5% and Eastern Mediterranean 2%. Nigeria, Democratic Republic of Congo (DRC), Mozambique, India and Uganda are the countries with almost half of the malaria reported cases globally. Nigeria, DRC, Burkina Faso, United Republic of Tanzania, Sierra Leone, Niger and India has more than half of malaria recorded death.

Dengue Fever (DF) is a viral infection transmitted by the bites of an infected Aedes aegypti mosquitoes. It is prevalent in subtropical and tropical regions. The disease is threatening about 40% of the world's population [6, 7]. Over 3 billion people are at risk of been infected with Dengue fever

[*]Department of Mathematics, Federal University of Technology, Minna
[†]General Studies Department, Newgate College of Health Technology, Minna
[‡]E-mail: dayofemi985@gmail.com

annually in over 125 endemic countries, and it is estimated to cause the death of about 10,000 people annually. Factors that account for the global transmission of dengue includes rapid population growth, increased international travel, and development of the agricultural sector, unplanned urbanization and global climate change. Ineffective mosquito control and inadequate health facilities also contribute to the global transmission [8, 9].

Dengue Fever and Malaria co-infection is rising in the tropics causing high morbidity and mortality globally [10]. The co-infection of Dengue Fever and Malaria is possible in an area where dengue and malaria vectors co-exist. The co-infection was first reported in 2005. Dengue Fever and Malaria co-infection exhibit clinical features of both dengue and malaria mono-infection resulting in misdiagnosis. Dengue and Malaria co-infection has been reported in 44 locations spread across 20 countries. The co-infection varies ranging between 0.1 – 23 % from south Asia, 0.01 – 9% from Africa, 0.5 – 2.5 % from South East Asia and 1 – 3 % from South America [11]. The high rate of the mobility of today's population and increased activities associated with movement of goods and services from one location to another is likely to increase the incidences of dengue and malaria co-infection [12].

Sensitivity Analysis is used to determine how a model response to changes in the value of the parameters of the model. Sensitivity Analysis is extremely important for mathematical models. It studies the variation of a model caused by variations in the inputs [13]. Atokolo and Omale [13] investigated the sensitivity analysis of typhoid fever transmission, the result shows that increase in enlightenment, campaign will lead to reduction in prevalence. Sirajo *et al.* (14) carried out a sensitivity analysis of parameters of Hepatitis B Model, the result revealed that vaccination, condom use and reduced-average sexual partner can reduce and control the spread of Hepatitis B. Marsudi *et al.* [15] studied the sensitivity analysis of the parameters of HIV/AIDS model with condom campaign and Antiretroviral Therapy (ARV).

In this study, analyze the parameters of the co-infection model of malaria-dengue fever to determine which is most sensitive.

2 Model Formulation

In this model, the total human population at time t denoted by N_h is divided into eight sub-classes which are susceptible humans (S_h), individuals exposed to malaria only (E_{hm}), individuals infected with malaria only (I_{hm}), individuals exposed to dengue fever only (E_{hd}), individuals infected with only dengue fever (I_{hd}), individuals exposed to malaria and dengue fever co-infection (E_{md}), individuals infected with malaria and dengue fever co-infection (I_{md}), individuals that recovered from malaria and dengue fever (R_h). The vector population includes the Malaria Parasite non-carrier vectors (S_m), Malaria parasite carrier vectors (I_m), Dengue virus non-carrier vectors (S_d) and Dengue fever carrier vectors (I_d).

2.1 Model Assumptions

The following Assumptions are made in formulating the model:

1. Recruitment into the population is into the susceptible class only
2. The recovered class includes those who recover from malaria only, dengue only and co-infection of both
3. Those who recover from malaria can be re-infected with malaria or dengue
4. Both the Exposed and Infected classes are involved in the transmission of the diseases.

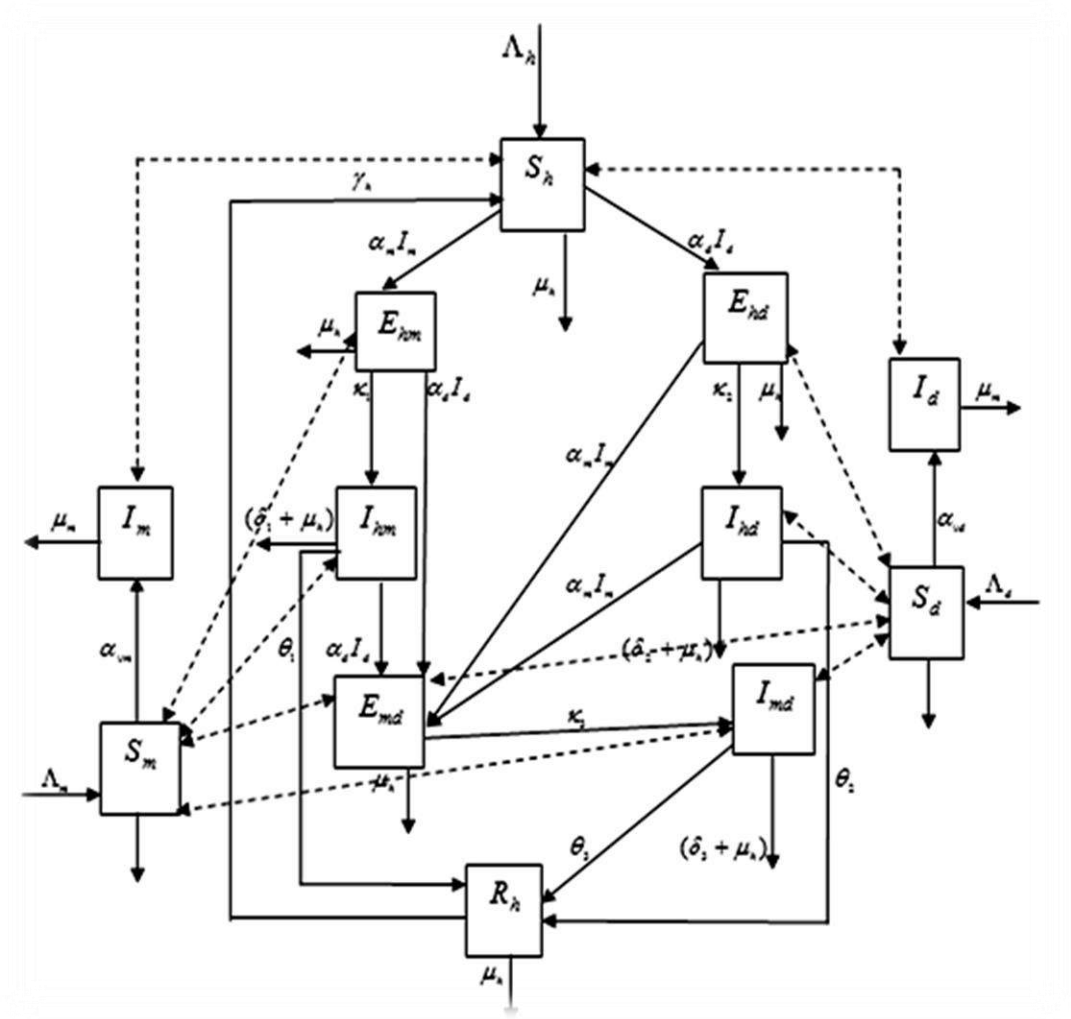

Figure 2.1: Schematic Diagram of the Model

Based on the assumptions, the equations governing the co-infection dynamics is given as,

$$\frac{dS_h}{dt} = \Lambda_h + \gamma_h R_{hm} - (\alpha_d I_d + \alpha_m I_m) S_h - \mu_h S_h$$

$$\frac{dE_{hm}}{dt} = \alpha_m I_m S_h - (\alpha_d I_d + \kappa_1 + \mu_h) E_{hm}$$

$$\frac{dI_{hm}}{dt} = \kappa_1 E_{hm} - (\alpha_d I_d + \delta_1 + \theta_1 + \mu_h) I_{hm}$$

$$\frac{dE_{hd}}{dt} = \alpha_d I_d S_h - (\alpha_m I_m + \kappa_2 + \mu_h) E_{hd}$$

$$\frac{dI_{hd}}{dt} = \kappa_2 E_{hd} - (\alpha_m I_m + \delta_2 + \theta_2 + \mu_h) I_{hd}$$

$$\frac{dE_{md}}{dt} = \alpha_d I_d E_{hm} + \alpha_d I_d I_{hm} + \alpha_m I_m E_{hd} + \alpha_m I_m I_{hd} - (\kappa_3 + \mu_h) E_{md}$$

$$\frac{dI_{md}}{dt} = \kappa_3 E_{md} - (\delta_3 + \theta_3 + \mu_h) I_{md}$$

$$\frac{dR_{hm}}{dt} = \theta_1 I_{hm} + \theta_2 I_{hd} + \theta_3 I_{md} - (\gamma_h + \mu_h) R_{hm}$$

$$\frac{dS_m}{dt} = \Lambda_m - \alpha_{vm}(E_{hm} + I_{hm} + E_{md} + I_{md}) S_m - \mu_m S_m$$

$$\frac{dI_m}{dt} = \alpha_{vm}(E_{hm} + I_{hm} + E_{md} + I_{md}) S_m - \mu_m I_m$$

$$\frac{dS_d}{dt} = \Lambda_d - \alpha_{vd}(E_{hd} + I_{hd} + E_{md} + I_{md}) S_d - \mu_d S_d$$

$$\frac{dI_d}{dt} = \alpha_{vd}(E_{hd} + I_{hd} + E_{md} + I_{md}) S_d - \mu_d I_d$$

Table 1: Model Variables

Symbols	Description
S_h	Susceptible Humans
E_{hm}	Exposed Humans with Malaria
I_{hm}	Humans infected with Malaria only
E_{hd}	Exposed Humans with Dengue Fever
I_{hd}	Humans infected with Dengue Fever only
E_{md}	Exposed Humans jointly infected with Malaria and Dengue Fever
I_{md}	Humans jointly infected with Malaria and Dengue Fever
R_h	Humans Recovered from Malaria and Dengue Fever
S_m	Malaria Parasite carrier vectors
I_m	Malaria Parasite non-carrier vectors
S_d	Dengue virus non-carrier vectors
I_d	Dengue virus carrier vectors

Table 2: Model Parameters

Symbols	Description
Λ_h	Recruitment rate of Human Population
Λ_m	Recruitment rate of Malaria Parasite Vectors
Λ_d	Recruitment rate of Dengue Virus Vectors
θ_1	Recovery rate for Humans infected with Malaria only
θ_2	Recovery rate for Human infected with Dengue only
θ_3	Recovery rate for Human jointly infected with Malaria and Dengue
γ_h	Rate at which recovered becomes susceptible
κ_1	Rate at which E_{hm} becomes I_{hm}
κ_2	Rate at which E_{hd} becomes I_{hd}
κ_3	Rate at which E_{md} becomes I_{md}
α_m	Transmission rate from Human to Malaria Parasite Vectors
α_d	Transmission rate from Human to Dengue Virus Carrier Vectors
α_{vm}	Probability for Malaria Parasite Vectors to be infected
α_{vd}	Probability for Dengue Virus Vectors to be infected
δ_1	Malaria Induced Death

δ_2	Dengue Induced Death
δ_3	Co-infection Induced Death
μ_h	Natural death rate for Humans
μ_m	Natural death rate of Malaria Parasite Vectors
μ_d	Natural death rate of Dengue Virus Vectors

3 Model Analysis

3.1 Model Equilibria Points

The Disease-Free Equilibrium (DFE) of the co-infection Model is given by

$$\varepsilon_0 = \left(S_h^0, E_{hm}^0, I_{hm}^0, E_{hd}^0, I_{hd}^0, E_{md}^0, I_{md}^0, R_{hm}^0, S_m^0, I_m^0, S_d^0, I_d^0\right)$$
$$= \left(\frac{\Lambda_h}{\mu_h}, 0,0,0,0,0,0,0, \frac{\Lambda_m}{\mu_m}, 0, \frac{\Lambda_d}{\mu_d}, 0\right)$$

while the Endemic Equilibrium point (EEP) is given by

$$\varepsilon_E = \left(S_h^*, E_{hm}^*, I_{hm}^*, E_{hd}^*, I_{hd}^*, E_{md}^*, I_{md}^*, R_{hm}^*, , S_m^*, I_m^*, S_d^*, I_d^*\right) =$$
$$\left(\begin{array}{c}
\frac{Q_6}{Q_4+Q_5}, \frac{\alpha_m I_m Q_6}{(\alpha_d I_d+\eta_1)(Q_4+Q_5)}, \frac{\kappa_1 \alpha_m I_m Q_6}{(\alpha_d I_d+z_1)(\alpha_d I_d+\eta_1)(Q_4+Q_5)}, \\
\frac{\alpha_d I_d Q_6}{(\alpha_m I_m+\eta_2)(Q_4+Q_5)}, \frac{\kappa_2 \alpha_d I_d Q_6}{(\alpha_m I_m+z_2)(\alpha_m I_m+\eta_2)(Q_4+Q_5)}, \\
\frac{\alpha_d I_d \alpha_m I_m Q_3 Q_6}{\eta_3(Q_4+Q_5)}, \frac{\alpha_d I_d \alpha_m I_m \kappa_3 Q_3 Q_6}{z_3 \eta_3(Q_4+Q_5)}, \frac{\Lambda_h Q_7}{(Q_4+Q_5)}, \\
\frac{\Lambda_m(\alpha_d I_d+\eta_1)(Q_4+Q_5)}{\alpha_{vm}\alpha_m I_m Q_1 Q_6+\mu_m(\alpha_d I_d+\eta_1)(Q_4+Q_5)}, \\
\frac{\Lambda_m \alpha_{vm}\alpha_m I_m Q_1 Q_6}{\mu_m(\alpha_{vm}\alpha_m I_m Q_1 Q_6+\mu_m(\alpha_d I_d+\eta_1)(Q_4+Q_5))}, \\
\frac{\Lambda_d(\alpha_m I_m+\eta_2)(Q_4+Q_5)}{\alpha_{vd}\alpha_d I_d Q_2 Q_6+\mu_d(\alpha_m I_m+\eta_2)(Q_4+Q_5)}, \\
\frac{\Lambda_d \alpha_{vd}\alpha_d I_d Q_2 Q_6}{\mu_d(\alpha_{vd}\alpha_d I_d Q_2 Q_6+\mu_d(\alpha_m I_m+\eta_2)(Q_4+Q_5))}
\end{array}\right)$$

where

$$Q_1 = \left(\left(1+\frac{\kappa_1}{(\alpha_d I_d + z_1)}\right) + \frac{\alpha_d I_d}{\eta_3}\left(\frac{(\alpha_d I_d+\rho_1)(\alpha_m I_m+z_2)(\alpha_m I_m+\eta_2) + (\alpha_m I_m+\rho_2)(\alpha_d I_d+z_1)(\alpha_d I_d+\eta_1)}{(\alpha_d I_d+z_1)(\alpha_d I_d+\eta_1)(\alpha_m I_m+z_2)(\alpha_m I_m+\eta_2)} \right)\left(1+\frac{\kappa_3}{z_3}\right) \right)$$

$$Q_2 = \left(\left(1+\frac{\kappa_2}{(\alpha_m I_m + z_2)}\right) + \frac{\alpha_m I_m}{\eta_3}\left(\frac{(\alpha_d I_d+\rho_1)(\alpha_m I_m+z_2)(\alpha_m I_m+\eta_2) + (\alpha_m I_m+\rho_2)(\alpha_d I_d+z_1)(\alpha_d I_d+\eta_1)}{(\alpha_d I_d+z_1)(\alpha_d I_d+\eta_1)(\alpha_m I_m+z_2)(\alpha_m I_m+\eta_2)} \right)\left(1+\frac{\kappa_3}{z_3}\right) \right)$$

$$Q_3 = \left(\frac{(\alpha_d I_d+\rho_1)(\alpha_m I_m+z_2)(\alpha_m I_m+\eta_2) + (\alpha_m I_m+\rho_2)(\alpha_d I_d+z_1)(\alpha_d I_d+\eta_1)}{(\alpha_d I_d+z_1)(\alpha_d I_d+\eta_1)(\alpha_m I_m+z_2)(\alpha_m I_m+\eta_2)} \right)$$

$$Q_4 = z_3\eta_3\mu_h\left(\frac{(\alpha_d I_d+\alpha_m I_m+\mu_h)(\alpha_d I_d+z_1)(\alpha_d I_d+\eta_1)}{(\alpha_m I_m+z_2)(\alpha_m I_m+\eta_2)} \right)$$

$$Q_5 = \gamma_h\left(\frac{z_3\eta_3(\alpha_d I_d+\alpha_m I_m+\mu_h)(\alpha_d I_d+z_1)(\alpha_d I_d+\eta_1)(\alpha_m I_m+z_2)}{(\alpha_m I_m+\eta_2) - \left(\begin{array}{c} \theta_1\kappa_1\alpha_m I_m z_3\eta_3(\alpha_m I_m+z_2)(\alpha_m I_m+\eta_2) \\ +\theta_2\kappa_2\alpha_d I_d z_3\eta_3(\alpha_d I_d+z_1)(\alpha_d I_d+\eta_1) \\ +\theta_3\kappa_3\alpha_d I_d\alpha_m I_m Q_3(\alpha_d I_d+z_1)(\alpha_d I_d+\eta_1) \\ (\alpha_m I_m+z_2)(\alpha_m I_m+\eta_2) \end{array} \right)} \right)$$

$$Q_6 = \Lambda_h z_3\eta_3(\gamma_h+\mu_h)(\alpha_d I_d+z_1)(\alpha_d I_d+\eta_1)(\alpha_m I_m+z_2)(\alpha_m I_m+\eta_2)$$

$$Q_7 = \theta_1\kappa_1 z_3\eta_3\alpha_m I_m(\alpha_m I_m+z_2)(\alpha_m I_m+\eta_2) + \theta_2\kappa_2 z_3\eta_3\alpha_d I_d(\alpha_d I_d+z_1)(\alpha_d I_d+\eta_1)$$
$$+\theta_3\kappa_3\alpha_m I_m\alpha_d I_d(\alpha_d I_d+z_1)(\alpha_d I_d+\eta_1)(\alpha_m I_m+z_2)(\alpha_m I_m+\eta_2)$$

3.2 Reproduction Number (R_0)

We apply the next generation method to compute the Reproduction Number. This is the expected number of secondary infections produced when one infected individual is introduced into a susceptible population. So $R_0 = \rho\left(FV^{-1}\right)$ where F is the matrix of new infections and V is the matrix consisting of the transition terms. The matrices are given by

$$F = \begin{pmatrix} 0 & 0 & 0 & 0 & 0 & 0 & \alpha_m \frac{\Lambda_h}{\mu_h} & 0 \\ 0 & 0 & 0 & 0 & 0 & 0 & 0 & 0 \\ 0 & 0 & 0 & 0 & 0 & 0 & 0 & \alpha_d \frac{\Lambda_h}{\mu_h} \\ 0 & 0 & 0 & 0 & 0 & 0 & 0 & 0 \\ 0 & 0 & 0 & 0 & 0 & 0 & 0 & 0 \\ 0 & 0 & 0 & 0 & 0 & 0 & 0 & 0 \\ \alpha_{vm} \frac{\Lambda_m}{\mu_m} & \alpha_{vm} \frac{\Lambda_m}{\mu_m} & 0 & 0 & \alpha_{vm} \frac{\Lambda_m}{\mu_m} & \alpha_{vm} \frac{\Lambda_m}{\mu_m} & 0 & 0 \\ 0 & 0 & \alpha_{vd} \frac{\Lambda_d}{\mu_d} & \alpha_{vd} \frac{\Lambda_d}{\mu_d} & \alpha_{vd} \frac{\Lambda_d}{\mu_d} & \alpha_{vd} \frac{\Lambda_d}{\mu_d} & 0 & 0 \end{pmatrix}$$

$$V = \begin{pmatrix} \eta_1 & 0 & 0 & 0 & 0 & 0 & 0 & 0 \\ -\kappa_1 & z_1 & 0 & 0 & 0 & 0 & 0 & 0 \\ 0 & 0 & \eta_2 & 0 & 0 & 0 & 0 & 0 \\ 0 & 0 & -\kappa_2 & z_2 & 0 & 0 & 0 & 0 \\ 0 & 0 & 0 & 0 & \eta_3 & 0 & 0 & 0 \\ 0 & 0 & 0 & 0 & -\kappa_3 & z_3 & 0 & 0 \\ 0 & 0 & 0 & 0 & 0 & 0 & \mu_m & 0 \\ 0 & 0 & 0 & 0 & 0 & 0 & 0 & \mu_d \end{pmatrix}$$

So

$$\rho\left(FV^{-1}\right) = R_0 = \max\{R_{0m}, R_{0d}\},$$

where

$$R_{0m} = \sqrt{\frac{\Lambda_h \Lambda_m \alpha_m \alpha_{vm} (z_1 + \kappa_1)}{\eta_1 z_1 \mu_h \mu_m^2}} \quad \text{and}$$

$$R_{0d} = \sqrt{\frac{\Lambda_h \Lambda_d \alpha_d \alpha_{vd} (z_2 + \kappa_2)}{\eta_2 z_2 \mu_h \mu_d^2}}.$$

4 Sensitivity Analysis

In this section, sensitivity analysis is carried out to identify the most influential parameter(s) on the reproduction number. The techniques in [16] is applied. Given a parameter, say ξ the sensitivity index of R_0 with respect to ξ is given by

$$\mathrm{K}_{\xi}^{R_0} = \frac{\partial R_0}{\partial \xi} \frac{\xi}{R_0}.$$

Since $R_0 = \max\{R_{0m}, R_{0d}\}$, we obtain the analysis for R_{0m} and R_{0d} separately, using values in Table 3 below.

Table 3: Parameter Values

Symbols	Values	Source
θ_1	0.99	Calculated
θ_2	2.5	Garba *et al.* (2008)
κ_1	0.058	Olaniyi *et al.* (2018)
κ_2	0.074	Assumed
α_m	0.75	Olaniyi and Obabiyi (2013)
α_d	0.833	Garba *et al.* (2008)
α_{vm}	0.5	Labadin *et al.* (2009)
α_{vd}	0.09	Garba *et al.* (2008)
δ_1	0.015	Calculated
δ_2	0.36	James and Eguda (2017)
μ_h	0.0116	Calculated
μ_m	0.75	Labadin *et al.* (2009)
μ_d	0.365	Blayneh *et al.* (2009)

The Sensitivity indices is given in Table 4 below.

Table 4: Sensitivity Indices

Parameter	Sensitivity Index
R_{0m}	Basic Reproduction number of Malaria
α_m	1.000000001
α_{vm}	1.000000000
δ_1	-0.002632231
θ_1	-0.249184537
κ_1	-0.561160644
μ_h	-1.187022586
μ_m	-2.00000000
R_{0d}	Basic Reproduction number of Dengue
α_d	1.000000000
α_{vd}	1.000000000
δ_2	-0.003149462
θ_2	-0.021871270
κ_2	-0.839363765
μ_h	-1.135615500
μ_d	-2.000000000

5 Discussion and Conclusion

As outline in Table 4 the parameters have negative or positive effects as indicated by the signs. Parameters with negative signs $(\delta_1, \delta_2, \theta_1, \theta_2, \kappa_1, \kappa_2, \mu_h, \mu_m, \mu_d)$ when increased with other parameters remaining constant will reduce the value of R_0. Otherwise, increasing any of the indices with positive signs will increase the value of the reproduction number (R_0). It is observed that the most sensitive parameters are the vectors death rate (μ_m, μ_d). This implies that control strategies that concentrate on eliminating or reducing the disease vectors will be most effective in reducing the transmission of malaria and dengue fever disease.

References

[1] Epelboin, L., Hanf, M., Dussart, P., Ouar-Epelboin, S., Djossou, F., Nacher, M. and Carme, B. (2012). Is dengue and malaria co-infection more severe than single infections? A retrospective matched-pair study in French Guiana, Malaria Journal, 11(142): 1-8.

[2] Kolawole, O. M., Seriki, A. A., Irekeola, A. A., Bello, K. E. and Adeyemi, O. O. (2017). Dengue virus and Malaria concurrent infection among febrile subjects within Ilorin metropolis, Nigeria, Journal of Medical Virology, 89 (8): 1347 – 1353.

[3] Aschale, Y., Mengist, A., Bitew, A., Kassie, B. and Talie, A. (2018). Prevalence of malaria and associated risk factors among asymptomatic migrant laborers in West Armachiho District, Northwest Ethiopia. Res. Rep. Trop. Med., 9: 95 – 101.

[4] Ashley, E.A., Phyo, P. A. and Woodrow, C.J. (2018). Malaria, Lancet, 391(10130): 1608–1621.

[5] Walker, N., Nadjm, B. and Whitty, C. (2017). Malaria. Medicine, 42, 52–58.

[6] Phaijoo, G. R. and Gurung, D. B. (2017). Modeling Impact of Temperature and Human Movement on the Persistence of Dengue Disease, Computational and Mathematical Methods in Medicine. https://doi.org/10.1155/2017/1747134

[7] Oyinloye, S. O., Wajiroko, M., Lawan, A. M. *et al.*, (2016). Dengue virus infection in northeast Nigeria: Case study of a squatters' Camp. International Journal of Perceptions in Public Health, 1(1): 59-65.

[8] Otu, A., Ebenso, B. and Chukwuekezie, O. (2019). Dengue fever- an update review and implications for Nigeria, and similar countries, Afri Health Sci., 19 (2): 2000 – 2007.

[9] Oladipo, E. K., Amanetu, C., Gbadero, T.A. and Oloke, J. K. (2014). Detectable anti-dengue virus IgM antibodies among healthy individuals in Ogbomoso, Oyo State, Nigeria, Am. J. Infect. Dis. 10: 64 -67.

[10] Sareen, R., Menka, K., Gupta, G. N. (2018). Plamodium Vivax and Dengue co-infection Emerging Challenge to Diagnosis, Journal of Advanced Medical Sciences, 2 (1): 4-6.

[11] Salam, N., Mustafa, S., Hafiz, A., Chaudhary, A. A., Deeba, F. and Parveen, S. (2018). Global prevalence and distribution of co-infection of Malaria, Dengue and Chikungunya: a systematic review. BMC Public Health, 18 (710): 1-20.

[12] Chong, S. E., Zaini, M. R. H., Suraiya, S., Lee, K. T. and Lim, J. A. (2017). The danger of

accepting a single diagnosis: case report of concurrent Plasmodium Knowlesi malaria and dengue infection. Malaria J., 16 (2): 1-8.

[13] Atokolo, W. and Omale, D. (2018). Sensitivity analysis of a transmission dynamics model for Typhoid fever and its control. Journal of Nigerian Society of Mathematical Biology, 1: 47-58.

[14] Sirajo, A., Akinwande, N. I.,, Awojoyogbe, O. B. and Abubakar, U. Y. (2013). Sensitivity Analysis of the Parameters of a Mathematical Model of Hepatitis B Virus Transmission., Universal Journal of Applied Mathematics, 1(4): 230-241.

[15] Marsudi, Noor, H. and Wibowo, R.B.E. (2017). Sensitivity Analysis of the Parameters of an HIV/AIDS Model with Condom Campaign and Antiretroviral Therapy, AIP Conf. Proc., 1913: 020019

[16] Chitnis, N., Hyman, J. and Cushing, J. (2008) Department of Public Health and Epidemiology, 70, 1272–1296.

Journal of the Nigerian Society for Mathematical Biology
Volume 4 (2021), pp. 76 – 95

Sensitivity analysis of Smartphone Virus infection transmission dynamics

T.I. Chinebu[*], G.C.E. Mbah[†], E.A. Jooda[*],

E.O. Ezennorom[‡] and I.V. Udegbe[‡]

Abstract

We proposed in this paper, a mathematical model for the sensitivity analysis of the Smartphone virus infection transmission dynamics using SEICQR. First, the model was well-posed as we proved that all its state variables are nonnegative for all time and then we determine a unique Smartphone virus infection free equilibrium state and indicate possibility of control of Smartphone virus infection. The basic Smartphone virus infection reproduction number, R_0, as a threshold parameter, in terms of the given model parameter was computed using the next generation method. Also, the sensitivity analysis of R_0 was determined to see parameters that positively contribute to the dynamics of Smartphone virus infection. The numerical simulation of the model was done using Runge-Kutta Fourth order (RK4) method in MATLAB to evaluate the effect of these parameters of the basic Smartphone reproduction number on the dynamics of the infection. The numerical results confirm the theoretical results of the sensitivity indices. Finally, these findings suggest that Smartphone virus infection will only be eradicated from the population with proper control strategies.

***Keywords*:** smartphone virus; sensitivity analysis; basic reproduction number; infection transmission dynamics.

1 Introduction

The Smartphone is small enough to fit in a pocket and it enable users to have a device with a good processing power, internet access and functions of traditional mobile phones in one device. However, the wealth of private information which is stored on those devices made them an

[*]Department of Applied Sciences, Federal College of Dental Technology and Therapy, P.M.B. 01473, Trans Ekulu, Enugu, Nigeria
[†]Department of Mathematics, University of Nigeria, Nsukka, Nigeria
[‡]Department of Computer Science, Madonna University Nigeria, Elele, Nigeria

interesting target for malicious users and cyber criminals [1], who then invade these Smartphone with virus. Smartphone virus is a mischief program written to proliferate from one phone to another and it takes control of Smartphone devices by exploiting its vulnerability. Continuous improvement in Smartphone device hardware and Smartphone communication technologies has led to a highly interconnected world, but also a world grown highly vulnerable. Cyber criminals have proven significantly efficient in uncovering new vulnerabilities in popular applications (apps) [2]. As a result, more and more Smartphone malware families are introduced every year [3]. Just in 2017, more than 20 million malware samples have been detected [4], while other studies show that the chances for monetization is a key factor responsible for the rise of Smartphone malware [5, 6].

The cyber attacker who was able to install malware on some system can install or delete programs, modify files, download sensitive information and use them to impersonate the user's action and keystrokes, capture users screen, use camera and retrieve photos or videos, use the infected system as a source of Distributed denial of service (DDoS)) attack [1, 7]. It's a method where cyber criminals flood a network with so much malicious traffic that it cannot operate or communicate as it normally would. This causes the site's normal traffic, also known as legitimate packets, to come to a halt. Smartphone can become infected either through downloading infected files using the phone internet browser, transferring files between phones using Bluetooth interface, synchronizing with an infected computer, assessing an infected physical memory card, opening infected files attached to multimedia message service (MMS) or email [8, 9]. Zhang [10] discovered that Smartphone virus can also propagate through multi-layered network. He concluded that Smartphone viruses can use any network (3G, 4G, Wi-Fi or Bluetooth).

When an unsuspected user accepts the infected attachment file, using a phone susceptible to the virus, then the virus is installed and infects the target phone which then begins to perform as an attacked phone [9]. Smartphone virus can seize the victims mobile device by running malicious exploit and this infected device will in turn, scan and infect other Smartphones in the mobile network [11].

Some response mechanisms completely stop further virus propagation, but others simply slow the propagation rate of the virus [12]. Both types of response can be used. Ideally, the response mechanism would always quickly and completely stop Smartphone virus propagation. However, some viruses spread so quickly that a first response mechanism that slows the spread could buy time to enable activation of a second response mechanism that completely halts the propagation process. Actually, in phone user education response, the consent of the phone user to accept the message and infect the phone is required, therefore, a user not accepting an infected message has a direct effect on virus propagation. Also, other response mechanism such as immunization can prevent infection even if the user accepts the MMS message attachment [12]. A virus scans of all MMS attachments as they pass through an MMS gateway is completely effective against viruses with known virus signature. For that reason, after the new virus signature is added to the list of known viruses, the gateway virus scan is able to completely halt virus propagation [13].

The immunization response mechanism operates using software placed directly on each Smartphone [14]. After a Smartphone service provider detects virus that exploits a vulnerable Smartphone, the service provider begins developing a patch to fix that vulnerability [15]. Once the patch is developed, the immunization software resident in each Smartphone automatically installs any immunization patch available [10]. Bandwidth constraint prevents most Smartphone from receiving the patch simultaneously, as the patch is rolled out to the entire Smartphone population uniformly over a period of time [16]. The more servers that are dedicated to distributing these patches, the faster the deployment to susceptible Smartphones in the network [17]. When the patch arrives at a particular Smartphone, it becomes immunized from virus if not infected, or the patch stops further propagation attempts from Smartphone if it is already infected [18].

Because Smartphone viruses have potential to attack in many different ways, an optimal response strategy must incorporate mechanisms to counteract a wide variety of virus behaviors. The hope of stopping Smartphone virus before it degrades the utility and value of a Smartphone is quick and concerted action on the part of all universal mobile telecommunications service (UMTS) data networks that their mobile devices use; Wi-Fi networks have no such protection. And while some carriers already filter their MMS streams to remove messages bearing malicious attachments, all should do so [6].

Some of the manufacturers have joined the trusted computing group, which has been hammering on industry standards micro circuiting inside phones that will make it harder for malware to get a sensitive data in the devices memory or to hijack its payment mechanism. Symbian released a version of its operating system that does an improved job of protecting key files which requires software to obtain digital certificate from the company. This Symbian system refuses to install programs not accompanied by a certificate. Unless disabled by a user the system effectively excludes all mobile malware discovered to date [6].

2 Related Literature

In Smartphone network environment, virus attack is a serious threat and is still multiplying as time continues to pass and it is very necessary to control these virus attacks in Smartphone. A number of mathematical models have been formulated to simulate, analyze and understand Smartphone virus propagation and its control strategies. In related works, Guillen et al [19] used the theory of optimal control that is associated to systems of ordinary differential equations to find a new function to control malware epidemic through time, while Liu and Zhong [20] employed the optimal control theory to study malware immunization strategies, aiming to keep the total economic loss of security investment and infection loss as low as possible.

Ruitenbeek and Stevens [13] proposed response mechanisms for mobile phone viruses and used their model to obtain insight on the effectiveness of the virus mitigation technique. To study the fundamental spreading patterns that characterize a mobile virus outbreak, Wang et al [11]

modeled the mobile benign worm based on two stages of repairing mechanisms. Chinebu et al [21] proposed an SVEIQRS model that control virus attack through vaccination, quarantine and treatment. Their model has a globally asymptotically stable virus free equilibrium when $R_0 < 1$ and a unique endemic equilibrium when $R_0 > 1$. Yang et al [22] proposed two different propagation models of mobile phone viruses under the complex network.

Our aim in this paper is to highlight the seriousness of Smartphone virus propagation, particularly exposed$(E(t))$Smartphone that is infected without symptom which can transmit the infection to susceptible$(S(t))$ Smartphone. Likewise, there can be transmission from infected Smartphone$(I(t))$ to susceptible. In addition, we included complication with virus infected Smartphone $(C(t))$. Furthermore, we have the quarantined Smartphone$(Q(t))$ and finally the recovered Smartphone$(R(t))$.

A continuous mathematical model we proposed in this paper and it describes the dynamics of a population infected by Smartphone virus. Moreover, we gave the model in section 3 and some basic properties of the model in section 4. Lastly, we presented the discussion and conclusion in section 5.

3 Mathematical Model Formulation

We consider a mathematical model SEICQR that describe the Smartphone virus infection transmission dynamics. The entire Smartphone population denoted by $N(t)$ was divided into six compartments.

3.1 Description of the Smartphone Model Compartments

The schematic diagram of the proposed Smartphone virus transmission dynamics is shown in Figure 1:

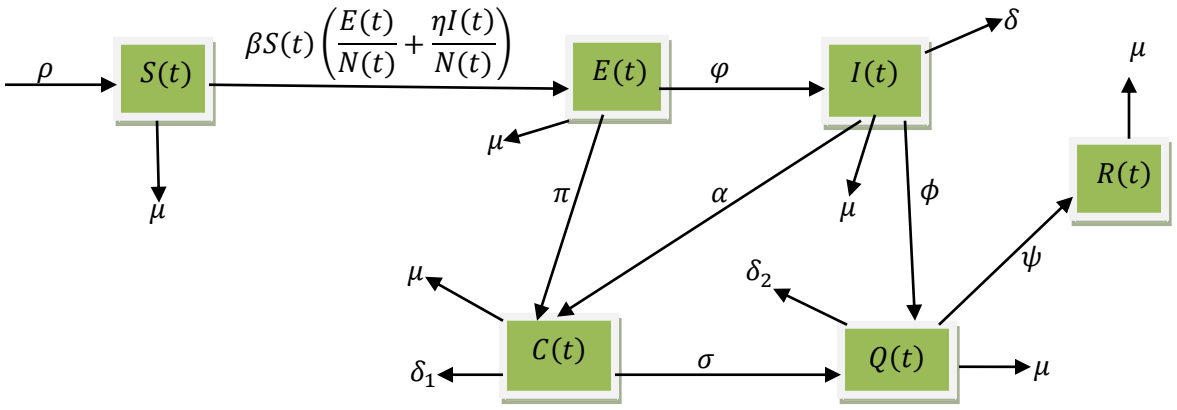

Figure 1: Schematic Diagram of the Model for Smartphone virus infection transmission dynamics.

Let us denote the force of infection by

$$\lambda = \beta\left(\frac{\eta E(t) + I(t)}{N}\right), \qquad (1)$$

where, β is the Smartphone virus infection transmission rate and η is the modification factor for the exposed Smartphones.

Compartment $(S(t))$ represents the number of Smartphone infected with virus. This compartment is increased by ρ, which denotes the incidence of susceptible Smartphone. The compartment is decreased by the amount μ (natural Death, i.e., Smartphones that can never be repaired again), $\frac{\beta\eta S(t)E(t)}{N}$ (The number of Smartphone that are infected with the virus by contact with the exposed Smartphone) and $\frac{\beta S(t)I(t)}{N}$ (The number of Smartphone that were infected with the virus by communication with infected Smartphone). Thus, we have

$$\frac{dS(t)}{dt} = \rho - \mu S(t) - \beta\left(\frac{\eta E(t) + I(t)}{N}\right)S(t) \qquad (2i)$$

Compartment $(E(t))$ represents the number of exposed Smartphones, that is, those that are infected without symptoms but can transmit the infection. The compartment $(E(t))$ is increased by the amount of $\frac{\beta\eta S(t)E(t)}{N}$ and $\frac{\beta S(t)I(t)}{N}$. It is decreased by natural death, denoted with μ, the number of Smartphones that become infectious, φ, and also by number of Smartphones that have upgraded to the development of rapid and dangerous virus, thereby, having complications due to antivirus deficiency and is denoted by π. This gives

$$\frac{dE(t)}{dt} = \beta\left(\frac{\eta E(t) + I(t)}{N}\right)S(t) - (\mu + \varphi + \pi)E(t) \qquad (2ii)$$

Compartment $(I(t))$ represents the number of infected Smartphones. The compartment $(I(t))$ is increased by the number of exposed Smartphones that becomes infectious and is denoted by φ. This compartment is decreased by α, that is, Smartphones that have severe complications such as Apps crashing over and over again. It is also decreased by, μ, natural death rate, δ, death rate due to virus infection and ϕ, progression rate from infected to quarantine. Therefore, we obtain

$$\frac{dI(t)}{dt} = \varphi E(t) - (\mu + \alpha + \phi + \delta)I(t) \qquad (2iii)$$

Compartment $(C(t))$ represents the number of infected Smartphones with complications. This compartment is increased by π and α, that is, progression rate from exposed and infected respectively to infected with complications. It is decreased by natural death, μ, death rate due to virus infection with complication δ_1 and progression rate from infected with complications to quarantine, σ. Then, we get

$$\frac{dC(t)}{dt} = \pi E(t) + \alpha I(t) - (\mu + \delta_1 + \sigma)C(t) \qquad (2iv)$$

Compartment $(Q(t))$ represents the number of Quarantined Smartphones with follow-up treatment. This compartment is increased by ϕ and σ, that is, progression rate from infected and infected with complications respectively to quarantined. It is decreased by the movement from quarantined to recovered Smartphones, ψ, natural death rate, μ and quarantined Smartphones that cannot be repaired again, δ_2. This, provides us with

$$\frac{dQ(t)}{dt} = \phi I(t) + \sigma C(t) - (\mu + \delta_2 + \psi)Q(t) \qquad (2v)$$

Compartment $(R(t))$ represents the number of recovered Smartphones. This is increased by recovery rate, ψ and is decreased by natural death rate, μ. Thus, we have

$$\frac{dR(t)}{dt} = \psi Q(t) - \mu R(t) \qquad (2vi)$$

Based on the above formulations from equations $(2i) to\ (2vi)$ and the schematic diagram, we thus present the Smartphone virus infection transmission dynamics model by the following systems of differential equation:

$$\left.\begin{aligned}
\frac{dS(t)}{dt} &= \rho - \mu S(t) - \lambda S(t) \\
\frac{dE(t)}{dt} &= \lambda S(t) - (\mu + \varphi + \pi)E(t) \\
\frac{dI(t)}{dt} &= \varphi E(t) - (\mu + \alpha + \phi + \delta)I(t) \\
\frac{dC(t)}{dt} &= \pi E(t) + \alpha I(t) - (\mu + \delta_1 + \sigma)C(t) \\
\frac{dQ(t)}{dt} &= \phi I(t) + \sigma C(t) - (\mu + \delta_2 + \psi)Q(t) \\
\frac{dR(t)}{dt} &= \psi Q(t) - \mu R(t)
\end{aligned}\right\} \qquad (3)$$

where the initial state are $S(0) \geq 0,\ E(0) \geq 0,\ I(0) \geq 0,\ C(0) \geq 0,\ Q(0) \geq 0,\ R(0) \geq 0$.

4 Basic Properties of the Model

4.1 Positivity of Solutions

For Smartphone virus infection transmission dynamics model system (3) to be epidemiologically and mathematically meaningful, it is important to prove that all its state variables are positive for all time. Therefore, solution of model system (3) with non negative initial data remains non-negative for all time $t \geq 0$. Thus, the total Smartphone population can be defined as

$$N(t) = S(t) + E(t) + I(t) + C(t) + Q(t) + R(t) \qquad (4)$$

Theorem 1: If $S(0) \geq 0, E(0) \geq 0, I(0) \geq 0, C(0) \geq 0, Q(0) \geq 0\ and\ R(0) \geq 0,$ the solutions $S(t), E(t), I(t), C(t), Q(t)\ and\ R(t)$ of system (3) are non negative for all $t \geq 0$.

Proof: It follows from equation (2i) that

$$\frac{dS(t)}{dt} = \rho - \mu S(t) - \beta\left(\frac{\eta E(t) + I(t)}{N(t)}\right)S(t)$$

$$\geq -\mu S(t) - \lambda S(t)$$

$$\frac{dS(t)}{dt} + (\mu + \lambda)S(t) \geq 0$$

Let $\mu + \lambda = F(t)$, then we have

$$\frac{dS(t)}{dt} + F(t)S(t) \geq 0$$

Multiplying both sides of this inequality by $\exp\left(\int_0^t F(s)ds\right)$ we get

$$\exp\left(\int_0^t F(s)ds\right).\frac{dS(t)}{dt} + F(t)\exp\left(\int_0^t F(s)ds\right)S(t) \geq 0$$

Then,

$$\frac{d}{dt}\left(S(t)\exp\left(\int_0^t F(s)ds\right)\right) \geq 0$$

Integrating this inequality from 0 to t we obtain:

$$\int_0^t \frac{d}{dt}\left(S(s)\exp\left(\int_0^t (\mu+\lambda)ds\right)\right)ds \geq 0$$

Therefore,

$$S(t) \geq S(0)\exp\left(\int_0^t (\mu+\lambda)ds\right)$$

This implies that $S(t) > 0 \ \forall\, t > 0$. Similarly, it can be proved that $E(t) \geq 0, I(t) \geq 0, C(t) \geq 0, Q(t) \geq 0 \ and \ R(t) \geq 0$ and this is done using the remaining sub equations of (3) and we have

$$E(t) \geq E(0)\exp\left(\int_0^t (\mu+\varphi+\pi)de\right)$$

$$I(t) \geq I(0)\exp\left(\int_0^t (\mu+\alpha+\phi+\delta)di\right)$$

$$C(t) \geq C(0)\exp\left(\int_0^t (\mu+\delta_1\ +\sigma)dc\right)$$

$$Q(t) \geq Q(0)\exp\left(\int_0^t (\mu+\delta_2\ +\psi)dq\right)$$

$$R(t) \geq R(0)\exp\left(\int_0^t (\mu)dr\right)$$

This completes the proof. It is important to note that system (3) will be analyzed in a feasible region

$$\Phi = \left\{(S, E, I, C, Q, R) \in \mathbb{R}_+^6 : S + E + I + C + Q + R \leq \frac{\rho}{\mu}\right\} \qquad (5)$$

which can easily be verified to be positively invariant with respect to model system (3). Therefore, model system (3) is epidemiologically and mathematically well posed in Φ [23].

4.2 The Basic Smartphone Virus Infection Reproduction Number, R_0

To compute the basic Smartphone virus infection reproduction number, we first calculate the Smartphone virus infection free equilibrium state of the model by setting the left hand side of system (3) to zero and obtain the Smartphone virus infection free equilibrium state as follows

$$H_0^* = \left(S_0(t), E_0(t), I_0(t), C_0(t), Q_0(t), R_0(t)\right) = \left(\frac{\rho}{\mu}, 0, 0, 0, 0, 0\right)$$

The rate of appearance of new virus infection in the population is given by the new infection terms in the exposed compartment [24][25][26]. Then new infections in compartments$E(t)\ I(t)\ and\ C(t)$ is given by

$$F := \begin{pmatrix} \frac{\beta\eta\rho}{\mu} & \frac{\beta\rho}{\mu} & 0 \\ 0 & 0 & 0 \\ 0 & 0 & 0 \end{pmatrix}$$

While the remaining transmission terms in compartments$E(t)\ I(t)\ and\ C(t)$ is given by

$$V := \begin{pmatrix} A & 0 & 0 \\ -\varphi & B & 0 \\ -\pi & -\alpha & G \end{pmatrix}$$

$$where\ A = \mu + \varphi + \pi, B = \mu + \alpha + \phi + \delta,\ \ G = \mu + \delta_1 + \sigma$$

The inverse of the transmission terms in compartments$E(t)\ I(t)\ and\ C(t)$ and FV^{-1} are respectively given by

$$V^{-1} \rightarrow \begin{pmatrix} \frac{1}{A} & 0 & 0 \\ \frac{\varphi}{A \cdot B} & \frac{1}{B} & 0 \\ \frac{\pi \cdot B + \varphi \cdot \alpha}{A \cdot B \cdot G} & \frac{\alpha}{B \cdot G} & \frac{1}{G} \end{pmatrix} \quad \text{and} \quad F \cdot V^{-1} \rightarrow \begin{pmatrix} \frac{\beta\eta\rho}{A \cdot \mu} + \frac{\varphi \cdot \beta\rho}{A \cdot B \cdot \mu} & \frac{\beta\rho}{B \cdot \mu} & 0 \\ 0 & 0 & 0 \\ 0 & 0 & 0 \end{pmatrix}$$

Therefore the basic Smartphone virus infection reproduction number R_0 is given by:

$$R_0 = \frac{\beta\eta\rho}{\mu A} + \frac{\varphi\beta\rho}{\mu AB} = \frac{\beta\eta\rho}{\mu(\mu+\varphi+\pi)} + \frac{\rho\varphi\beta}{\mu(\mu+\varphi+\pi)(\mu+\alpha+\phi+\delta)}$$

$$R_0 = \frac{\beta\rho}{\mu(\mu+\varphi+\pi)}\left(\eta + \frac{\varphi}{(\mu+\alpha+\phi+\delta)}\right) \quad (6)$$

4.3 Endemic Equilibrium Point

Here we discuss the point at which the virus infection cannot be totally eradicated from the population. We therefore let H_1^{**} be the Smartphone virus infection endemic equilibrium of the model. Thus, we have

$$\mathrm{H}_1^{**} = \left(S_1(t), E_1(t), I_1(t), C_1(t), Q_1(t), R_1(t)\right)$$

$$\left.\begin{aligned}
S_1(t) &= \frac{\rho}{\mu+\lambda^{**}} \\
E_1(t) &= \frac{\lambda^{**}\rho}{A(\mu+\lambda^{**})} \\
I_1(t) &= \frac{\lambda^{**}\varphi\rho}{AB(\mu+\lambda^{**})} \\
C_1(t) &= \frac{\lambda^{**}\rho}{AG(\mu+\lambda^{**})}\left(\pi + \frac{\alpha\varphi}{B}\right) \\
Q_1(t) &= \frac{\lambda^{**}\rho}{AK(\mu+\lambda^{**})}\left(\frac{\phi\varphi}{B} + \frac{\sigma\pi}{G} + \frac{\sigma\alpha\varphi}{BG}\right) \\
R_1(t) &= \frac{\lambda^{**}\psi\rho}{\mu AK(\mu+\lambda^{**})}\left(\frac{\phi\varphi}{B} + \frac{\sigma\pi}{G} + \frac{\sigma\alpha\varphi}{BG}\right)
\end{aligned}\right\} \quad (7)$$

But the force of infection$\lambda^{**} = \beta\left(\frac{\eta E(t)+I(t)}{N}\right)$, substituting (7) into the force of infection gives

$$\lambda^{**}(a_2(\lambda^{**})^2 + a_1\lambda^{**} + a_0) = 0 \quad (8)$$

$$\left.\begin{aligned}
a_2 &= \mu AB^2GK + \mu ABGK + \mu\pi AB^2GK + \mu\alpha\varphi ABK + \mu\varphi ABG + \mu\sigma\pi AB^2 + \mu\sigma\alpha\varphi AB \\
&\quad + \phi\varphi\psi ABGK + \sigma\pi\psi AB^2GK + \sigma\varphi\psi\alpha AB \\
a_1 &= \mu^2AB^2GK + \mu^2\varphi ABGK + \mu^2\pi AB^2K + \mu^2\varphi\alpha AB + \mu^2\varphi ABG + \mu^2\sigma\pi AB^2 + \mu^2\varphi ABGK \\
&\quad + \mu\phi\varphi\psi ABGK + \mu\sigma\pi\psi AB^2GK + \mu\sigma\varphi\psi\alpha AB^2 \\
a_0 &= \mu^2A^2B^2GK(1-R_0)
\end{aligned}\right\}$$

The root $\lambda^{**} = 0$ of (8) correspond to Smartphone virus infection free equilibrium H_0^*. It is important to know that the coefficient a_0 is always positive if and only if $R_0 < 1$ and negative if and only if $R_0 > 1$.

4.4 Boundedness of Solution

Theorem 2: Assume that the initial condition of Smartphone virus transmission dynamics of model system (3) $S(0) \geq 0, E(0) \geq 0, I(0) \geq 0, C(0) \geq 0, Q(0) \geq 0 \; and \; R(0) \geq 0$ with the set $\Phi = \left\{(S, E, I, C, Q, R) \in \mathbb{R}_+^6 : S + E + I + C + Q + R \leq \frac{\rho}{\mu}\right\}$ satisfying $N(0) \leq \frac{\rho}{\mu}$. Then, whenever the solution exists on an interval Φ, it satisfies the following bundedness

$$N(t) \leq \frac{\rho}{\mu}$$

Proof: From equation (4) we obtain the total Smartphone population as

$$N(t) \leq \rho - \mu N - \delta I - \delta_1 C - \delta_2 Q \tag{9}$$

Applying Barkhoff and Rota [29] theorem to equation (9) and having in mind that in the absence of virus infection, $\delta = \delta_1 = \delta_2 = 0$, then we have

$$0 \leq N(t) \leq \frac{\rho}{\mu} \; as \; t \to \infty \tag{10}$$

Since $I(t) \geq 0$ we have from (5) that

$$N(t) \leq \rho - \mu N$$

Using comparison theorem by Lakshmikanthan et al [30], Zhang [31], it can be shown that

$$N(t) \leq N(0)e^{-\mu t} + \frac{\rho}{\mu}(1 - e^{-\mu t}) \tag{11}$$

Whenever $(0) \leq \frac{\rho}{\mu}$, we have $N(t) \leq \frac{\rho}{\mu}$, and Consequently, $I(t) \leq \frac{\rho}{\mu}$.

4.5 Existence of Solution

Theorem 3: The system (3) that satisfies a given initial condition $S(0), E(0), I(0), C(0), Q(0), R(0)$ has a unique solution.

Proof: Let

$$Y = \begin{bmatrix} S(t) \\ E(t) \\ I(t) \\ C(t) \\ Q(t) \\ R(t) \end{bmatrix} \; and \; \mathfrak{O}(Y) = \begin{bmatrix} \frac{dS(t)}{dt} \\ \frac{dE(t)}{dt} \\ \frac{dI(t)}{dt} \\ \frac{dC(t)}{dt} \\ \frac{dQ(t)}{dt} \\ \frac{dR(t)}{dt} \end{bmatrix}$$

So that system (11) can be written in the following form:

$$\mathfrak{O}(Y) = VY + F(Y) \tag{12}$$

Where

$$V := \begin{pmatrix} -\mu & 0 & 0 & 0 & 0 & 0 \\ 0 & -A & 0 & 0 & 0 & 0 \\ 0 & \varphi & -B & 0 & 0 & 0 \\ 0 & \pi & \alpha & -G & 0 & 0 \\ 0 & 0 & \phi & \sigma & -K & 0 \\ 0 & 0 & 0 & 0 & \psi & -\mu \end{pmatrix} \quad \text{and}$$

$$F(Y) = \begin{bmatrix} -\beta\left(\frac{\eta E(t) + I(t)}{N}\right)S(t) \\ +\beta\left(\frac{\eta E(t) + I(t)}{N}\right)S(t) \\ 0 \\ 0 \\ 0 \\ 0 \end{bmatrix}$$

$$where \; A = \mu + \varphi + \pi, \qquad B = \mu + \alpha + \phi + \delta, \;\; G = \mu + \delta_1 + \sigma \; and \;\; K = \mu + \delta_2 + \psi$$

$$F(Y_1) - F(Y_2) = \begin{bmatrix} -\beta\left(\frac{\eta E(t) + I(t)}{N}\right)S(t) \\ +\beta\left(\frac{\eta E(t) + I(t)}{N}\right)S(t) \\ 0 \\ 0 \\ 0 \\ 0 \end{bmatrix} - \begin{bmatrix} -\beta\left(\frac{\eta E(t) + I(t)}{N}\right)S(t) \\ +\beta\left(\frac{\eta E(t) + I(t)}{N}\right)S(t) \\ 0 \\ 0 \\ 0 \\ 0 \end{bmatrix} \tag{13}$$

$$|F(Y_1) - F(Y_2)|$$

$$= \left|-\beta\left(\frac{\eta E_1(t) + I_1(t)}{N}\right)S_1(t) + \beta\left(\frac{\eta E_2(t) + I_2(t)}{N}\right)S_2(t)\right|$$

$$+ \left|\beta\left(\frac{\eta E_1(t) + I_1(t)}{N}\right)S_1(t) - \beta\left(\frac{\eta E_2(t) + I_2(t)}{N}\right)S_2(t)\right|$$

$$\leq 2\beta\left(|\eta S_1(t)|\left|\frac{E_1(t) - E_2(t)}{N}\right| + |S_1(t) - S_2(t)|\left|\frac{\eta E_2(t) + I_1(t)}{N}\right| + |S_2(t)|\left|\frac{I_1(t) - I_2(t)}{N}\right|\right)$$

$$\leq 2\beta\left(\left|\frac{\eta E_1(t)S_1(t) + I_1(t)S_1(t)}{N}\right| - \left|\frac{\eta E_2(t)S_2(t) + I_2(t)S_2(t)}{N}\right|\right)$$

$$\leq \Gamma(|Y_1 + Y_2|)$$

By letting equation (10) be equal to $\Pi_0 \in \mathbb{R}_+^6 \; and \; \lim_{t\to\infty} Sup\, N(t) \leq \Pi_0$, which concludes that $S(t), E(t), I(t), C(t), Q(t), R(t) \leq \Pi_0 \; as \; t \to \infty$, where

$$\Gamma = 2g\Pi_0$$

$$|\mathfrak{O}(Y_1) - \mathfrak{O}(Y_2)| \leq \|\mathrm{V}\||Y_1 - Y_2| + \Gamma|Y_1 - Y_2| \leq \Pi|Y_1 - Y_2|$$

$$where \qquad \Pi = Max(\Gamma, \|V\|) < \infty$$

Therefore,it follows that the function $\mathfrak{O}$ is uniformly Lipschitz continuous and with the restriction on $S(0) \geq 0, E(0) \geq 0, I(0) \geq 0, C(0) \geq 0, Q(0) \geq 0 \; and \; R(0) \geq 0$, we see that a solution of system (12) exists [27].

4.6 Sensitivity Analysis of the Model R_0

Let the normalized forward sensitivity index of the basic reproduction number of the model R_0, which is differentiable with respect to a given parameter ω, be defined by

$$\Gamma_{\omega}^{R_0} = \frac{\partial R_0}{\partial \omega} . \frac{\omega}{R_0}$$

Thus, we compute an analytical expression for the sensitivity of R_0, with the value of $R_0 = 0.627$using equation (6), to each parameter that it includes. The value of the parameters and the sensitivity indices obtained are represented in table 1. Remember that the Sensitivity index may depend on many parameters of the system, but also can be constant, independent of any parameter [28].

Table 1: The effect of the parameters on R_{02}.

Parameters	Value	Effect on R_{02}
ρ	100	$+1$
μ	0.057	-14.301887
β	0.0065	$+1$
η	0.0002	$+0.046864$
φ	0.0045	$+0.906593$
π	0.04	-0.375563
α	0.21	-0.010300
ϕ	0.83	-0.040708
δ	0.01	-0.000490

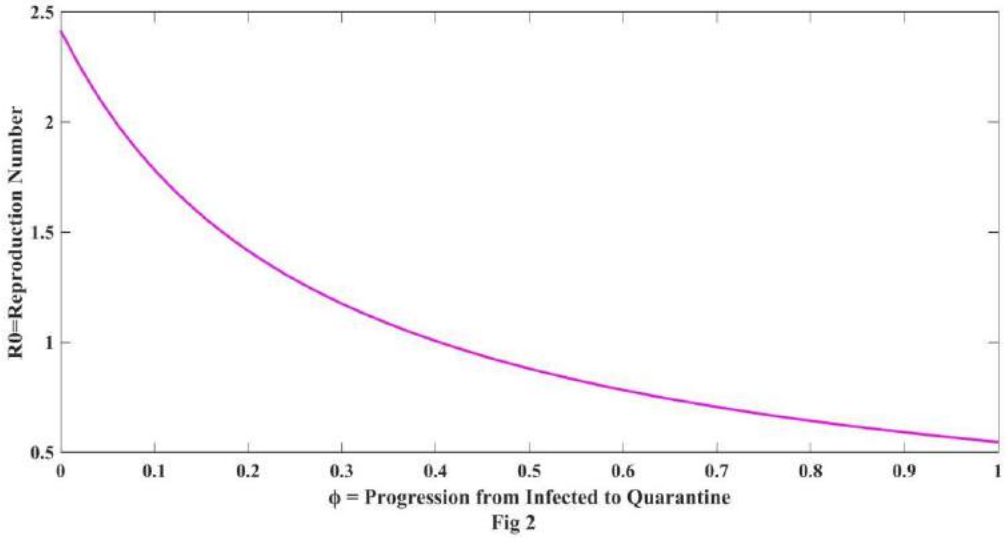

Figure 2: Impact of ϕ (progression from infected to quarantine) on the Smartphone virus infection transmission dynamics in the population

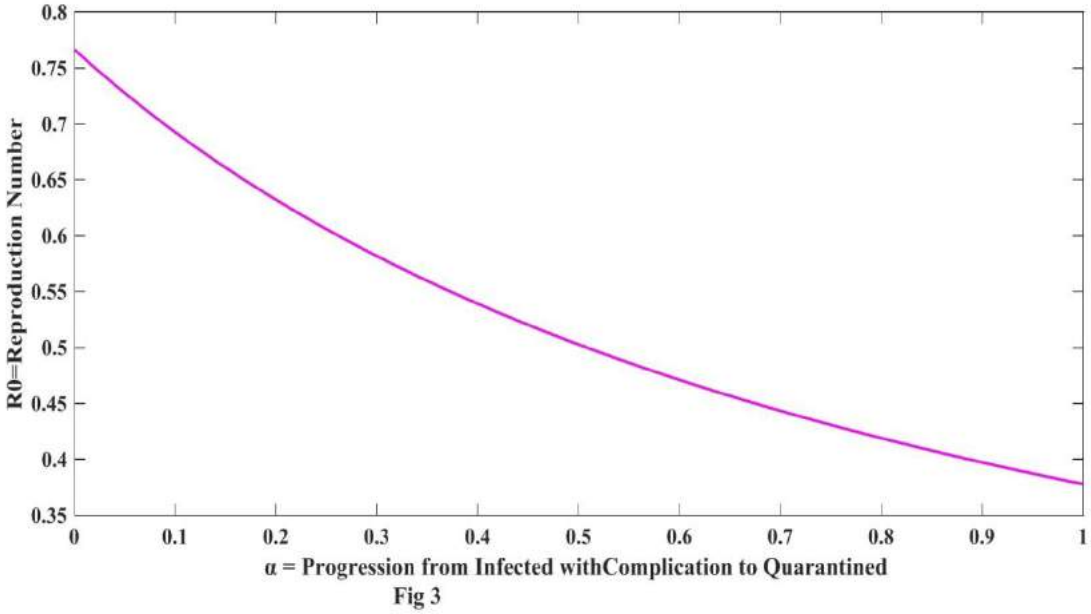

Figure 3: Impact of α (Smartphones with severe complications such as Apps crashing over and over again) on the Smartphone virus infection transmission dynamics in the population

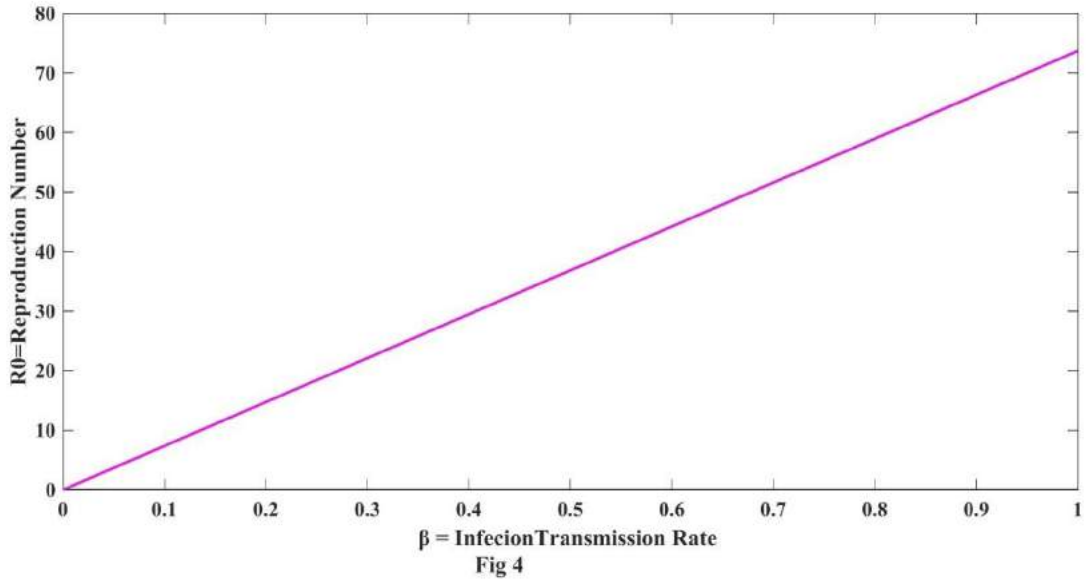

Figure 4: Impact of β (Smartphone virus infection transmission rate) on the Smartphone virus infection transmission dynamics in the population.

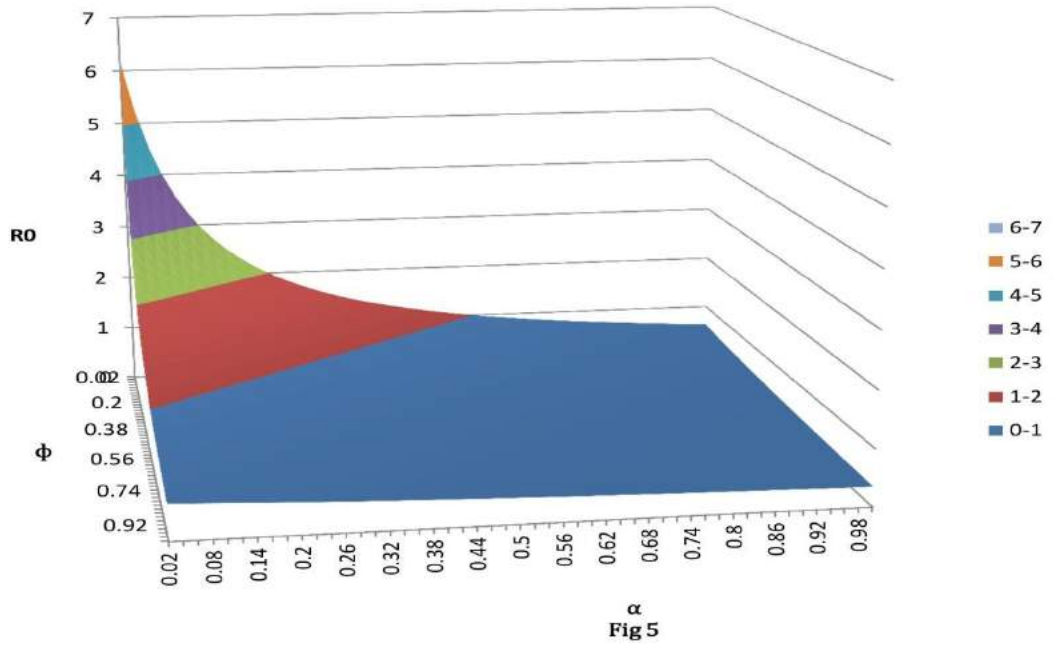

Figure 5: Impact of ϕ (progression from infected to quarantine) and α (Smartphones with severe complications such as Apps crashing over and over again) on the dynamics of Smartphone virus infection in the population.

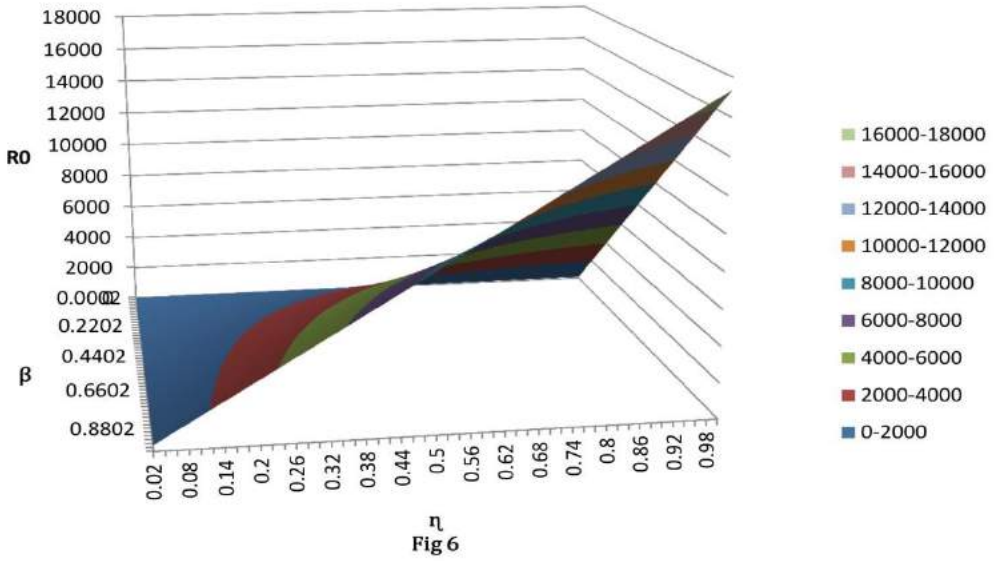

Figure 6: Impact of β (Smartphone virus infection transmission rate) and η (modification factor for the exposed Smartphone) on the dynamics of Smartphone virus infection in the population.

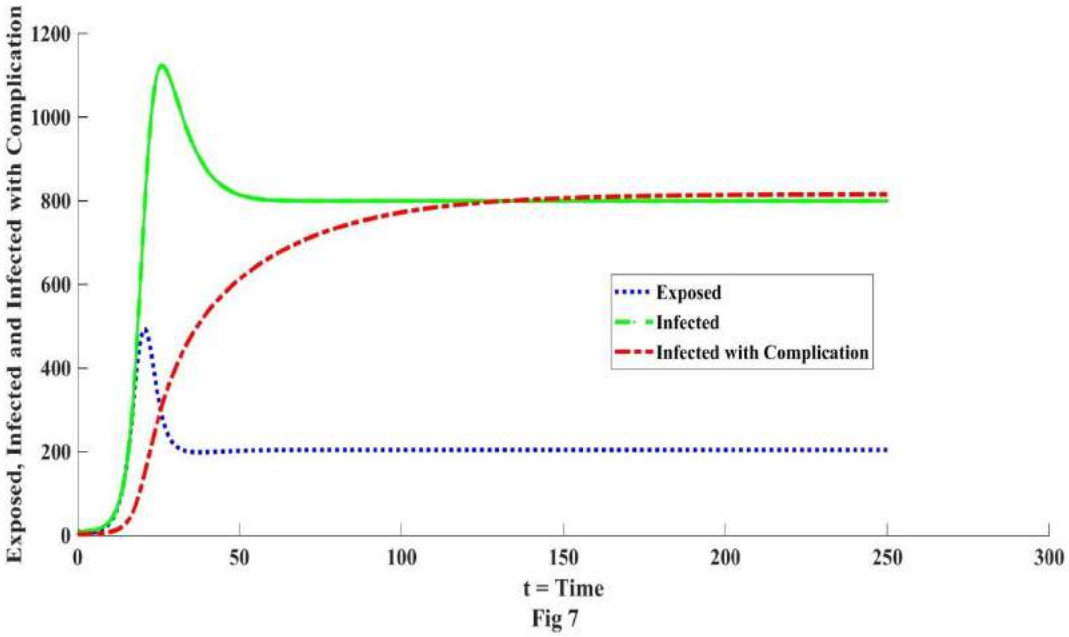

Figure 7: Simulation of the dynamic behavior of model system (3) (Exposed, Infected and Infected with complication) generated in Matlab.

5 Discussion and Conclusion

5.1 Discussion

From Table 1 above, we observe that $\Gamma_{\beta}^{R_0} = \Gamma_{\rho}^{R_0} = +1$. This implies that increasing (decreasing) β or ρ or both by a certain percentage always increases (decreases) R_0 by the same percentage. Thus, sensitivity indices with positive sign show that the value of R_0 increases as these values increase, while the remaining indices that are negative, indicates that the value R_0 decreases as they increase. The estimation of a sensitive parameter should be carefully done, since a small perturbation in such parameter leads to relevant quantitative changes. On the other hand, the estimation of a parameter with a small value for the sensitivity index does not require as much attention to estimate, because a small perturbation in that parameter leads to small changes [29]. This simply means that Smartphone will be infected, repaired (disinfected with antivirus) and eventually recover and retain the infection or obtain immunity. These parameters with negative index reduce the rate at which the infection multiplies in Smartphone population and the virus may eventually be eradicated.

In this work, the analytic results obtained are discussed as follows. The basic Smartphone virus infection reproduction number, R_0,which is the threshold parameter that predicts whether an infection can spread were used as a guide to Smartphone manufacturers and antivirus software

developers on the amount of effort needed to control or eradicate virus infection in Smartphone. The results of the numerical simulation of the sensitivity analysis of the basic Smartphone virus infection reproduction number were discussed in this section. The parameter values and sensitivity indices are shown in table 1. The main aim is to assess the feasibility of the dynamics of Smartphone virus infection for different value of the parameters of the basic reproduction number.

Figures 2, 3 and 5 confirm our theoretical analysis that negative sensitivity indices contribute in decreasing R_0 as their value increases. Similarly, figures 4 and 6 represents positive sensitivity indices and it shows that as the value of these parameters increases, R_0 is also increased. Figure 7 shows that the prevalence of Smartphone virus infection increases to a climax, decreases and remains almost stable through the horizon at an alarming rate. Actually the climax indicates the maximum point of the epidemic and the almost stable horizon indicates endemicity of Smartphone virus infection. Therefore, the study confirms that without adequate control measure, Smartphone virus will continuously invade and destroy Smartphones and the virus cannot be eradicated in the population.

5.2 Conclusion

In this work, we computed the sensitivity analysis of the basic reproduction number to study Smartphone virus infection transmission dynamics. The model parameters are given in section (3) and the model equations was derived with the aid of the schematic diagram in figure 1. The Smartphone virus free equilibrium state of the model was determined. The basic Smartphone virus infection reproduction number R_0, for the model was computed using next generation method. The model showed that the stable Smartphone virus infection free equilibrium coexists with the Smartphone virus infection endemic equilibrium in the population. The model suggests that without adequate control measure, Smartphone virus will continuously invade and destroy Smarphones and the virus cannot be eradicated in the population.

Reference

[1] Milosevic, N., Dehghantanha, A. and Choo, K. K. R. (2017) Machine Learning Aided Malware Classification of Android. Computers and Electrical Engineering, 61: 266 – 274.

[2] Kouliaridis, V., Barmpatsalou, K., Kambourakis, G. and Chen, S. (2020). A Survey on Mobile Malware Detection Techniques, IEICE Transacions on Information and Systems vol. E103 No. 2.

[3] Peng, S., Min, W., Wang, G. and Yu, S. (2014). Propagation of Smartphone worm Based on Semi-Markov Process and Social Relationship Graph. Comput. Secr., 44: 92-103.

[4] McAfee. "Mobile Threat Report", hppts://www.mcafee.com/enterprise/en-us/assets/reports/rp-mobile-threat-report-2018.pdf, accessed May 10, 2018.

[5] Symantec, Motivations of Recent Android Malware, hppts://www.symantec,com/content/en/us/enterprise/media/security_response /whitepapers/motivations_of_recent_android_malware.pdf, accessed Dec 10, 2018.

[6] Hypponen, M. (2006) Malware goes Mobile. Scientific American, Inc. www.Sciam.com.
[7] Skoudis, E. and Zeltser, L. (2004). Malware: fighting malicious code. Prentice Hall Professional, New Jersey, USA.
[8] Chandrasekar, S. and Jayaprakasan, V. (2014) Automatic Detection and Restraining Mobile Virus Propagation using Android, International Journal of Computer Science and Mobile Computing, 3(1): 526-532.
[9] Chinebu, T.I., Udegbe, I.V. and Eberendu, A.C. (2021) Epidemic Model and Mathematical Study of Impact of Vaccination for the Control of Malware in Computer Network, Journal of Advances in Mathematics and Computer Science, 36(3):72-96.
[10] Zhang, C. (2018) Global behavior of a computer virus propagation model on multilayer networks, Security and Communication Networks, 9(6).
[11] Wang, M., Chen, Z., Xu, L. and Zhan, H. (2014) Spread and control of mobile benign worm based on two-stage repairing mechanism, Journal of Applied Mathematics.
[12] Fan, Y., Zheng, K. and Yang, Y. (2010) Epidemic model of mobile phone virus for hybrid spread mode with preventive immunity and mutation", in Proc. 6th International Conference on Wireless Communications Networking and Mobile Computing (WiCOM 2010), Chengdu, China, 1-5.
[13] Van, R.E., Courtney, T., Sander, W.H. and Stevens, F. (2007). Quantifying the Effectiveness of Mobile Phone Viruses response mechanism. In Proceeding of the 37th Annual IEEE/IFTP International Conference on Dependable System and Networks (DNS 07), 790-799.
[14] Racic, R., Ma, D. and Chen, H. (2006). Exploiting MMS vulnerabilities to stealthily exhaust mobile phone's battery. In 2006 Securecomm and Workshops (pp. 1-10). IEEE.
[15] Yang, L.X., Li, P., Yang, X. and Tang, Y.Y. (2017). Distributed interaction between computer virus and patch: A modeling study, arXiv preprint arXiv:1705.04818.
[16] MadhuSudanan, V. and Geetha, R. (2020) Dynamics of epidemic computer virus spreading model with delays, Wireless Personal Communications, 115(3): 2047-2061.
[17] Batista, F.K. and del Rey, Á.M., Quintero-Bonilla, S., and Queiruga-Dios, A. (2017) A SEIR Model for Computer Virus Spreading Based on Cellular Automata, In International Joint Conference SOCO'17-CISIS'17-ICEUTE'17 León, Spain, September 6–8, 2017, Proceeding (pp. 641-650).Springer.
[18] Van, R.E, Courtney, T., Sander, W.H. and Stevens, F. (2007) Quantifying the Effectiveness of Mobile Phone Viruses response mechanism. In Proceeding of the 37th Annual IEEE/IFTP International Conference on Dependable System and Networks (DNS 07), 790-799..
[19] Guillen, J.D.H., del Rey, A.M. and Vara, R.C. (2020) On the Optimal Control of a Malware Propagation model, Mathemaics, doi: 10.3390/math8091518.
[20] Liu, W. and Zhong, S. (2017) Web Malware Spread Modelling and Optimal Control Strategies. Scientific Reports, doi:10.1038/srep42308.
[21] Chinebu, T.I., Eberendu, A.C. and Udegbe, I.V. (2021) Analysis of a Mathematical Model for the Dynamics of Smartphone Virus Propagation: a guide from epidemiological model, Global Scienific Journals, 9(6).
[22] Yang, W., Wei, X., Guo, H., An, G., Guo, L. and Yao, Y. (2014). Modeling the propagation of Mobile Phone Virus under Complex Network. The Scientific World Journal, doi.org/10.1155/2014/207457.
[23] Hethcote, H.W. (2000). The mathematics of infectious diseases", SIAM Rev. 42 (4):599- 653.
[24] van den Driessche, P. and Watmough, J. (2002). Reproduction numbers and sub-threshold

endemic equilibria for compartmental models of disease transmission, Mathematical Biosciences, 180(1-2): 29-48.
[25] Heffernan, J.M. (2005). Perspective on the Basic reproduction Ratio. J. R Soc. Interface, 2: 281-293.
[26] Ameh, E.J. The Basic Reproduction number: Bifurcation and stability, PGD Project at AIMS.
[27] Rosa, S. and Torres, D.F.M. (2018). Parameter Estimation, Sensitivity Analysis and Optimal Control of a Periodic Epidemic Model with Application to HRSV in Florida State., Optim. Inf. Comput., 6: 139 – 149.
[28] Mikucki, M.A. (2012) Sensitivity Analysis of the Basic Reproduction Number and other Quantities for Infectious Disease Model. Ph.D Thesis Colorado State University.
[29] Birkhoff, G. and Rota, G.C. (1989) Ordinary Differential Equations, 4th Edition. New York: John Wiley and Sons, Inc.
[30] Lakshmikantham, V., Leela, S. and Martynyu, K.A. (1989) Stability Analysis of Nonlinear Systems, Marcel Dekker Inc. New York.
[31] Zhang, S.N. (1988) Comparison theorems on boundedness. Funkcial Ekvac, 31:179-196.

Journal of the Nigerian Society for Mathematical Biology

Scope: The Journal of the Nigerian Society for Mathematical Biology (JNSMB), the official journal of the Nigerian Society for Mathematical Biology, disseminates original research findings relating mathematics to the biological sciences. The aim of the journal is to cause to be published research that shows the connection between applied mathematicians, statisticians, operations researchers, physicists, engineers, computer scientists and specialists in the fields of agriculture, public health, epidemiology, pharmacy, life sciences and other bio-medical fields at the crossroad of theoretical, experimental and field biology with the mathematical sciences, in order to provide solutions to problems that cut across these fields through exchange of ideas and collaborations.

Submitted papers should provide rigorous mathematical analysis of the biological issues being discussed. At the same time, the results obtained should be useful in a biological context and easily understandable by non-mathematicians. The Journal also welcomes experimental results from any biological process. The journal will accept different kinds of articles, ranging from review articles to special invitations. All submitted manuscript will be assessed by the Editor-in-Chief before being sent out for peer-review.

Areas covered include, cellular and sub-cellular biology, physiology, epidemiology, ecology, development and morphogenesis, genetics, neurobiology, population biology, immunology, molecular biology, DNA and protein structures and functions, plant biology, animal biology, eco-toxicology, pharmacokinetics, public health, bio-engineering, bio-statistics, bio-fluid dynamics, and computational biology.

Manuscript Information and guidelines for Authors

This is to invite you to submit high-quality research articles to the Journal of the Nigerian Society for Mathematical Biology (JNSMB).

Manuscripts should be written either using MS Word or in LaTeX (most preferred). Initial submissions for review can be in MS Word or PDF. There will be a page restriction of a maximum of 26 pages per accepted article. The article should be concise and details of well established mathematical methods should be omitted. Articles that do not contain significant mathematical content and results will not be accepted for publication.

Citations within the manuscript should be done using the number system i.e., "Following the idea in [7], we have that …". Theorems, Lemmas, Propositions, Remarks, e.t.c., should be numbered using the Section number where they appear e.g., Theorem 2.1 will appear in Section 2.

References should follow the format shown below:

[1] Anderson, R. M. and May, M. (1991). Infectious Diseases of Humans: dynamics and Control. Oxford University Press, UK.

[2] Castillo-Chavez, C. and Song, B. (2004). Dynamical models of tuberculosis and their applications, Math. Biosci. Eng., 1: 361-404.

References should be in alphabetical order in the list of references, which should be the last section in the manuscript.

Manuscripts should be submitted to the Editor-in-Chief, via the following email address: mcsb@uniben.edu. Please note that this is the **only** acceptable channel for manuscript submission at this time.

There is a publication charge for each accepted article. Payment details will be corresponded to the author(s) at the time of manuscript acceptance for publication in the JNSMB.

Subscription rates: This is subject to change from time to time. Please, contact the Editor-in-Chief for the current rates, for local and foreign subscriptions.

Journal of the Nigerian Society for Mathematical Biology, Volume 4 (2021)

Contents